Techno-Economic Analysis of Hybrid Concentrating Solar Power Systems

Jin Han Lim

Thesis submitted for the degree of Doctor of Philosophy

School of Mechanical Engineering

Faculty of Engineering, Computer & Mathematical Sciences

The University of Adelaide, South Australia

March 2017

Table of contents

Abstract

This thesis presents the outcomes of techno-economic studies of power generation using hybrid Concentrating Solar Power (CSP) systems, in particular, the Hybrid Solar Receiver Combustor (HSRC). The HSRC technology consists of a device that integrates a combustor into a tubular solar cavity receiver to enable a schedulable firm supply of electricity. Two innovative configurations of the HSRC were investigated; one operating with conventional combustion while the other operating with Moderate or Intense Low-oxygen Dilution (MILD) combustion. The HSRC was developed to lower the overall cost of renewable electricity generation by reducing the installed capital cost, fuel consumption and parasitic losses of a conventional hybrid Concentrating Solar Power (CSP) plant. The HSRC technology was also developed to provide a firm supply of electricity with lower emissions relative to current state-of-the-art hybrid CSP systems.

The thesis presents an assessment of the HSRC, which was based on operation with conventional combustion, with an analytical model that calculates the heat transfer, mass flow rates and energy into and out of the device. A systematic investigation of the influence of controlling parameters on the performance of the device was undertaken. The performance of the HSRC was analysed with a pseudo-dynamic model that accounts for variations in CSP input using historical solar data from sites in USA and Australia.

The thermal efficiency of the HSRC was found to be similar to a conventional system of two stand-alone systems, namely; a solar-only cavity receiver and a conventional natural gas boiler, also termed Solar Gas Hybrid (SGH). Additionally, it was found that the HSRC system benefits from the reduction in start-up and shut-down losses, incurred by a backup boiler, and a decrease in parasitic losses due to the integration of solar and combustion in one device.

The HSRC was estimated to reduce the overall Levelised Cost of Electricity (LCOE) by up to 17% relative to the SGH system. The sensitivities to key parameters of the LCOE were also assessed, and the results were found to be highly influenced by the price of the fuel (natural gas). In addition, configurations of the HSRC that enable it to operate in the conditions required for MILD combustion were also identified. This is desirable as the combustion regime is known to offer greater compactness, lower NO_x emissions, and potential fuel savings due to higher and more uniform heat transfer relative to current state-of-the-art combustion systems. Operating in this combustion regime resulted in a more compact device and an estimated LCOE reduction of up to 4% relative to the HSRC operating with conventional combustion for the same reference receiver size of $30MW_{th}$.

This thesis also evaluated the potential to lower the cost of hybrid CSP systems by modularising selected components (e.g. heliostat, tower and receiver) in a CSP plant. It was found that the energy losses in a system of small-sized modules employing molten salt as its heat transfer fluid are dominated by electrical trace heating due to the increased in piping length relative to their larger receiver counterpart. However, this can be reduced by a significant amount using alternative heat transfer fluids with a lower melting point such as sodium. In addition, for modularisation to be cost effective, access to alternative, lower-cost manufacturing methods is required. Specifically, the benefit of standard learning rates is insufficient to lower the LCOE on its own.

Declaration

I certify that this work contains no material which has been accepted for the award of any other degree or diploma in my name, in any university or other tertiary institution and, to the best of my knowledge and belief, contains no material previously published or written by another person, except where due reference has been made in the text. In addition, I certify that no part of this work will, in the future, be used in a submission in my name, for any other degree or diploma in any university or other tertiary institution without the prior approval of the University of Adelaide and where applicable, any partner institution responsible for the joint-award of this degree.

I give consent to this copy of my thesis when deposited in the University Library, being made available for loan and photocopying, subject to the provisions of the Copyright Act 1968.

I acknowledge that copyright of published works contained within this thesis resides with the copyright holder(s) of those works.

I also give permission for the digital version of my thesis to be made available on the web, via the University's digital research repository, the Library Search and also through web search engines, unless permission has been granted by the University to restrict access for a period of time.

Jin Han Lim Date

19/03/2017

Acknowledgement

I would like to express my most sincere gratitude to those who have helped me in my journey towards completing this thesis.

Firstly, I would like to thank my supervisors Professor Graham ‘Gus’ Nathan, Professor Bassam Dally and Dr. Alfonso Chinnici for helping me significantly in many different ways. I thank Professor Nathan for sharing his extensive knowledge in the field of hybrid solar energy systems, and for his enthusiasm and motivation, all of which have helped me tremendously throughout my postgraduate studies. He has also acted as an advisor/mentor, providing me with career guidance, in addition to immensely improving my technical writing skills with his thorough feedback and attention to detail. I also thank Professor Dally for his eagerness to meet datelines and willingness to help and provide advice at all time, as well as for sharing his technical knowledge in the field of MILD combustion. Furthermore, I would like to thank Dr. Chinnici for his support and guidance, and for sharing his knowledge, both in the fields of MILD combustion and analytical modelling. He is ever willing to help, acting not only as a supervisor, but also as a friend.

I would also like to acknowledge the university and Professor Nathan for providing me with financial support through the Divisional Scholarship and a further supplementary scholarship through the Linkage Grant.

Finally, I would like to say, from the bottom of my heart, thank you, to my parents, my partner, my brother and other close family members for their unconditional love and support. I also thank the HSRC team for the collective work that we have accomplished together, colleagues for being my lunch buddies and for keeping my spirits up and motivation levels high, and Associate Professor Eric Hu for sharing his technical knowledge and for his supervision in the first two years of my candidature.

CHAPTER 1

INTRODUCTION

1.1Background

Environmental concerns and emission targets over the last few decades have fuelled much of the effort in developing technologies and regulatory framework to tackle climate change [1, 2]. This is because the majority of scientists established that climate change is linked to an increase in human induced greenhouse gas emissions which poses major risks to not only the society, but also the economy and the environment [2, 3]. A warmer climate is predicted to increase the frequency of extreme weather incidents, such as heatwaves, torrential rain and droughts [2]. One of the major contributors to climate change is human induced emission of greenhouse gases, such as carbon dioxide, water vapour, nitrous oxides and methane, into the atmosphere [2]. These gases store heat radiated from the surroundings in the atmosphere. Since the 1950s, the concentration of greenhouse gases, especially carbon dioxide, has increased substantially as a result of human dependence on fossil fuels for energy conversion [4]. In addition, a study performed by the Energy Information Administration (EIA) has found that the consumption of fossil fuels may potentially increase by an additional 27% over the next 20 years [5]. It was determined that such an increase would result in a global temperature rise of around 1.4°C over the next century [2]. To prevent such rise in temperature and its long-term effects, there is a need to reduce greenhouse gas emissions as soon as practical. Several solutions have been proposed and those include: increasing the penetration of renewable energy generation, deployment of carbon capture and storage technologies and improving the energy efficiency of existing electricity generation systems and electrical appliances.

Two of the most prominent methods to harness renewable energy from the sun to generate electricity are solar photovoltaic (PV) cells and Concentrating Solar Power (CSP) technologies. The use of solar energy to displace fossil fuels is expected to significantly decrease the level of greenhouse gas emissions to the atmosphere [6-8]. In recent times, there has been an increase in interest in CSP technologies, comparable with solar PV research, especially for large scale

solar power generation as CSP has several advantages over solar PV [1]. The advantages include CSP potentially achieving higher solar-to-electricity efficiencies, lower investment costs for storage and wider hybridization options, although solar PV is currently cheaper if considering only electricity generation [9]. The International Energy Agency (IEA) has predicted that the CSP industry will potentially account for 28% of total global electricity generation over the next few decades [6]. However, it is common knowledge that solar resource is intermittent and varies in nature. Hence, there is a need to cost effectively address this issue.

Two of the solutions that have been proposed to address the intermittency and variability of solar resource are to introduce storage technologies, and hybrids with traditional combustion technologies [10-14]. Of the various types of storage technologies, Thermal Energy Storage (TES) is the most widely deployed storage system in CSP plants around the world. This is because TES has a high energy density and high energy conversion efficiency [12, 15]. When coupled with a CSP plant, TES enables electricity to be dispatched when solar radiation levels are below its useful threshold thus increasing the plant's solar fraction and enables load shifting capabilities [16]. However, storing enough solar energy via TES to enable a continuous dispatch of electricity [17], especially in 'island' electrical networks or stretched capacity wires as found in Australia, is unlikely to be financially beneficial. Meanwhile, hybrids of CSP with fossil fuel systems are attractive in the short term to provide firm supply, mitigate greenhouse gas emissions and capitalize on the lower cost of energy from readily available fossil fuels [18]. This implies that a combination of CSP and fossil fuelled systems offers the potential to reduce greenhouse gas emissions at a moderate cost, while providing a firm supply of electricity [19, 20]. Hence, it is likely that the introduction of hybrid CSP-combustion systems will be one of the stepping stones towards the path of greenhouse gas emission mitigation.

One of the recently proposed concepts is the Hybrid Solar Receiver Combustor (HSRC), which integrates the functions of a solar-only cavity receiver and a natural gas combustor into a single

tubular receiver [21, 22]. It was previously found that the device offers significant potential advantages over an equivalent configuration of a solar-only cavity receiver and a backup gas boiler, termed the Solar Gas Hybrid (SGH). In particular, the HSRC was estimated to reduce the Levelized Cost of Electricity (LCOE) of the overall power system which includes hot and cold storage tanks, a steam generator and an Electrical Power Generating System (EPGS), by up to 11% for a $100MW_{th}$ receiver size [21]. However, this estimate is based on the assumption that the capital cost of the HSRC is double that of a solar-only cavity receiver. It was also assumed that the performance of both the solar receiver and the combustor within the HSRC achieves a similar efficiency relative to its standalone counterparts. In addition, the previous analysis assumed an annually averaged performance of the CSP plant, and did not account for the additional potential benefits of the HSRC relative to the SGH, such as eliminating the start-up and shut-down losses of a conventional backup boiler, and reducing electrical trace heating required to maintain the temperature of the Heat Transfer Fluid (HTF) (assumed to be molten salt) above its freezing point. Hence, further analyses are required to refine the previous assumptions and to account more reliably for solar resource variability. Also, the additional benefits of the HSRC in reducing start-up and shut-down losses and electrical trace heating losses relative to the SGH have not yet been assessed.

Previous assessments were based on the HSRC operating with conventional combustion, as is the case for most of the current state-of-the-art boiler technologies. The challenge with conventional combustion is that it produces relatively high volumes of greenhouse gas and NO_x emissions [23], which play a key role in the formation of acid rain and photochemical smog [24]. Therefore, it is necessary to incorporate the use of a low emission combustion technology in the HSRC. One of such methods is the use of Moderate or Intense Low-oxygen Dilution (MILD) combustion. This combustion method is known to offer lower NO_x emissions, greater compactness and potential fuel savings due to higher and more uniform heat transfer relative

to standard combustion systems [25, 26]. Hence, it is desirable to identify configurations of the HSRC that enables it to operate in the conditions required for MILD combustion. The economic trade-off of this configuration compared with other equivalent hybrid CSP-fossil fuel technologies also needs to be assessed.

Another proposed method to lower the cost of hybrid CSP plants is the concept of modularisation of selected components in the plant, e.g. heliostats, towers and solar receivers [27]. This concept is driven by both the potential use of lower-cost materials, and the potential to lower the components' cost by mass production of standardized components of significantly smaller scale [27]. Another advantage is that modular systems can be constructed in phases, which allows cash-flow to be generated in stages [28]. Yet, these potential advantages should be compared with the disadvantages of modular systems that include an increase in the initial capital cost and Operations and Maintenance (O&M) costs. To date, no previous assessment has been reported of the economic merit of modularisation of hybrid CSP plants. Therefore, there is a need to evaluate the conditions where it is economically beneficial to implement modular hybrid CSP systems. It is also of interest to determine the conditions in which the HSRC will add value to a modular CSP system.

1.2 Project aims

Based on the above background, the motivation behind this work is based on the need to identify cost effective CSP hybridization options, with combustion technology, that has the potential to provide a firm supply of electricity and also offer low greenhouse gas and NO_x emissions.

The specific aims of this thesis are the following:

- To investigate the influence of the controlling parameters of the HSRC, such as length to diameter ratio of its cavity and length of the heat exchanger, on its performance and weight (which is the key driver of its cost);
- To more reliably estimate the economic benefits of the HSRC relative to the SGH by accounting for solar resource variability;
- To account for the additional benefits of the HSRC technology relative to the SGH system by assessing both the influence of start-up and shut-down losses of a backup boiler and electrical trace heating losses for both systems;
- To identify configurations of the HSRC that enables it to operate in the conditions required for MILD combustion and to estimate the potential economic benefit of this configuration relative to other equivalent hybrid CSP systems;
- To identify conditions where economic benefits can be derived from modularising selected components in a hybrid CSP plant;
- To identify conditions where the cost of the HSRC would be lower compared with the SGH for a modular system.

1.3 Thesis outline

This thesis comprises a portfolio of publications that are either in press or submitted for publication. This document is presented in seven chapters as outlined in the following:

Chapter 2 presents background literature regarding the research topic and identifies the gaps in current knowledge and understanding. In particular, it provides an overview of current CSP technologies and introduces the types of hybrid CSP power plants and thermal energy storage

systems. This chapter also assesses the challenges with current state-of-the-art hybrid CSP systems and introduces the HSRC technology.

Chapter 3 consists of the first published paper entitled: “Analytical assessment of a novel hybrid solar tubular receiver and combustor”. The paper reports on the study of the HSRC with an analytical model that was used to calculate the heat transfer, mass flow rates and energy into and out of the device. The influence of variation of the controlling parameters of the HSRC, such as length to diameter ratio of its cavity and length of the heat exchanger, on its performance and weight was evaluated.

Chapter 4 consists of the second published paper entitled: “Impact of start-up and shut-down losses on the economic benefit of an integrated hybrid solar cavity receiver and combustor”. The paper identifies further potential advantages of employing the HSRC relative to the SGH by eliminating start-up and shut-down losses of a conventional backup boiler and decreasing the amount of electrical trace heating needed to prevent the HTF from solidifying. The previously developed analytical model of the HSRC (from Chapter 3) was extended to incorporate other components of a CSP system such as heliostat field, storage tanks, a steam generator and an EPGS. The model also accounts for the variability in solar resource by using a five-year time-series of historical Direct Normal Irradiation (DNI) data at one-hour time-steps as input. The LCOE of each of the systems analysed were calculated by varying the size of the power block and DNI data location.

Chapter 5 consists of the third published paper titled: “Assessment of the potential benefits and constraints of a hybrid solar receiver and combustor operated in the MILD combustion regime”. The paper identifies configurations of the HSRC to operate with a low emission combustion technology. In particular, this chapter identifies configurations of the HSRC that enable it to operate with MILD Combustion. The economic benefits of the HSRC operating in

the MILD combustion regime relative to other equivalent hybrid CSP systems were also assessed.

Chapter 6 consists of the fourth paper submitted for publication titled: “Techno-economic evaluation of modular hybrid concentrating solar power systems”. This paper evaluates a method to potentially lower the cost of hybrid CSP systems involving the modularisation of selected components in a CSP plant. Modularisation of both HSRC and SGH systems were considered for the same sized power block. The trade-offs between the pros and cons of modularisation for both systems were assessed with a pseudo-dynamic model.

Finally, Chapter 7 presents the conclusions of the work presented in this thesis while Chapter 8 presents recommendations for future work.

1.4 Publications resulting from this work

This study has produced four journal papers and two peer reviewed conference papers.

List of Journal papers:

- Lim, JH, Nathan, GJ, Hu, E & Dally, BB 2016, 'Analytical assessment of a novel hybrid solar tubular receiver and combustor', Applied Energy, vol. 162, pp. 298-307.
- Lim, JH, Hu, E & Nathan, GJ 2016, 'Impact of start-up and shut-down losses on the economic benefit of an integrated hybrid solar cavity receiver and combustor', Applied Energy, vol. 164, pp. 10-20.
- Lim, JH, Chinnici, A, Dally, BB & Nathan, GJ 2016, 'Assessment of the potential benefits and constraints of a hybrid solar receiver and combustor operated in the MILD combustion regime', Energy, vol. 116, Part 1, pp. 735-745.

- Lim, JH, Dally, BB, Chinnici, A & Nathan, GJ 2016, 'Techno-economic evaluation of modular concentrating solar thermal hybrid power systems', Energy (submitted September 2016 – manuscript number: EGY-D-16-02670).

Conference papers:

- Lim, JH, Nathan, G, Dally, B & Chinnici, A 2016, 'Techno-economic assessment of a hybrid solar receiver and combustor', AIP Conference Proceedings, vol. 1734, no. 1, p. 070020.
- Lim, JH, Chinnici, A, Dally, B & Nathan, GJ 2017, 'Assessing the techno-economics of modular hybrid solar thermal systems', AIP Conference Proceedings (submitted).

1.5 Format

This thesis has been submitted in the publication format, as it includes publications that have either been published or are currently under review. It follows the formatting requirements of The University of Adelaide. The printed and online copies of the thesis are identical. The online version is available as a PDF and can be viewed with any PDF viewing software.

References

1. Hoffschmidt, B., et al., *Concentrating Solar Power*. Comprehensive Renewable Energy, 2012. **3**: p. 595-636.
2. Authority, C.C., *Reducing Australia's Greenhouse Gas Emissions: Targets and Progress Review—Final Report*, in *Climate Change Authority, Melbourne*. 2014.
3. Olivier, J.G., et al., *Trends in global CO2 emissions: 2015 Report*. 2015, PBL Netherlands Environmental Assessment Agency The Hague.
4. Yamasaki, A., *An overview of CO2 mitigation options for global warming-Emphasizing CO2 sequestration options.* Journal of Chemical Engineering of Japan, 2003. **36**(4): p. 361-375.
5. Figueroa, J.D., et al., *Advances in CO 2 capture technology—the US Department of Energy's Carbon Sequestration Program.* International journal of greenhouse gas control, 2008. **2**(1): p. 9-20.
6. International Energy Agency, *Solar Energy Perspectives*. 2011.
7. Wagner, S.J. and E.S. Rubin, *Economic implications of thermal energy storage for concentrated solar thermal power*. 2012.
8. van der Zwaan, B. and A. Rabl, *Prospects for PV: a learning curve analysis.* Solar Energy, 2003. **74**(1): p. 19-31.
9. Faraz, T. *Benefits of concentrating solar power over solar photovoltaic for power generation in Bangladesh*. in *Developments in Renewable Energy Technology (ICDRET), 2012 2nd International Conference on the*. 2012. IEEE.
10. Pasamontes, M., et al., *Hybrid modeling of a solar-thermal heating facility.* Solar Energy, 2013. **97**: p. 577-590.
11. Fath, H.E.S., *Technical assessment of solar thermal energy storage technologies.* Renewable Energy, 1998. **14**(1-4): p. 35-40.
12. Tian, Y. and C.Y. Zhao, *A review of solar collectors and thermal energy storage in solar thermal applications.* Applied Energy, 2013. **104**: p. 538-553.
13. Zhang, H.L., et al., *Concentrated solar power plants: Review and design methodology.* Renewable and Sustainable Energy Reviews, 2013. **22**: p. 466-481.
14. Kolb, G.J., *Economic evaluation of solar-only and hybrid power towers using molten-salt technology.* Solar Energy, 1998. **62**(1): p. 51-61.
15. Gil, A., et al., *State of the art on high temperature thermal energy storage for power generation. Part 1-Concepts, materials and modellization.* Renewable and Sustainable Energy Reviews, 2010. **14**(1): p. 31-55.
16. Kearney, D. and H. Price. *Assessment of thermal energy storage for parabolic trough solar power plants*. in *2004 International Solar Energy Conference, July 11, 2004 - July 14, 2004*. 2004. Portland, OR, United states: American Society of Mechanical Engineers.
17. Kueh, K.C., G.J. Nathan, and W.L. Saw, *Storage capacities required for a solar thermal plant to avoid unscheduled reductions in output.* Solar Energy, 2015. **118**: p. 209-221.
18. Ordorica-Garcia, G., A.V. Delgado, and A.F. Garcia, *Novel integration options of concentrating solar thermal technology with fossil-fuelled and CO_2 capture processes.* Energy Procedia, 2011. **4**: p. 809-816.
19. Powell, K.M. and T.F. Edgar, *Modeling and control of a solar thermal power plant with thermal energy storage.* Chemical Engineering Science, 2012. **71**: p. 138-145.
20. Moore, J. and J. Apt, *Can hybrid solar-fossil power plants mitigate CO2 at lower cost than PV or CSP?* Environmental Science and Technology, 2013. **47**(6): p. 2487-2493.

21. Nathan, G.J., D.L. Battye, and P.J. Ashman, *Economic evaluation of a novel fuel-saver hybrid combining a solar receiver with a combustor for a solar power tower.* Applied Energy, 2014. **113**: p. 1235-1243.
22. Nathan, G.J., et al., *A Hybrid Receiver-Combustor*, A.R.I.P. Ltd, Editor. 2013.
23. Szegö, G.G., B.B. Dally, and G.J. Nathan, *Scaling of NOx emissions from a laboratory-scale mild combustion furnace.* Combustion and Flame, 2008. **154**(1–2): p. 281-295.
24. Baukal Jr, C.E., *Heat Transfer*, in *The John Zink Combustion Handbook*. 2001, John Zink Company LLC. p. 106.
25. Tsuji, H., et al., *High Temperature Air Combustion*. 2003, Boca Paton: CRC Press.
26. Cavaliere, A. and M. de Joannon, *Mild Combustion.* Progress in Energy and Combustion Science, 2004. **30**(4): p. 329-366.
27. Vast Solar, *Dissemination Report: Heliostat Field and High Temperature Receiver Development*. 2014.
28. Johansson, T.B., *Renewable energy: sources for fuels and electricity*. 1993: Island press.

CHAPTER 2

LITERATURE REVIEW

2.1 Concentrating Solar Power (CSP)

Concentrating Solar Power (CSP) systems harness thermal energy from the sun to generate electricity and have been in operation since 1980s, with large scale systems being deployed commercially with an estimated total operational capacity of ~4800MW_e worldwide [1, 2]. Recently, the construction of two of the largest CSP plants in the world in Arizona and Southern California was completed [3]. In addition, CSP is also one of Australia's most viable options for renewable energy [4]. This is because solar radiation levels in Australia are extremely high, with the country receiving among the highest average amount of solar radiation per square metre annually worldwide [5]. There are many additional drivers for CSP technology deployment in Australia. The most important of those, are the need for carbon emission reduction technologies to meet Australia's commitments in the recent Conference of the Parties (COP 21) [6], energy security in the future due to the finite amount of fossil fuels [7] and the need for cost effective energy storage (thermal) to account for the mismatch between supply and demand in the electricity market. However, the progress of the CSP industry in Australia has been slow due to the technology's high capital costs. In addition, a High Temperature Solar Thermal roadmap commissioned on behalf of the Council of Australian Governments concluded that the CSP sector has a major opportunity for development in Australia, if carbon dioxide emitted prices in the range of $50AUD per tonne are introduced [7]. Nevertheless, many market and political analysts believe that such high carbon prices are unlikely to be introduced in the near future. Therefore, it is desirable to increase the market penetration of CSP in Australia [7] and also lower the cost of the technology so that it becomes competitive with current electricity generation technologies, i.e. there is a need for innovative technologies to reduce the cost of CSP systems.

2.2 CSP concentrator technologies

Concentrating Solar Power (CSP) systems operate on a relatively simple principle: reflect sunlight via a reflective surface onto a very small area either in a line, or a point, to increase the temperature of a Heat Transfer Fluid (HTF) to levels of up to 1000°C [3, 8]. The thermal energy transferred to the HTF can be used to generate electricity through either a gas, steam or combined cycle turbine. Figure 1 presents the four current state-of-the-art CSP concentrator technologies (clockwise from top left) [8]:

a) Linear Fresnel Reflector (LFR)

b) Central Receiver (Tower)

c) Parabolic Trough

d) Parabolic Dish

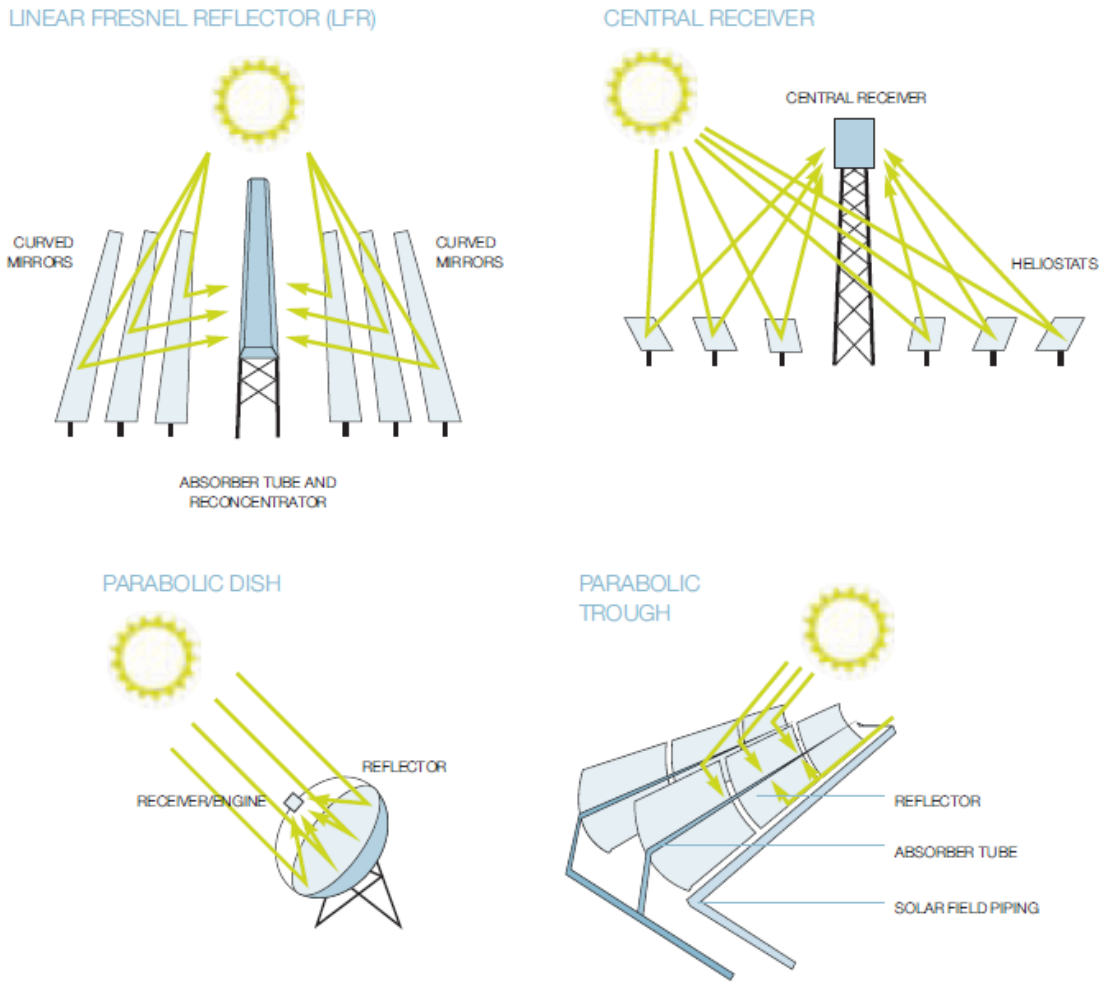

Fig. 1. Diagrams of state-of-the-art Concentrating Solar Power (CSP) concentrator technologies, namely the Linear Fresnel Reflector (LFR), Central Receiver (Tower), Parabolic Trough and Parabolic Dish [9].

The following is a summary of the operating principles for the four main CSP concentrator technologies.

2.2.1 Linear Fresnel Reflector (LFR)

Linear Fresnel Reflector (LFR) concentrator consists of mirrors, radiation receivers and support structures. This technology employs an array of long rows of mirrors that are either straight or slightly curved that concentrate incoming direct normal irradiance (DNI) from the

sun onto fixed linear receivers mounted to structures placed above the mirrors [4]. The radiation receivers are made up of absorber tubes enclosed in an evacuated glass envelope to reduce heat losses [10]. A HTF is circulated inside the absorber tubes to carry the heat from the incoming DNI. This heat is then either stored or used directly to generate electricity via a steam turbine in an Electrical Power Generating System (EPGS). Systems that use LFR concentrators usually operate at temperatures of up to 250°C making them more suited for direct steam generation [11]. The main advantage of LFR is its simple design of flexibly bent mirrors and fixed receivers, which require lower investment costs. However, LFRs are typically less efficient than other similar technologies such as Parabolic Troughs due to a lower optical efficiency, (higher cosine losses, daily profile, etc.) resulting from the concentrators' geometric properties. This results in low solar concentration ratios of ~10 to ~40 [11]. It is also more expensive to couple this technology with thermal energy storage due to its low operational temperatures [8].

2.2.2 Central Receiver (Tower)

The Central Receiver or tower concentrator technology consists of a large field of mirrors, called heliostats, that track DNI and focus it onto a receiver mounted on the top of a tall tower [12]. For current power systems that use this technology, their receiver typically comprises of tubes carrying the heat from the DNI via a HTF to either a storage tank or the EPGS. An advantage of this technology is the ability to operate at higher temperatures in excess of 500°C, potentially up to 1000°C [12] because the system operates by focusing the incoming DNI onto a common point, instead of a line. This enables Central Receiver systems to convert solar radiation into useful work at higher temperatures, relative to LFRs and Parabolic Troughs [13]. Central Receivers have a higher potential than other CSP concentrator technologies as they have been proven to work in large scales of up to 377MW_e (gross turbine capacity of the Ivanpah system in USA), albeit with a higher capital cost from building the tower and employing a control system to focus the mirrors [7, 14, 15]. However, this cost has been

projected to decrease in the near future when more operating experience is gained [8], with the technology predicted to produce the lowest cost of all CSP technologies within the next 30 years [16]. Presently there are two commercial towers, PS10 and PS20, in Spain that use cavities, as part of the solar power towers. Cavities are known to have lower radiative and convective losses relative to conventional tower technologies and are able to operate at higher temperatures. A potential improvement has been identified, by mounting a separate cavity receiver with an aperture cover, on top of a solar tower, to further decrease radiative and convective losses [17-19]. However, it is worth noting that cavities have restricted acceptance angles and therefore cannot be coupled efficiently with surround heliostat fields unless multiple cavities are used on a single tower. Therefore, considering both the potential and future low cost of the Central Receiver system, further research into innovative technologies that utilise this concentrator to harness CSP is necessary.

2.2.3 Parabolic Trough

Similar to the LFR system, the Parabolic Trough technology consists of mirrors, heat receivers and support structures. However, the mirrors are shaped into a parabola, which concentrates DNI onto a receiver tube at the focal line of the collector. A single-tracking axis is used to focus the mirrors and direct them towards the incoming DNI, which is used to heat the HTF in the receiver system [20]. Most plants that are currently in operation use synthetic oils as its HTF because these fluids can operate at temperatures up to 400°C. Modern plants use molten salt (a combination of sodium nitrate and potassium nitrate) as their HTF because the fluid can operate at higher temperatures of up to 565°C. This higher operating temperature results in an increase in the thermodynamic performance of a power plant. Parabolic Trough is the most widely used CSP concentrator technology in the world with it being installed in more than 80% of all CSP plants in operation and under construction [2, 10, 21]. This is because of the maturity

of the technology, as it has been proven in large scale electricity generation systems, especially in Spain and USA [13].

2.2.4 Parabolic Dish

Dishes are of parabolic shape to efficiently focus solar radiation onto a point receiver mounted on the axis and at the focal point of the dish. The main advantage of dishes is that it can achieve the highest optical efficiency of all CSP concentrator systems. Another advantage is that the technology has been demonstrated to achieve concentration ratios of up to 3000 and operate at very high temperatures of up to 1400°C [22]. The heat concentrated by the dish system is usually used to generate electricity directly. However, it is the least mature of all CSP systems with many of the existing systems still being in the demonstration phase [8]. One of the challenges faced is that the dish system may not be suitable to be used with thermal storage due to the dish system's small scale and extremely high operating temperatures. The current market niche for this technology is typically small scale, off-grid power applications [22-25].

2.3 Thermal Energy Storage

Storing excess energy from CSP is necessary to address the intermittent and varying characteristic of solar power [26, 27]. Storing thermal energy at times when the solar energy harnessed is in excess of the load enables a more robust system that can provide power when solar power is below its useful threshold. This increases the system's reliability to dispatch schedulable power and is therefore essential to any system that depends on solar energy [28]. There are several ways to store solar energy including thermal, electrical, chemical and mechanical methods. From all the available storage methods, thermal energy storage is the most efficient and cost effective [13]. The selection of medium for thermal energy storage applications is important as it directly affects the design, equipment selection, and both capital

and operational costs [29]. The three forms of thermal energy storage from solar energy are: sensible heat storage, latent heat storage and chemical storage.

2.3.1 Sensible heat storage

Sensible heat storage involves the addition of heat to a material to increase its temperature without changing its phase or chemical composition. Examples of such materials are liquids, e.g. molten salt, water and synthetic oils, and solids, e.g. rocks, concrete and bricks. When selecting the materials to be used for thermal energy storage, the following characteristics are required [30, 31]:

- Low cost;
- High thermal conductivity to enhance the transfer of heat in and out of the HTF;
- High thermal storage density to increase the total energy stored per degree temperature rise;
- Chemically and mechanically stable during charging and discharging to prevent reaction and dissociation;
- Non-toxic, to reduce risk and operation cost;
- Non-corrosive, to minimize construction material cost and maintenance.

Heat can be stored in a range of materials at different temperatures, classified as low (<100°C), medium (between 100°C and 500°C) and high (>500°C). The most suitable material for storing solar power at low temperatures is water due to its high thermal capacity. Another advantage is that heat can be stored at atmospheric pressure at low temperatures. However, one of the limitations is the temperature range (below 100°C at atmospheric conditions), resulting in a large amount of material required (which will increase the cost). It is also desirable to operate at higher temperatures to achieve higher thermodynamic efficiencies.

One of the current state-of-the-art material used for sensible thermal energy storage in CSP systems is molten salt, which is a combination of potassium nitrate (40%) and sodium nitrate (60%). This is because molten salt is known to have high thermal stability when operating at higher temperatures of around 500°C to 600°C, but is typically presently only heated up to 565°C in industrial applications [32, 33]. In addition, molten salt has properties that are comparable to water at high temperature (similar viscosity and low vapour pressure) [34]. For these reasons, molten salt is the HTF chosen for several CSP plants around the world [35, 36].

Another material that is currently being considered in the CSP industry is sodium [37, 38]. This is because, relative to molten salt, sodium has a higher heat transfer coefficient and thermal conductivity. Therefore, sodium reduces the risk of hot spots (thus reducing pipe stresses) [37]. More importantly, the freezing temperature of sodium is much lower at ~97°C [39] compared with molten salt at ~220°C [32, 40]. Hence, the amount of electrical energy required to maintain the temperature of sodium above its freezing point is much lower, relative to molten salt. Additionally, sodium is able to operate, while remaining chemically stable, at higher temperatures of up to 800°C [41] compared with molten salt, which can only operate up to temperatures of approximately 565°C [42]. However, the cost of sodium is higher than molten salt by a factor of ~2 and it must be completely isolated from the environment [37]. Failure to do so will result in fire accidents as sodium is very reactive with air. Some examples are a sodium leakage and fire in Jemalong Solar Station [43] and a sodium fire accident at the Plataforma Solar de Almeria (PSA) facility [44].

2.3.2 Latent heat storage

Latent heat storage involves materials that undergo a change in phase, either from solid to solid, solid to liquid or liquid to vapour, after the addition of heat. Due to its low volumetric expansion rate, the solid to liquid phase change is preferable over the liquid to vapour phase change, while

because of its high latent heat, it is preferable over the solid-solid transition. It is advantageous over sensible heat storage as it potentially uses much less storage space [26]. However, the disadvantages relative to sensible heat storage are that there is a need for a significantly larger heat transfer area and higher costs [26]. In addition, this technology has not yet been demonstrated in large scale CSP systems.

2.3.3 Chemical storage

Chemical energy storage is the least developed of all the storage technologies [45], although it has the potential to provide high energy storage densities compared with the other two aforementioned technologies [46]. For chemical energy storage, the heat from the solar receiver is used to drive a completely reversible chemical reaction [47], with the chemical undergoing an endothermic reaction when being heated and an exothermic reaction when releasing energy. Hence, the products can be stored as chemicals at ambient temperature for a longer duration with lower losses relative to sensible storage. This may increase the overall system efficiency. The stored heat can also be released at a constant rate and potentially higher temperature than the stored heat, as long as this heat is removed at a rate that would prevent self-heating/cooling [48]. These advantages make chemical energy storage a suitable alternative to traditional sensible and latent heat storage applications.

Several reactions have been proposed for chemical energy storage: redox reactions of metal oxides [49, 50], dissociation of ammonia [7, 51-53], decomposition of calcium hydroxide [54, 55], and reforming of methane [56]. Despite the distinct advantages for each of these innovative concepts, these technologies have not been proven in large-scale CSP applications.

2.4 Hybrid CSP-combustion plants

It has been shown that firm supply of CSP accounting for eventualities like a period of extended cloud cover, thermal storage capacities of up to 10 days is required, even for sites with a good

solar resource [57]. Such large thermal storage capacities are deemed uneconomic with presently available technology [27, 58]. In fact, increasing thermal storage beyond three hours has been reported to increase the capital cost of a CSP plant significantly [7]. To address this matter, hybrids of CSP with fossil fuels technologies were proposed due to their complementary nature. A hybrid CSP-combustion system is defined as a system which uses a combination of both CSP and combustion to generate electricity [59]. There is a trade-off between CSP and combustion, with CSP technologies offering low net greenhouse gas and NO_x emissions at the expense of higher cost [60] due to the intermittency of the solar resource [61], while the combustion of fossil fuels produces greenhouse gases and other pollutants but at a lower cost and higher availability [62, 63]. Moreover, it is advantageous to use CSP over many other renewable energy technologies because the former utilises heat as an intermediate energy carrier [59]. Therefore, many methods of hybridising traditional power plants with CSP have been proposed. These hybridization methods can be classified into three main categories: hybrid CSP-Rankine cycle (steam power plants), hybrid CSP-Brayton cycle (gas power plants) and hybrid CSP-combined cycle power plants.

2.4.1 Hybrid CSP-Rankine cycle

Zoscak and Wu were the pioneers in solar hybridisation of Rankine cycle (steam power) plants [64]. They studied several possible ways to utilise solar radiation in a fossil-fuelled steam powered plant such as feedwater heating, steam superheating, air preheating and water evaporation. They discovered that it is possible to obtain a maximum solar fraction, defined as the ratio of the amount of input energy contributed by a solar energy system to the total input energy, of 0.27 with more than one of the methods mentioned. Pai analysed the concept of integrating a solar concentrator field with a modern thermal power station, in particular a 210MW coal-fired power plant, by preheating feedwater up to temperatures of 241°C [65]. The author found that there are significant savings in coal of around 47,000 tonnes annually. By

increasing the preheating temperature to up to 330°C, the level of coal savings can potentially be doubled. Deng proposed a hybrid solar and coal-fired steam power plant with secondary air preheating [66]. Using GateCycle sofware, the authors estimated solar-to-power efficiencies of up to 24.1%, and this value is higher than existing hybrid solar-feedwater systems. Ying and Hu proved that a high thermodynamic efficiency of a regenerative Rankine plant can be obtained by utilising low-grade solar thermal to pre-heat feedwater in a boiler [67]. Their analysis is based on an exergy merit index (EMI), defined as the ratio of work generated by the saved steam to the exergy supplied by the solar heat. With the feedwater preheating concept (for inlet temperatures of up to 286°C), the EMI can reach values greater than 100% while a solar-only power system can never reach such high EMI values. Yang et al. also demonstrated that medium to low temperatures from solar energy could be used in regular coal-fired plants to generate electricity efficiently [68]. Additionally, You and Hu investigated the optimal efficiency for a combined system of a regenerative-reheat Rankine power cycle and a parabolic trough collector which heats the HTF to a temperature of up to 390°C [69]. The authors concluded that the reheat-regenerative arrangement is suitable for medium-temperature solar thermal power generation. Eck et al. presented the scientific results from the European Direct Solar Steam (DISS) project in real solar conditions (for steam temperatures of around 400°C and a pressure of 100 bar) [70]. The authors investigated three modes of operation of a direct steam generation collector field, the once-through mode, the recirculation mode and the injection mode. They found that direct steam generation via parabolic troughs is feasible, and that the recirculation process is the most attactive option for commercialisation. However, it is worth noting that direct steam generation with CSP was proven to be uneconomical as the system does not allow thermal storage and faces the challenge of boiling in horizontal pipes [71]. Yan et al. analysed the economic benefits of using CSP to preheat the feedwater in a range of subcritical, critical and supercritical coal-fired power plants in temperature ranges between

90°C to 260°C [72]. The authors found that fuel savings of up to 20% can potentially be achieved, and that the benefits of hybridisation increases with the size of the power plant. Odeh et al developed a model of a solar electric generation system using a thermo-hydrodynamic model of a direct steam collector combined with a model of a traditional steam power house [73]. The authors used hourly radiation data from different sites across Australia (Alice Springs and Darwin) in their model. They confirmed the feasibility of the system in Australia. Popov analysed an option to utilise Linear Fresnel mirrors for feedwater heating in a fossil fuelled power station [74].

The use of solar energy reduces the fuel input into the system, with solar shares reaching up to 23% and achieving efficiencies of up to 39% for the best solar hour of the year. It is also worth noting that there are some hybrid CSP-Rankine cycles that are commercially available but are typically limited to a low solar share of less than 15% [75]. Therefore, it is necessary to identify innovative hybrid CSP technologies that enable higher solar shares. However, it is also important to consider the trade-off between overall cost of the power plant and high solar share.

2.4.2 Hybrid CSP-Brayton cycle

A hybrid CSP-Brayton cycle uses heat from the solar resource and the combustion of fossil fuel to increase the temperature of pressurised air before introducing it into the gas turbine [76]. Typically, CSP is first used to preheat pressurised air from the compressor. This process is completed within a pressurised solar receiver, and the heated air is then passed into an after-burner (a combustion chamber). The after-burner provides heat to compensate for the periods where the solar resource is below its useful threshold [77]. In these hybrid CSP-gas turbine systems, the solar share increases with temperature of the pressurised air from the solar receiver. It was previously found that this type of system at large scales of 16MW manages to achieve a 16% annual solar share with an operating temperature of 800°C [78]. This value of

solar share will increase with operating temperature (if solar energy provides the heat required). Hence, the solar receiver is a key component of the hybrid system.

Several configurations of solar receivers for pressurised air have been proposed based on either direct or indirect heating. The direct heating method involves the heat from the absorber to be transferred to the pressurised gas directly, via a transparent window. This method enables the air to be heated to temperatures of up to 1300°C [79, 80] due to its high heat transfer rate [81]. However, the transparent window is vulnerable to high pressure and this vulnerability increases as the size of the window increases. It was also shown that the construction of the window requires special materials that can withstand high temperature fluctuations and stress, and this can subsequently increase cost [80, 82, 83]. For the indirect heating method, the window is replaced with a heat transfer medium. However, the heat transfer rate for this method is limited by the thermal conductivity of the selected medium. A 3kW high-temperature indirect pressurised air solar receiver that can achieve a thermal efficiency of 36% when operating at a pressure of 5 bars and temperature of around 1062°C was recently developed by Hischier et al [81]. The authors predicted that the thermal efficiency of the receiver will increase with temperature and scale, and reach up to 90% for a 200kW device. However, this concept has not yet been demonstrated commercially.

Furthermore, there has been limited research on methods to provide a constant heat source to a solar receiver in industrial applications, to address the issue of intermittency of solar power. A separate combustion system is usually used to provide heat during periods of low solar irradiance. It was previously shown that there is potential to lower the cost of CSP systems by combining the solar receiver with another heating source, such as combustion, into the same device [17, 84]. Hence, further evaluations are necessary to verify the potential benefits of these systems.

2.4.3 Hybrid CSP-combined cycle

Typically, in a hybrid CSP-combined cycle system, the heat from CSP is used to either heat pressurised gas in the gas turbine, or a heat source to the bottoming Rankine cycle. Oda and Hashem studied the use of the heat from CSP for feedwater preheating with a Rankine cycle, and an air heater solar receiver for a gas turbine [85]. They found that the cycles were limited to a 30% thermal efficiency. Price et al. studied a $30MW_e$ hybrid combined cycle power plant which uses heat from CSP that is transferred to a nitrate-salt as a HTF in a solar tower system [86]. This system also employs the use of a salt/air heat exchanger to heat pressurised air when the solar resource is above its useful threshold, with the system achieving a peak solar share of 27%. Allani, Favrat and Von proposed a hybrid combined cycle consisting of a solar field and a Rankine cycle plant that would also enable a higher thermodynamic efficiency as well as high CO_2 mitigation albeit higher cost of implementation [87]. Kribus et al. [88] performed an analysis on a solar-driven combined cycle plant consisting of both Rankine and Brayton cycles. They found that there is potential for a high performance coupled with low installation cost [88]. The results from their analysis show that for a large-scale combined cycle plant of 34MW, a solar capacity factor of 0.242 is achievable with a turbine inlet temperature of 1200°C. The calculated Levelised Cost of Electricity (LCOE) for this system was $0.067-0.078/kWh, 25% lower than that of the other conventional systems. In addition, Segal and Epstein studied a method to maximize the overall efficiency of three components in a hybrid CSP system, i.e. heliostat field and tower, the solar receiver and the power block [89]. They found that the efficiency of the system increases from ~35% to ~55% with an increase of temperature from ~730°C to ~1730°C. Additionally, Dunham and Lipinski studied the theoretical efficiency of both a single Brayton and a combined Brayton-Rankine power cycle to be used in a distributed-scale solar thermal power system and it was found that for applications that require low power, Brayton-Rankine systems performed better [90]. Li and Yang proposed an integrated solar

combined cycle with direct steam generation with two-stage solar input, increasing the solar share to 27% of the total power output and achieving a maximum thermal efficiency of 53% [91]. Although there have been many hybrid CSP-combined systems proposed, effort in the CSP community has now shifted away from combined cycles in recent times because of the high capital cost and poor suitability to intermittent operation.

In short, although there are numerous hybrid CSP-combustion technologies that are currently either under research and development stage or commercially deployed, there is still a need to identify cost reductions options while achieving a high solar share. Such cost reduction options may include combining different methods of hybridisation, or sharing infrastructure used for solar and combustion heating processes.

2.5 Challenges with current state-of-the-art CSP and hybrid CSP plants

Although both CSP and hybrid CSP plants have been in operation for many years, there are still numerous challenges associated with their operation. These challenges are classified into three different sections, namely; operational, financial and emissions from backup combustion systems.

2.5.1 Operational

Two major operational problems associated with CSP plants are high parasitic losses, and high fuel consumption from the backup combustion systems. Since one the current state-of-the-art HTF used in most plants is molten salt, due to reasons identified in Section 2.3.1, it is important to maintain the temperature of the salt above its freezing point of ~240°C [12, 16, 92]. This is usually done with an electrical trace heating system, which brings significant challenges [93-96]. Firstly, this system can consume a significant fraction of the total power produced if not properly managed [94]. This is further highlighted when non-uniform heating of the pipes during installation of the Solar Two project led to a five-month delay and resulted in

unnecessary expenditure due to the need to reinstall the entire electrical trace heating system [16]. Hence, there is a need to reduce these losses to derive further economic benefit from both CSP and hybrid CSP systems.

Another limitation with current hybrid CSP systems is the losses due to the start-up and shutdown of a conventional backup boiler. For a conventional hybrid CSP system with a backup boiler, it is necessary to operate the boiler in "stand-by" mode for periods. To do this, the boiler needs to be maintained at a sufficiently high temperature to allow it to be brought online either during periods of low solar insolation, or when power from the thermal storage medium is unavailable. This results in additional fuel consumption due to start-up and shut-down losses during transitions between solar-only and combustion-only modes of operation. Additionally, a conventional boiler is limited by its minimum capacity in which it needs to operate, with a turndown ratio of maximum to minimum throughput being between 3 to 4 [97]. Moreover, the boiler's operation is limited by the maximum admissible thermal stress for the walls of its components and any violations of these limits can potentially reduce the life-time of each component [98]. These limitations associated with the use of a conventional boiler as a backup to a CSP plant result in the need for an alternative method of hybridisation of a CSP system.

2.5.2 Financial

The high capital cost of CSP systems is a significant barrier to their penetration in the current renewable energy market [8]. Wustenhagen and Menichetti previously demonstrated that the financial risk to investors increase with the capital cost of a renewable energy system [60]. Additionally, subsidies introduced by the government, such as renewable energy certificates, and/or carbon taxes fail to fully mitigate long term financial risks because they are vulnerable to changes in government policy [99]. To a certain extent, hybrid CSP-fossil fuel systems

reduce these risks due to the lower cost of fossil fuels relative to CSP, but further approaches to lower the overall capital cost of these systems are required.

A concept recently proposed to lower the capital cost of hybrid CSP systems is the modularisation of selected components in a power plant [19]. This concept is driven by the potential to lower the cost of the modularised components by mass production at a smaller scale. Other advantages are claimed with the use of lower-cost materials [18] which offer the potential to reduce the system's overall LCOE. Furthermore, modular systems allow cash-flow to be generated in stages because the power plant can be constructed in stages [100]. Nonetheless, these potential advantages must be compared with the disadvantages of employing modular systems, i.e. higher operation and maintenance costs and increased thermal and parasitic losses (due to a higher surface area to volume ratio). To the knowledge of the author, both the economic benefit and the trade-off between the advantages and disadvantages of the concept of modularisation are yet to be assessed.

2.5.3 Pollutant emissions from backup combustion systems

To provide a continuous supply of electricity, CSP plants are often coupled with a backup fossil-fuelled combustion system. The disadvantage of these systems is the generation of a significant amount of greenhouse gas and NO_x emissions from the combustion of fossil fuels [101, 102]. This is because most of the large scale systems use fossil fuel combustion processes which are known to produce pollutants such as SO_x, NO_x and particulates [103]. It was previously found that the key parameters influencing the volume of these emissions are the flame temperature, residence time of hot gases in the flame and the total oxygen concentration in the flame [103]. It is important to note that these parameters are both interdependent and plant specific. Several research groups have been developing technologies to lower combustion

pollutant emissions by controlling these parameters [102-105]. Such technologies include oxy-fuel combustion and Moderate Intense Low-oxygen Dilution (MILD) combustion.

Oxy-fuel combustion involves combining high concentrations of oxygen (usually of greater than 95% purity) and recycled flue gas during the combustion of fuel [105]. The recycled flue gas is used to control the flame temperature in the boiler and compensates for the missing N_2 that usually carries the heat through the boiler. Oxy-fuel combustion typically uses coal, although other fuels have also been considered. The temperature of the flame is usually higher than that of conventional combustion due to the lack of N_2 dilution [105]. Another low emission technology that has been proposed is Moderate or Intense Low-oxygen Dilution (MILD) combustion, a rapidly developing technology, based on the principles of heat and flue gas recirculation [104, 106-108]. MILD combustion involves exhaust gas and heat recirculation at above auto-ignition temperature which results in a volumetric reaction at moderate temperatures. This combustion technology operates with a range of different fuels, usually producing a lower temperature flame relative to conventional combustion due to the dilution of the combustion air [101]. Research has shown that the net radiation flux from such combustion mode is higher than conventional combustion despite the lower maximum temperature of the gases inside the boiler or furnace. It has also been shown that both oxy-fuel and MILD combustion offers many significant potential benefits over conventional combustion [104, 109]. These advantages include ultra-low pollutant emissions with a reduction in NO_x emissions of up to 70% relative to conventional combustion and high thermal efficiency. MILD combustion also offers an increased thermal field uniformity and enhanced combustion stability. Compared with oxy-fuel combustion, the MILD combustion technology does not require an extra air separation unit or the use of a pure oxygen stream, which will increase the overall cost of the system [110]. Therefore, to reap further benefits from using renewable energy, in particular, low carbon and NO_x emissions, while providing a firm supply of

electricity, it is necessary to integrate low emissions technologies, e.g. MILD combustion, into hybrid CSP-combustion systems.

2.6 Hybrid Solar Receiver Combustor

The concept of a Hybrid Solar Receiver Combustor (HSRC), where a solar cavity receiver and a combustor are integrated into a single tubular device, was proposed by Nathan et al [17, 111]. This concept seeks to combine the infrastructure used to collect the heat from both solar radiation and combustion. This is because the heat of combustion is best collected in a single, central device, both to capitalize on economies of scale and to minimize heat losses [17]. Kolb has previously identified the economic benefit of sharing infrastructure, i.e. the condenser and turbine, in a power plant [112]. He showed that the cost of the solar component of energy can potentially be reduced by up to 50% compared with standalone plants by combining the infrastructure. In addition, Mehos et al. proposed a hybrid device where a combustor is mounted behind a receiver cavity with separate chambers for each component [84]. However, this device has separate chambers for the solar receiver and the combustor. Hence, to the knowledge of the author, the only device that fully integrates a combustor into a solar receiver is the HSRC.

The HSRC concept is novel and is based on a device that operates as a CSP receiver with a combustor that shares the same heat exchange surface. Sharing the same heat exchange surface enables lower heat convection and thermal radiation losses throughout the entire device. This increases the thermal efficiency of the device. In addition, the device also takes advantage of economy of scale, especially when mounted on a solar power tower [17]. At times where solar power is unavailable or below its useful threshold, the combustor will be used to supply heat to the same chamber as that of the solar receiver. This is advantageous because for a conventional solar power tower system, a minimum threshold of intensity is required to heat

the HTF to a high enough temperature before the heat from the fluid can be utilised. The combustor will provide the heat required to raise the temperature of the HTF to its operating temperature. The HSRC is proposed to operate in three modes, namely, Solar-Only, Combustion-Only and Mixed-mode where both CSP and combustion are introduced simultaneously into the device.

An evaluation has previously been performed to determine the economic benefits of implementing the device as part of an electricity generating system. Previous results suggest that the HSRC offers potential advantages over other equivalent configurations of proposed hybrid systems and stand-alone solar power towers [17]. The advantages, relative to other hybrid systems, include a potential decrease of 24% in the overall Levelised Cost of Electricity (LCOE) and a reduction of the overall capital cost by 51% compared with its equivalent hybrid for a system size of $100MW_e$. However, all the calculations assumed that the HSRC is capable of achieving similar combustion efficiency as a regular gas boiler for two times the capital cost of a solar receiver. Additionally, the analysis also assumed, both, the annual capacity factor and the start-up and shut-down times of the HSRC. Further, the previous estimates were based only on average performance and did not account for the dynamic variability of the solar resource. A more detailed analysis is therefore required, to calculate these parameters, i.e. efficiency, capacity factor, and start-up and shut-down times of the HSRC. As the previous model did not account for variability in solar radiation flux, it is necessary to develop a more accurate model to utilise historical time-series of the solar resource. Moreover, no detailed design procedure is available that calculates dimensions or cost as a function of design specification.

The current configuration of the HSRC employs the use of a conventional flame in both Combustion-Only mode and Mixed-mode of operation [111]. This method of combustion is currently state-of-the-art and is used in most combustion technologies. However, the use of a

conventional flame generally produces high CO_2 and NO_x emissions, which are the leading causes of global warming and ozone layer destruction, respectively [113]. Therefore, research into approaches to lower these emissions have been the focus in recent times [106-108, 113]. A potential approach to address this limitation for the case of the HSRC is to integrate MILD combustion into the device because of the reasons described in Section 2.5.3. MILD combustion is also more suited to the HSRC relative to other low NO_x combustion technologies (such as oxy-fuel combustion) because it operates with a lower temperature that will not limit the type of HTF utilised in the device (some HTFs will decompose at high temperatures). Also, operating in the MILD combustion regime does not require the use of additional components such as an air separation unit, required for oxy-combustion. MILD combustion also typically operates with a gaseous fuel, which is desirable as the fuel needs to be pumped up a tall tower (operating with a liquid or solid fuel will no doubt increase the associated parasitic pumping losses). Therefore, there is a need to identify configurations of the HSRC to meet the parameters required to achieve the MILD combustion regime. The economic trade-off between this new configuration and the original concept, in addition to other hybrid CSP-combustion systems also requires significant consideration.

2.7 Levelized Cost of Electricity

The Levelized Cost of Electricity (LCOE) is typically used to estimate the cost of electricity generation from an electrical power generating system [7]. The LCOE of a system considers the capital cost of the plant and ongoing costs such as Operation and Maintenance (O&M), fuel, decommissioning and carbon emissions [114]. It also accounts for financial parameters e.g. Internal Rate of Return or Discount factors. The value of LCOE for a power plant is usually expressed in terms of $/MWh [27]. Noteworthy, is that there are many methods to obtain the inputs required to calculate the LCOE of a power generating system. These inputs also typically vary with different conditions such as location, climate, fuel cost etc. [17]. Therefore, when

performing a comparison between different types of technologies, it is necessary to use consistent cost correlations and financial parameters. To estimate the benefits of the integration of a solar cavity receiver and a gas boiler (HSRC technology) requires the LCOE of the system to be calculated relative to an equivalent system using consistent inputs to avoid the challenge of obtaining absolute values for a particular location.

2.8 Summary of literature review and gaps

To summarize, there is a need to identify methods to lower the capital cost and increase the solar share of CSP/hybrid-CSP systems, in particular, those employing Central Receiver systems to harness solar energy. One of the potential methods to improve the efficiency of Central Receiver systems is to employ the use of cavity receivers that are mounted on top of the towers, which needs to be assessed further. In addition, despite an increasing number of research projects on hybrid CSP-combustion technologies, there has been little focus on the benefits of sharing the same infrastructure for CSP and combustion processes. The HSRC has been shown to offer many potential advantages over its equivalent standalone system, but assumptions from previous studies need to be justified to improve the overall accuracy of the analysis. Therefore, this project aims to reduce the uncertainties of the previous assumptions, and to further the development of the HSRC technology by also incorporating MILD combustion technology into the device. In addition, the project also aims to identify and assess other cost-effective approaches to hybridization of CSP systems, such as the concept of modularisation of selected components in the power plant.

References

1. Hinkley, J., et al., *Concentrating solar power–drivers and opportunities for cost-competitive electricity.* Clayton South: CSIRO, 2011.
2. Liu, M., et al., *Review on concentrating solar power plants and new developments in high temperature thermal energy storage technologies.* Renewable and Sustainable Energy Reviews, 2016. **53**: p. 1411-1432.
3. Pool, S. and J. Dos Passos Coggin, *Fulfilling the Promise of Concentrating Solar Power*, S. Progress, Editor. 2013.
4. Clean Energy Council, *Concentrated solar thermal energy fact sheet*. 2012.
5. Lovegrove, K. and M. Dennis, *Solar thermal energy systems in Australia.* International Journal of Environmental Studies, 2006. **63**(6): p. 791-802.
6. Boisgibault, L. *COP21 objectives: towards a joint energy transition in the Mediterranean?* in *COP21*. 2015. IPEMED.
7. Lovegrove, K., et al., *Realising the potential of concentrated solar power in Australia*. 2012.
8. IRENA, I., *Renewable energy technologies: Cost analysis series*, in *Concentrating solar power*. 2012.
9. Richter, C., S. Teske, and R. Short, *Concentrating Solar Power Global Outlook 09*, R. Short and T. Writer, Editors. 2009.
10. International Renewable Energy Agency, *Concentrating Solar Power*. 2013.
11. Kalogirou, S.A., *Solar energy engineering: processes and systems*. 2013: Academic Press.
12. Behar, O., A. Khellaf, and K. Mohammedi, *A review of studies on central receiver solar thermal power plants.* Renewable and Sustainable Energy Reviews, 2013. **23**: p. 12-39.
13. Tian, Y. and C.Y. Zhao, *A review of solar collectors and thermal energy storage in solar thermal applications.* Applied Energy, 2013. **104**: p. 538-553.
14. Sargent & Lundy LLC Consulting Group, *Assessment of Parabolic Trough and Power Tower Solar Technology Cost and Performance Forecasts*. 2003, NREL: Chicago, Illinois.
15. Romero, M. and J. González-Aguilar, *Solar thermal CSP technology*. Wiley Interdisciplinary Reviews: Energy and Environment, 2014. **3**(1): p. 42-59.
16. Reilly, H.E. and G.J. Kolb, *An evaluation of molten-salt towers including results of the solar two project*. 2001: Albuquerque, New Mexico.
17. Nathan, G.J., D.L. Battye, and P.J. Ashman, *Economic evaluation of a novel fuel-saver hybrid combining a solar receiver with a combustor for a solar power tower.* Applied Energy, 2014. **113**: p. 1235-1243.
18. Vast Solar, *Dissemination Report: Heliostat Field and High Temperature Receiver Development*. 2014.
19. Fisher, J., *Low cost, high efficiency, dispatchable concentrated solar thermal power (CSP).* 2015, Vast Solar.
20. Kearney, A. and ESTELA, *Solar thermal electricity 2025*. 2010: Brussels.
21. Hachicha, A.A., et al., *Heat transfer analysis and numerical simulation of a parabolic trough solar collector.* Applied Energy, 2013. **111**: p. 581-592.
22. Mancini, T., et al., *Dish-Stirling systems: An overview of development and status.* Journal of Solar Energy Engineering, 2003. **125**(2): p. 135-151.
23. Stine, W.B. and R.B. Diver, *A compendium of solar dish/Stirling technology*. 1994, DTIC Document.
24. Keck, T. and W. Schiel. *EnviroDish and EuroDish System and Status*. in *Proceedings of ISES Solar World Congress*. 2003.

25. Lopez, C.W. and K.W. Stone. *Design and performance of the Southern California Edison Stirling dish*. in *Solar Engineering, Proc. of ASME Int. Solar Energy Conf*. 1992.
26. Fath, H.E.S., *Technical assessment of solar thermal energy storage technologies.* Renewable Energy, 1998. **14**(1-4): p. 35-40.
27. Wagner, S.J. and E.S. Rubin, *Economic implications of thermal energy storage for concentrated solar thermal power.* 2012.
28. Medrano, M., et al., *State of the art on high-temperature thermal energy storage for power generation. Part 2-Case studies.* Renewable and Sustainable Energy Reviews, 2010. **14**(1): p. 56-72.
29. Yilmazoglu, M.Z., *Effects of the selection of heat transfer fluid and condenser type on the performance of a solar thermal power plant with technoeconomic approach.* Energy Conversion and Management, 2016. **111**: p. 271-278.
30. Becker, M., *Comparison of heat transfer fluids for use in solar thermal power stations.* Electric Power Systems Research, 1980. **3**(3): p. 139-150.
31. Wyman, C., J. Castle, and F. Kreith, *A review of collector and energy storage technology for intermediate temperature applications.* Solar Energy, 1980. **24**.
32. Vignarooban, K., et al., *Heat transfer fluids for concentrating solar power systems – A review.* Applied Energy, 2015. **146**(0): p. 383-396.
33. Frazer, D., et al., *Liquid Metal as a Heat Transport Fluid for Thermal Solar Power Applications.* Energy Procedia, 2014. **49**: p. 627-636.
34. Sohal, M.S., et al., *Engineering Database of Liquid Salt Thermophysical and Thermochemical Properties*. 2010, Idaho National Laboratory. p. 2.
35. Kolb, G.J., *An evaluation of possible next-generation high-temperature molten-salt power towers.* Sandia National Laboratories, Albuquerque, NM, Report No. SAND2011-9320, 2011.
36. Herrmann, U., B. Kelly, and H. Price, *Two-tank molten salt storage for parabolic trough solar power plants.* Energy, 2004. **29**(5-6): p. 883-893.
37. Boerema, N., et al., *Liquid sodium versus Hitec as a heat transfer fluid in solar thermal central receiver systems.* Solar Energy, 2012. **86**(9): p. 2293-2305.
38. Pacio, J., et al., *Thermodynamic evaluation of liquid metals as heat transfer fluids in concentrated solar power plants.* Applied Thermal Engineering, 2013. **60**(1–2): p. 295-302.
39. Benoit, H., et al., *Review of heat transfer fluids in tube-receivers used in concentrating solar thermal systems: Properties and heat transfer coefficients.* Renewable and Sustainable Energy Reviews, 2016. **55**: p. 298-315.
40. Dunn, R.I., P.J. Hearps, and M.N. Wright, *Molten-salt power towers: newly commercial concentrating solar storage.* Proceedings of the IEEE, 2012. **100**(2): p. 504-515.
41. Pacio, J., et al., *Liquid Metals as Efficient Coolants for High-intensity Point-focus Receivers: Implications to the Design and Performance of Next-generation CSP Systems.* Energy Procedia, 2014. **49**: p. 647-655.
42. Fernández, A.G., et al., *Corrosion of alumina-forming austenitic steel in molten nitrate salts by gravimetric analysis and impedance spectroscopy.* Materials and Corrosion, 2014. **65**(3): p. 267-275.
43. Bartos, N. and J. Fisher. *Experiences from using molten sodium metal as a heat transfer fluid in concentrating solar thermal power systems*. in *Asia-Pacific Solar Research Conference*. 2015. Queensland.
44. Coventry, J., et al., *Sodium receivers for solar power towers: a review*, in *Energy Procedia*. 2015.

45. Glatzmaier, G., *Summary Report for Concentrating Solar Power Thermal Storage Workshop: New Concepts and Materials for Thermal Energy Storage and Heat-Transfer Fluids, May 20, 2011*. 2011, National Renewable Energy Laboratory (NREL), Golden, CO.
46. Gil, A., et al., *State of the art on high temperature thermal energy storage for power generation. Part 1-Concepts, materials and modellization.* Renewable and Sustainable Energy Reviews, 2010. **14**(1): p. 31-55.
47. Prieto, C., et al., *Review of technology: Thermochemical energy storage for concentrated solar power plants.* Renewable and Sustainable Energy Reviews, 2016. **60**: p. 909-929.
48. Harries, D.N., et al., *Concentrating solar thermal heat storage using metal hydrides.* Proceedings of the IEEE, 2012. **100**(2): p. 539-549.
49. Kodama, T. and N. Gokon, *Thermochemical cycles for high-temperature solar hydrogen production.* Chemical reviews, 2007. **107**(10): p. 4048-4077.
50. Tescari, S., et al., *Design of a thermochemical storage system for air-operated solar tower power plants.* Energy Procedia, 2015. **69**: p. 1039-1048.
51. Lovegrove, K., et al., *Developing ammonia based thermochemical energy storage for dish power plants.* Solar Energy, 2004. **76**(1): p. 331-337.
52. Lovegrove, K., A. Luzzi, and H. Kreetz, *A solar-driven ammonia-based thermochemical energy storage system.* Solar Energy, 1999. **67**(4): p. 309-316.
53. Dunn, R., K. Lovegrove, and G. Burgess, *A review of ammonia-based thermochemical energy storage for concentrating solar power.* Proceedings of the IEEE, 2012. **100**(2): p. 391-400.
54. Samms, J. and B. Evans, *Thermal dissociation of Ca (OH) 2 at elevated pressures.* Journal of Applied Chemistry, 1968. **18**(1): p. 5-8.
55. Schmidt, P., *On the design of a reactor for high temperature heat storage by means of reversible chemical reactions.* 2011.
56. Fedders, H. and B. Höhlein, *Operating a pilot plant circuit for energy transport with hydrogen-rich gas.* International Journal of Hydrogen Energy, 1982. **7**(10): p. 793-800.
57. Kueh, K.C., G.J. Nathan, and W.L. Saw, *Storage capacities required for a solar thermal plant to avoid unscheduled reductions in output.* Solar Energy, 2015. **118**: p. 209-221.
58. Zhang, H.L., et al., *Concentrated solar power plants: Review and design methodology.* Renewable and Sustainable Energy Reviews, 2013. **22**: p. 466-481.
59. Williams, T.A., M.S. Bohn, and H.W. Price, *Solar thermal electric hybridization issues*. 1994. Medium: ED; Size: 9 p.
60. Wüstenhagen, R. and E. Menichetti, *Strategic choices for renewable energy investment: Conceptual framework and opportunities for further research.* Energy Policy, 2012. **40**: p. 1-10.
61. Philibert, C., *The present and future use of solar thermal energy as a primary source of energy.* International Energy Agency, Paris, France, 2005.
62. Mills, A.F. and V. Ganesan, *Heat Transfer*. 2nd ed. 1999: Pearson Education.
63. Moore, J. and J. Apt, *Can hybrid solar-fossil power plants mitigate CO2 at lower cost than PV or CSP?* Environmental Science and Technology, 2013. **47**(6): p. 2487-2493.
64. Zoschak, R.J. and S.F. Wu, *Studies of the Direct Input of Solar Energy to a Fosil-Fuelled Central Station Steam Power Plant.* Solar Energy, 1975. **17**(5): p. 297-305.
65. Pai, B.R., *Augmentation of thermal power stations with solar energy.* Sadhana, 1991. **16**(1): p. 59-74.
66. Deng, S., *Hybrid Solar and Coal-Fired Steam Power Plant Based on Air Preheating.* Journal of Solar Energy Engineering, 2014. **136**(2): p. 021012.

67. Ying, Y. and E.J. Hu, *Thermodynamic advantages of using solar energy in the regenerative Rankine power plant.* Applied Thermal Engineering, 1999. **19**(11): p. 1173-1180.
68. Yang, D. and T. Chen, *HGSSP - A computer program for simulation of once-through boiler start-up behavior.* Heat Transfer Engineering, 2001. **22**(5): p. 50-60.
69. You, Y. and E.J. Hu, *A medium-temperature solar thermal power system and its efficiency optimisation.* Applied Thermal Engineering, 2002. **22**(4): p. 357-364.
70. Eck, M., et al., *Applied research concerning the direct steam generation in parabolic troughs.* Solar Energy, 2003. **74**(4): p. 341-351.
71. Krüger, D., et al., *Experiences with direct steam generation at the Kanchanaburi solar thermal power plant.* 2012.
72. Yan, Q., et al., *Evaluation of solar aided thermal power generation with various power plants.* International Journal of Energy Research, 2011. **35**(10): p. 909-922.
73. Odeh, S.D., M. Behnia, and G.L. Morrison, *Performance evaluation of solar thermal electric generation systems.* Energy Conversion and Management, 2003. **44**(15): p. 2425-2443.
74. Popov, D., *An option for solar thermal repowering of fossil fuel fired power plants.* Solar Energy, 2011. **85**(2): p. 344-349.
75. Meehan, R. and M. Rudge, *Hybridisation of Fossil Fuel Energy Generation in Australia*, in *Public Report, November*. 2013.
76. Schwarzbözl, P., et al., *Solar gas turbine systems: Design, cost and perspectives.* Solar Energy, 2006. **80**(10): p. 1231-1240.
77. Barigozzi, G., et al., *Thermal performance prediction of a solar hybrid gas turbine.* Solar Energy, 2012. **86**(7): p. 2116-2127.
78. European Comission, *SOLGATE - Solar hybrid gas turbine electric power system*. 2005.
79. Karni, J., et al., *The DIAPR: a high-pressure, high-temperature solar receiver.* Journal of solar energy engineering, 1997. **119**(1): p. 74-78.
80. Pritzkow, W.E., *Pressure loaded volumetric ceramic receiver.* Solar energy materials, 1991. **24**(1): p. 498-507.
81. Hischier, I., *Development of a pressurized receiver for solar-driven gas turbines*. 2011, Diss., Eidgenössische Technische Hochschule ETH Zürich, Nr. 19723, 2011.
82. Posnansky, M. and T. Pylkkänen, *Development and testing of a volumetric gas receiver for high-temperature applications.* Solar energy materials, 1991. **24**(1-4): p. 204-209.
83. Avila-Marin, A.L., *Volumetric receivers in solar thermal power plants with central receiver system technology: a review.* Solar Energy, 2011. **85**(5): p. 891-910.
84. Mehos, M.S., et al., *Combustion system for hybrid solar fuel receiver*. 2004: United States.
85. Oda, S.D. and H.H. Hashem, *A case study for three combined cycles of a solar-conventional power generation unit.* Solar & wind technology, 1988. **5**(3): p. 263-270.
86. Price, H.W., D.D. Whitney, and H. Beebe, *SMUD Kokhala power tower study*. 1997, National Renewable Energy Laboratory, Golden, CO (United States).
87. Allani, Y., D. Favrat, and S.M.R. Von, *CO2 mitigation through the use of hybrid solar-combined cycles.* Energy Conversion and Management, 1997. **38**(9999): p. S661-S667.
88. Kribus, A., et al., *A solar-driven combined cycle power plant.* Solar Energy, 1998. **62**(2): p. 121-129.
89. Segal, A. and M. Epstein, *Optimized working temperatures of a solar central receiver.* Solar Energy, 2003. **75**(6): p. 503-510.

90. Dunham, M.T. and W. Lipinski, *Thermodynamic analyses of single brayton and combined brayton-rankine cycles for distributed solar thermal power generation.* Journal of Solar Energy Engineering, Transactions of the ASME, 2013. **135**(3).
91. Li, Y. and Y. Yang, *Thermodynamic analysis of a novel integrated solar combined cycle.* Applied Energy, 2014. **122**: p. 133-142.
92. Rodriguez-Garcia, M.-M., M. Herrador-Moreno, and E. Zarza Moya, *Lessons learnt during the design, construction and start-up phase of a molten salt testing facility.* Applied Thermal Engineering, 2014. **62**(2): p. 520-528.
93. Pacheco, J.E., et al., *SUMMARY OF THE SOLAR TWO TEST AND EVALUATION PROGRAM.* 2000.
94. Pacheco, J.E., *A nightly conditioning method to reduce parasitic power consumption in molten-salt central-receiver solar-power plants*. 1995, Sandia National Labs., Albuquerque, NM (United States).
95. Kearney, D., et al., *Engineering aspects of a molten salt heat transfer fluid in a trough solar field.* Energy, 2004. **29**(5–6): p. 861-870.
96. Kearney, D., et al., *Assessment of a Molten Salt Heat Transfer Fluid in a Parabolic Trough Solar Field.* Journal of Solar Energy Engineering, 2003. **125**(2): p. 170-176.
97. Eoff, D., *Understanding Fuel Savings In the Boiler Room.* ASHRAE Journal, 2008. **50**(12): p. 38-43.
98. Kruger, K., R. Franke, and M. Rode. *Optimization of boiler start-up using a nonlinear boiler model and hard constraints*. 2004. Elsevier Ltd.
99. Wohlgemuth, N. and R. Madlener. *Financial support of renewable energy systems: investment vs operating cost subsidies*. in *NAEE Conference" Towards an Integrated European Energy Market", Bergen, Norway*. 2000.
100. Johansson, T.B., *Renewable energy: sources for fuels and electricity*. 1993: Island press.
101. Tsuji, H., et al., *High Temperature Air Combustion*. 2003, Boca Paton: CRC Press.
102. Baukal Jr, C.E., *Heat Transfer*, in *The John Zink Combustion Handbook*. 2001, John Zink Company LLC. p. 106.
103. Jenkins, B. and P. Mullinger, *Industrial and Process Furnaces*. 2008: Butterworth Heinemann. 544.
104. Cavaliere, A. and M. de Joannon, *Mild Combustion.* Progress in Energy and Combustion Science, 2004. **30**(4): p. 329-366.
105. Wall, T., et al., *An overview on oxyfuel coal combustion—State of the art research and technology development.* Chemical Engineering Research and Design, 2009. **87**(8): p. 1003-1016.
106. Sabia, P., et al., *Dynamic Behaviors in Methane MILD and Oxy-Fuel Combustion. Chemical Effect of CO2.* Energy & Fuels, 2015. **29**(3): p. 1978-1986.
107. Sabia, P., et al., *Modeling Negative Temperature Coefficient region in methane oxidation.* Fuel, 2012. **91**(1): p. 238-245.
108. De Joannon, M., et al., *Optimal post-combustion conditions for the purification of CO 2-rich exhaust streams from non-condensable reactive species.* Chemical Engineering Journal, 2012. **211**: p. 318-326.
109. Li, P.F., et al., *Progress and recent trend in MILD combustion.* Science China Technological Sciences, 2011. **54**(2): p. 255-269.
110. Toftegaard, M.B., et al., *Oxy-fuel combustion of solid fuels.* Progress in Energy and Combustion Science, 2010. **36**(5): p. 581-625.
111. Nathan, G.J., et al., *A Hybrid Receiver-Combustor*, A.R.I.P. Ltd, Editor. 2013.
112. Kolb, G.J., *Economic evaluation of solar-only and hybrid power towers using molten-salt technology.* Solar Energy, 1998. **62**(1): p. 51-61.

113. Rafidi, N., W. Blasiak, and A.K. Gupta, *High-temperature air combustion phenomena and its thermodynamics.* Journal of Engineering for Gas Turbines and Power, 2008. **130**(2).
114. International Energy Agency and OECD Nuclear Energy Agency, *Projected Costs of Generating Electricity*. 2010.

Statement of Authorship

Title of Paper	Analytical assessment of a novel hybrid solar tubular receiver and combustor
Publication Status	☑ Published ☐ Accepted for Publication ☐ Submitted for Publication ☐ Unpublished and Unsubmitted w ork w ritten in manuscript style
Publication Details	Lim, JH, Nathan, GJ, Hu, E & Dally, BB 2016, 'Analytical assessment of a novel hybrid solar tubular receiver and combustor', Applied Energy, vol. 162, pp. 298-307.

Principal Author

Name of Principal Author (Candidate)	Jin Han Lim		
Contribution to the Paper	Performed the literature review. Wrote the manuscript. Developed the analytical model required for analysis. Took primary responsibility for responding to the reviewers.		
Overall percentage (%)	60		
Certification:	This paper reports on original research I conducted during the period of my Higher Degree by Research candidature and is not subject to any obligations or contractual agreements with a third party that would constrain its inclusion in this thesis. I am the primary author of this paper.		
Signature		Date	18/7/16

Co-Author Contributions

By signing the Statement of Authorship, each author certifies that:

i. the candidate's stated contribution to the publication is accurate (as detailed above);

ii. permission is granted for the candidate in include the publication in the thesis; and

iii. the sum of all co-author contributions is equal to 100% less the candidate's stated contribution.

Name of Co-Author	Professor Graham Nathan		
Contribution to the Paper	Supervised the work done. Suggested different approaches to analytical modelling. Suggested methods for validation and verification of model developed. Assisted with editing the manuscript.		
Signature		Date	19/7/16

Name of Co-Author	Associate Professor Eric Hu		
Contribution to the Paper	Supervised the work done. Provided assistance in developing analytical model. Assisted with editing the manuscript.		
Signature		Date	19/7/2016

Name of Co-Author	Professor Bassam Dally		
Contribution to the Paper	Supervised the work done. Assisted with editing the manuscript. Provided assistance with addressing comments from reviewers.		
Signature		Date	18/7/16

CHAPTER 3

ANALYTICAL ASSESSMENT OF A NOVEL HYBRID SOLAR TUBULAR RECEIVER AND COMBUSTOR

Applied Energy 162 (2016) 298–307

Contents lists available at ScienceDirect

Applied Energy

journal homepage: www.elsevier.com/locate/apenergy

Analytical assessment of a novel hybrid solar tubular receiver and combustor

Jin Han Lim *, Graham J. Nathan, Eric Hu, Bassam B. Dally

Centre for Energy Technology, School of Mechanical Engineering, The University of Adelaide, SA 5005, Australia

HIGHLIGHTS

- We present a novel hybrid between a solar cavity receiver and a combustor.
- The economic benefit of this integration is confirmed.
- The combustor can achieve the same efficiency as a conventional boiler.

ARTICLE INFO

Article history:
Received 3 April 2015
Received in revised form 6 October 2015
Accepted 7 October 2015

Keywords:
Concentrating solar-thermal
Hybrid Solar Receiver Combustor (HSRC)
Hybrid

ABSTRACT

This paper presents a novel hybrid between a tubular solar receiver and a combustor, called the Hybrid Solar Receiver Combustor (HSRC), and reports on the development and application of an analytical model to describe its performance. The analytical model accounts for the variability of the solar resource with a pseudo steady state balance of the mass and energy flow, which calculates the heat transfer throughout the device. A systematic investigation of the influence of variation in all controlling parameters on performance and weight is undertaken. The results provide new understanding of the performance of the device relative to the solar-only and combustion-only counterparts, and further justification for its ongoing development.

1. Introduction

The growth of the renewable energy sector has continued world-wide, driven by policies that seek to mitigate climate change, reduce air pollution, and access the growing market in this field, together with recognition of the finite reserves of fossil fuels. Among all renewable energy sources, solar energy is receiving particular attention because it is both clean and abundant [1]. Concentrating solar thermal, CSP, energy, currently has a lower penetration than solar photovoltaic, PV, but is undergoing rapid recent growth in the number and size of power plants being built worldwide [2]. However, in common with wind and solar PV, a key barrier to the ongoing growth in the penetration of CSP is the challenge associated with managing the intermittent and variable nature of the resource, which adds to the cost. One opportunity to mitigate this challenge is through the use of hybrid systems that combine fossil and renewable energy sources into one plant. The ready availability and stored chemical energy in fossil fuels especially, and biomass to a lesser extent, means that hybrid systems are expected to make an important contribution to the ongoing penetration of renewable energy [3]. In this regard, CSP is particularly well suited to hybridisation with combustion plants because the thermal nature of both types of technology makes them synergistic. However, nearly all previous reports of hybrid concepts between CSP and combustion employ standalone solar receivers and combustors, which are designed to run in a series or parallel, rather than to be directly integrated. To the best knowledge of the authors, while a few concepts of integrated systems have been proposed [4], none of these directly integrate a tubular solar receiver and a combustor. Furthermore none of them report any analysis of the effect of such integration on performance. Hence the overall aim of this assessment is to present and analyse the performance of a novel concept of hybrid between a solar receiver and a combustor that seeks to harness the energy from both sources in a single device.

The device used to harness the concentrated solar radiation is called a solar receiver. Of the wide range of solar receivers that have been developed, the vast majority heat the medium indirectly through tubes. These tubular receivers can be used to heat either the working fluid (e.g. steam), or a heat transfer fluid, HTF, which can also provide thermal storage, such as a molten salt. Tubular

* Corresponding author. Tel.: +61 425748780.
E-mail address: jin.lim@adelaide.edu.au (J.H. Lim).

http://dx.doi.org/10.1016/j.apenergy.2015.10.048
0306-2619/

Nomenclature

$(GS_1)_R$	total exchange area between combustion gases and receiver tubes (m^2)
$\dot{V}$	volumetric flow rate (m^3/s)
A	area (m^2)
C	heat capacity rate (W/K)
c_p	specific heat capacity (J/kg K)
C_s	cold surface fraction
D_c	diameter of cavity (m)
f	friction factor
h	heat transfer coefficient (W/m^2 K)
L_c	length of cavity (m)
$\dot{m}$	mass flow rate (kg/s)
OD	outer diameter (m)
P	pressure (Pa)
Pr	Prandtl number
$\dot{Q}$	heat transfer rate (W)
Re	Reynolds number
T	temperature (°C)
U	overall heat transfer coefficient (W/m^2 K)
u	specific internal energy (kJ/kg)
u_m	mean velocity (m/s)
$\dot{W}$	electric power (W)

Greek symbols

ε	emissivity
η	efficiency
ρ	density
σ	Stefan–Boltzmann constant

Abbreviations

CPC	compound parabolic concentrator
CSR	concentrated solar radiation
CSP	concentrating solar power
EPGS	electricity power generating system
HSRC	Hybrid Solar Receiver Combustor
HTF	heat transfer fluid
HX	heat exchanger
HXT	heat exchanger tube
LCE	levelized cost of electricity
LHV	lower heating value
MSEE	molten salt electric experiment
PV	photovoltaic
RT	receiver tube

Subscripts

ap	aperture
c	cold
comb	combustion
conv	convection
elec	electric
h	hot
int	internal
noz	nozzle opening
rad	radiation
s	surface
sec	secondary
th	thermal

receivers offer both advantages and disadvantages over direct heat-transfer receivers, such as the particle vortex reactor of Z'Graggen et al. [5]. Other devices include volumetric receivers, typically used to heat air for a Brayton cycle, although these suffer the disadvantage of requiring a window if the air is to be pressurised before heating [5]. The advantages of mechanical robustness and relative ease of sealing typically outweigh the disadvantage of a lower exergetic efficiency and a lower maximum operating temperature, which is limited by the temperature of the tubes [6,7], under current conditions. In addition, while tubular receivers are most commonly employed for Rankine cycles at present, they are also applicable to other power cycles, such as supercritical CO_2 and to high temperature reactors [6,8]. Hence, there is an ongoing need to continue to develop tubular receivers.

There are many drivers to hybridise solar energy with combustion technologies. The current cost of implementing a solar-only system would require an unreasonably large amount of storage to meet 100% of electricity demand at any site [9]. This is, in part, because although thermal storage is currently among the lowest cost of energy storage technology, it nevertheless remains expensive with a current price of US$90/kW h_{th}, although this price is expected to decrease to US$22/kW h_{th} by 2020 [10]. In contrast, the current price of fossil fuelled electricity is presently significantly lower than that of grid-connected solar only power plants (presently ~US$0.06/kW h in USA from natural gas compared with a projected cost of ~US$0.14/kW h for solar power towers [11]). To address this issue, Kolb identified certain configurations of CSP hybrids, with Rankine cycle boilers that are economically beneficial [12]. Ying and Hu proved that a highly thermodynamically efficient way to utilise low-grade solar thermal heat is to pre-heat feedwater in a regenerative Rankine cycle boiler [13]. Yang et al. [14] also demonstrated that medium to low temperatures from solar energy could be used in regular coal-fired plants to generate electricity efficiently. Similarly, Zoschak and Wu found that an instantaneous fraction defined as the ratio of the solar energy input to the total input energy, of 0.27 could be achieved in a fossil fuelled steam powered plant through feedwater heating, steam superheating, air preheating and/or water evaporation [15]. However, the intermittent nature of the resource means that the average solar fraction is typically around 0.05. A range of investigations have found that the use of CSP to heat the feedwater of a Rankine cycle with a combined cycle can lower costs of CO_2 mitigation relative to stand-alone CSP [16,17]. However, of all these processes that employ solar tubular receivers and combustion boilers, none of them report any assessment of the potential benefits of directly integrating the solar receiver with a combustor.

CSP is particularly well suited to hybridisation with combustion technology, since both employ thermal power systems. CSP is receiving growing interest due to its potential to achieve energy storage at a relatively low cost and high efficiency [18]. Solar Power Towers are particularly well suited because their high concentration ratio allows them to achieve higher temperatures than parabolic troughs [9], while their larger scale compared to dishes leads to lower surface-area to volume ratio, and hence lower heat losses. Towers are also considered to have greater long-term potential owing to their higher efficiency than troughs [9] and greater potential to achieve economy of scale [18]. Hence, it is highly desirable to develop hybrids with the tower system.

Nathan et al. [19] first proposed the concept of directly integrating the functions of both a solar-receiver and a combustor into a Solar Power Tower system, or on the ground surrounded by a heliostat field with a beam-down configuration. The integration of a solar cavity receiver and a combustor is known to yield the following benefits [19]:

- Eliminating the boiler as a separate component, reducing the total heat-exchange area and heat losses. This also reduces the capital cost.
- The Hybrid Solar Receiver Combustor, HSRC, reduces energy losses as it avoids start-up and shut-down if a small thermal storage unit is used.
- The device also allows for more Concentration Solar Radiation, CSR, to be harvested near the lower flux limits of solar day. This is because for a regular solar cavity receiver, the minimum threshold of intensity to harvest CSR is set by the need to heat the tubes to its operating temperature while for the HSRC, the CSR is only required to supplement the heat from the flame, which means that a positive input can be obtained for lower solar heat fluxes.

The authors reported a first order techno-economic analysis that identified that the overall capital cost of an electricity generation plant can be reduced by 51% and its solar component by 12% compared with stand-alone counterpart on the assumption that the cost of the hybrid receiver–combustor was double that of the solar only receiver. They also found that the implementation of the device would reduce the overall LCE by 24% and its solar component by 11% under the same assumption. This analysis further assumed that the performance of both the solar receiver and of the combustor within the hybrid device to be comparable with that of the stand-alone counter-parts and that the cost of the combined unit is twice that of the stand-alone solar receiver. However, to date no detailed concept or analysis of the device which demonstrates that this performance can be achieved has been presented.

For the reasons described above, the aims of the present investigation are as follows:

- To present a novel configuration of hybrid device that integrates the functions of a tubular solar receiver and a combustor, the HSRC.
- To develop an analytical model of the HSRC.
- To identify suitable configurations for which the performance of the hybrid device in the Solar-Only and Combustion-Only modes can be equivalent to the stand-alone alternatives i.e. a regular solar cavity receiver using molten salt, and a conventional steam boiler.
- To assess the sensitivity of the performance of the HSRC to variation in both key dimensionless ratios including the length to diameter ratio of the cavity (L_c/D_c) and size of the HXT and connector tubes (CT) used, together with the effect of scale.
- To estimate the total weight of the device and compare this with that of the stand-alone concept counterpart to provide a guide for economic savings that can be made through the HSRC concept.

2. Hybrid Solar Receiver Combustor concept

The novel HSRC device proposed by Nathan et al. [20] is shown in Figs. 1 and 2. It comprises a cavity solar tubular receiver that is also designed with an integrated combustion system. The concentrated solar radiation (CSR) enters through the aperture, which can be fitted with a compound parabolic concentrator (CPC) to lower radiant losses. The heat is captured with a thermal fluid in the receiver tubes (RT), which can be used for any thermal process but is analysed here in an electricity power generation system. To compensate for those times when the solar flux is below the minimum useful threshold, the aperture can be shut to allow the device to operate as a combustor. The use of a fuel allows the device to be kept running at all times if desired, avoiding the start-up and shut-down losses suffered by conventional solar thermal power systems. It can also be run in combination with thermal storage to increase solar share [20]. Furthermore, the fuel can be used to supplement the solar flux during periods of moderate solar flux, in which case the shutter remains open. The HSRC can thus be operated in 3 alternative modes: Solar-Only, Combustion-Only and a Mixed-Mode in which both solar and combustion are used together [21,22].

To recover the sensible heat from the combustion products, a heat exchanger (HX) system is incorporated into the device. The hot combustion products pass through the heat exchanger tubes (HXT) and are cooled with cold ambient air in the Combustion-Only and mixed modes. The preheated air is then fed to the combustion process. The cooled combustion products are then blown across the aperture to form a curtain that minimises the convective losses through the aperture. Alternatively, the jet can be used to provide flue gas recirculation for NO_x control.

3. Analytical model

An analytical model, which can be run in a pseudo steady state mode, is used to calculate the heat transfer, mass flow rates and energy into and out from each component of the system. Each term is described with a mathematical equation with a mass and energy balance calculated both in the Solar-Only and Combustion-Only modes of operation.

Fig. 3 shows the flow of energy through the HSRC in the Solar-Only mode of operation. An energy flux of concentrated solar radiation, $\dot{Q}_{solar,in}$, from the heliostat field is introduced into the device through the aperture, with the shutter open. The solar radiation is then used to heat the cavity of the HSRC lined with receiver tubes, RT, filled with a HTF. In the present analysis we consider this to be molten salt although an alternative HTF or the working fluid could be employed. The useful heat, $\dot{Q}_{useful}$, from the heat transfer fluid is then transferred to the electrical power generating system (EPGS). The main losses from the system are the radiative and convective losses from the opening of the aperture, $\dot{Q}_{ap,loss}$, and the nozzle opening which is used for the introduction of fuel and air into the device and significantly smaller in diameter relative to the aperture, $\dot{Q}_{noz,loss}$, together with the wall losses, $\dot{Q}_{wall,loss}$. Pumps are also required for the operation of device, whose energy consumption is classified as a parasitic loss ($\dot{W}_{pump}$). The net electricity power supplied, $\dot{W}_{elec,net}$, will depend on the type of power cycle used. In both systems, the EPGS is assumed to be the same, avoiding the need to model this directly.

In the Combustion-Only mode of operation, the heat input from the fuel, $\dot{Q}_{fuel,in}$, heats the RT with the aperture shutter closed to avoid unnecessary losses as can be seen from Fig. 4. The combustion products are then passed through a heat exchanger (HX), which recovers a fraction of the sensible exhaust heat, $\dot{Q}_{hotgas,out}$, by preheating the combustion air, termed, $\dot{Q}_{secair,in}$, by an amount that depends on the effectiveness of the HX. In the Solar-Only mode, there is no flow through the HX. However, with the shutter open, the main losses from the system are the radiant opening losses through the aperture, together with some additional losses through the burner nozzle, $\dot{Q}_{noz,loss}$. The wall losses, $\dot{Q}_{wall,loss}$, are present for all modes, while the sensible heat in the exhaust, $\dot{Q}_{exhaust}$, and the parasitic losses required to operate the pumps and fans, $\dot{W}_{pump}$ and $\dot{W}_{fan(forced\ draft\&induced\ draft)}$, are present in the combustion mode. In all cases, the heat from the heat transfer fluid is transferred to the Electrical Power Generating System, EPGS to produce electricity, $\dot{W}_{elec,net}$. Given the high efficiency of modern generators, the generator losses are ignored in this analysis. In addition, the model does not calculate the conversion of heat to electrical power partly because the final efficiency step will vary from case to case

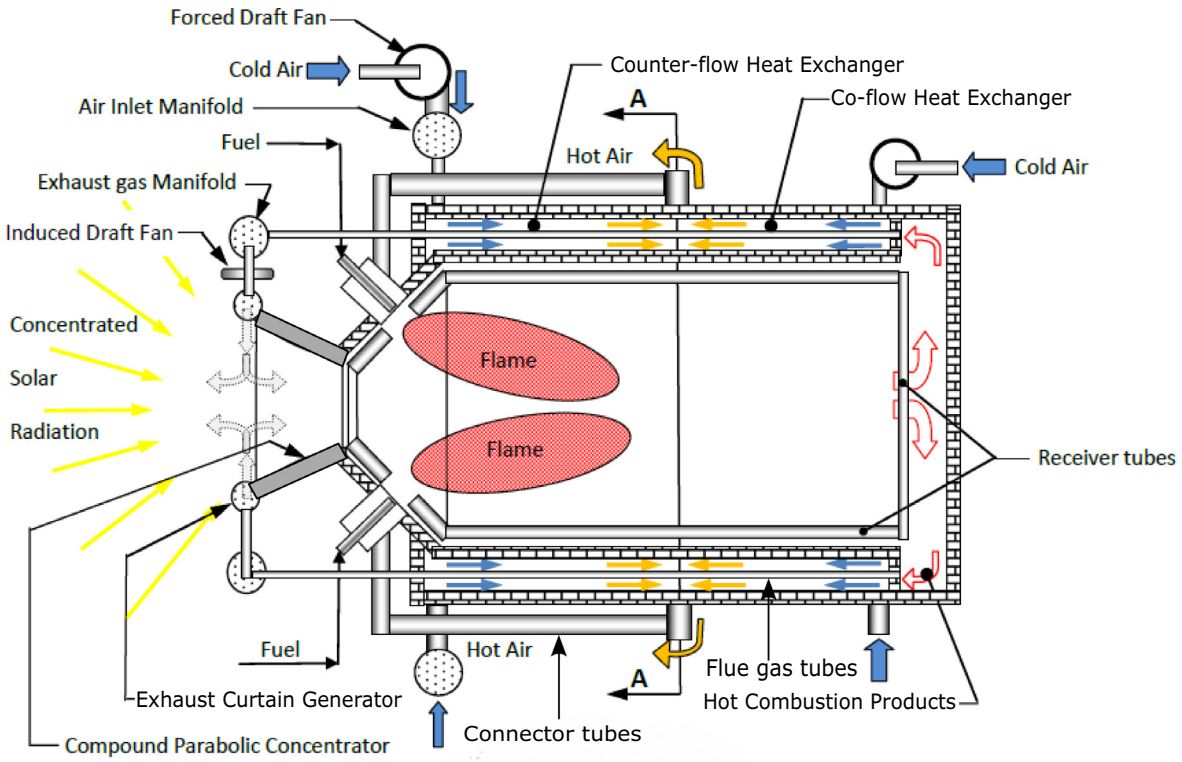

Fig. 1. Schematic diagram of the conceptual design of the Hybrid Solar Receiver Combustor, HSRC [19].

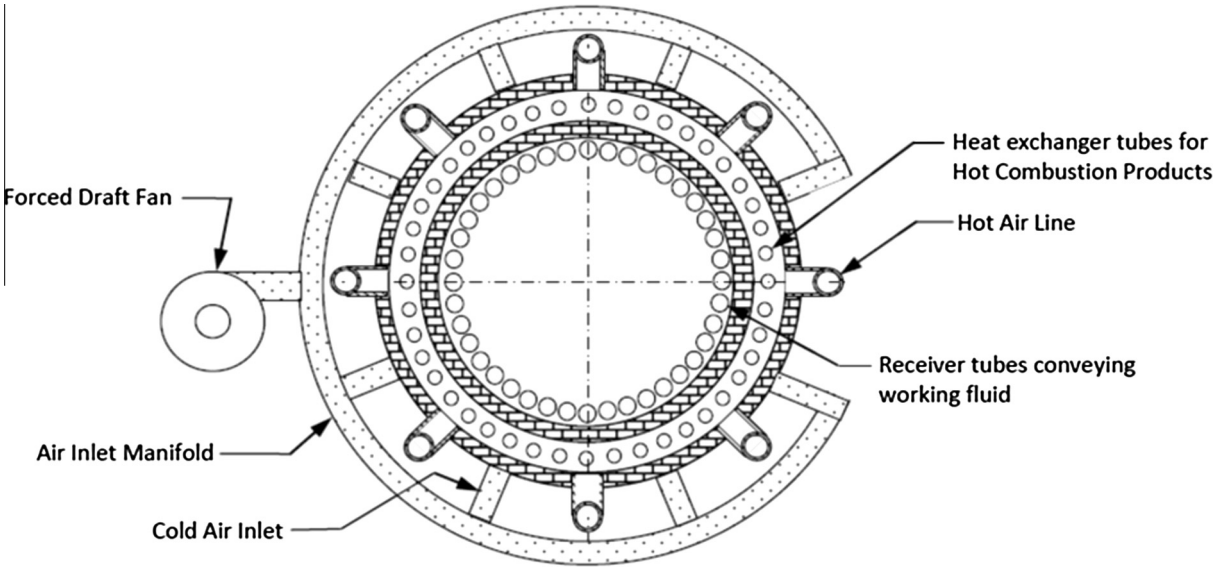

Fig. 2. End view of HSRC [19].

and partly because this step will be the same in the two types of hybrid that are being compared.

4. Methodology

4.1. Solar-Only

MATLAB was used as a tool to develop the analytical model that calculates the performance of the HSRC. The model is based on the mass and energy balance equations, with the thermal efficiency for the Solar-Only mode calculated following Steinfeld and Schubnell [23]:

$$\eta_{solar\text{-}only} = \frac{\dot{Q}_{useful}}{\dot{Q}_{solar,in}}. \tag{1}$$

Here $\dot{Q}_{useful}$ is the rate of energy transferred to the HTF:

$$\begin{aligned}\dot{Q}_{useful} &= \dot{Q}_{HTF} = h_{RT\ \text{to}\ HTF} A_{RT}(T_{RT} - T_{HTF}) \\ &= \dot{m}_{HTF} c_{p,HTF}(T_{HTF,out} - T_{HTF,in}).\end{aligned} \tag{2}$$

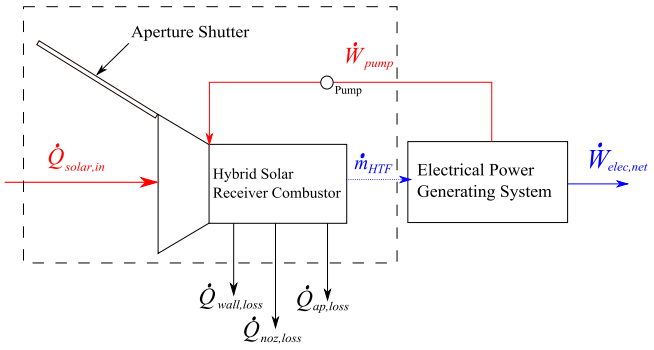

Fig. 3. Energy balance for the HSRC system in the Solar-Only mode with boundary of the modelled system.

where $h_{RT\ to\ HTF}$ is the heat transfer coefficient between the RT and HTF, noting that the fluid flow is assumed to be fully developed and turbulent [24]. This is confirmed by calculations which found that the Reynolds number is in the range ~4000 for all cases of length to diameter of the cavity ratio (L_c/D_c) and an entry length ~95 for an L_c/D_c ratio of 2. Here, the HTF is assumed to be a molten salt because the properties of the fluid are known and because these fluids are arguably the state-of-the-art in commercial solar thermal systems worldwide [25]. In addition, the heat storage capacity of molten salt is higher than that of air and water, which makes it more suitable for storage. Furthermore, the pressure drop associated with the fluid was calculated independently and found to be much lower than air and water, which means that the pumping power requirement is lower than the fan power. Following Hoffschmidt et al. [2], the inlet and outlet temperatures of the molten salt at either end of the RT are taken to be 290 °C and 565 °C, respectively. The average of these temperatures is used to calculate the heat transfer from the RT to the HTF. The mass flow rate of the HTF, $\dot{m}_{HTF}$, is also adjusted to maintain the difference between the outlet and inlet temperatures of the HTF.

$\dot{Q}_{solar,in}$ is the total amount of incoming solar radiation into the device. This includes the useful energy and the sum of the energy losses associated with the device.

In the analytical model, the HSRC is assumed to have an absorptivity of unity, given that it is a cavity receiver and so approaches a black body. The value of $\dot{Q}_{solar,in}$ matches the sum of the useful heat and the losses through an energy balance, (the power requirement from the fans and pumps, $\dot{W}_{fan+pump}$, is calculated separately as explained in Section 4.3) as follows:

$$\dot{Q}_{solar,in} = \dot{Q}_{useful} + \dot{Q}_{noz,loss} + \dot{Q}_{wall,loss} + \dot{Q}_{ap,loss}. \quad (3)$$

Heat transfer is calculated by assuming isothermal wall conditions for each type of surface so that all emissivities are constant (gray surface) [26]. It is important to note that although the heat flux distribution in the cavity is not uniform, the temperature of the tubes is influenced most strongly by the temperature of the HTF (i.e. molten salt) within them. In addition, it is not possible to calculate the actual distribution without detailed design of a solar field, a receiver and a power cycle, none of which are yet available. For the present analysis the tubes are assumed to be oriented axially, with the cold fluid inlet closest to the aperture, although other configurations are possible. This configuration minimises the risk of damage to the tubes and also minimises radiation losses because the coldest end of the tubes is closest to the aperture. On this basis, the present assumption of isothermal walls is reasonable for the present comparative analysis of the device in the Solar-Only mode. The same approach has been used by Wu et al. [27] and Xiao et al. [28] which justifies this assumption. The radiative and convective losses through the nozzle and aperture openings are calculated by the following equations [29]:

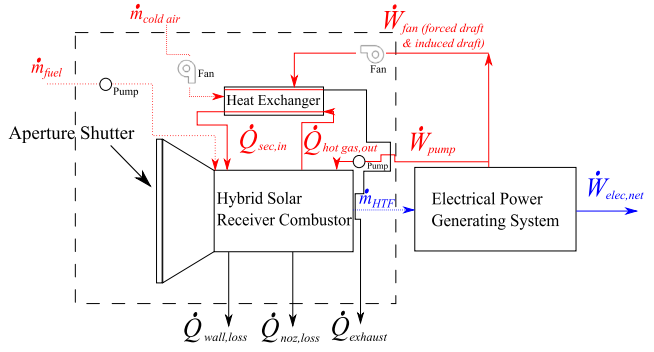

Fig. 4. Energy balance for the HSRC system in the Combustion-Only mode with boundary of the modelled system.

$$\dot{Q}_{noz,loss} = \dot{Q}_{rad,noz} + \dot{Q}_{conv,noz}, \quad (4)$$

where

$$\dot{Q}_{rad,noz} = \varepsilon_{eff}\sigma A_{noz}(T_{RT}^4 - T_{\infty}^4), \quad (5)$$

where the effective emissivity,

$$\varepsilon_{eff} = \frac{1}{1 + \left(\frac{1-\varepsilon_{RT}}{\varepsilon_{RT}}\right)\frac{A_{ap}}{A_{RT}}}, \quad (6)$$

and $\dot{Q}_{conv,noz} = 0.1\dot{Q}_{rad,noz}$, (7)

The convective losses through the nozzle are estimated to be 10% of the radiative losses as it is difficult to accurately estimate these losses due to external factors such as wind speed and optimum cavity position (such as the tilt angle). This percentage is deemed a reasonable assumption based on the studies performed by Jilte et al. and Leibfried and Ortjohann [29,30]. A similar approach is used to calculate $\dot{Q}_{ap,loss}$ where the size of the area of the nozzle is replaced with the size of the aperture. The wall losses throughout the device are estimated as follows [31]:

$$\dot{Q}_{wall,loss} = U_{wall}A_{wall}(T_{wall,in} - T_{\infty}), \quad (8)$$

where U_{wall} is the overall heat transfer coefficient across the shell of the HSRC, and depends on the wall thickness of the device. The wall is further assumed to be made of 3 layers, a refractory layer, an insulation layer and a steel casing to minimize wall heat losses. $T_{wall,in}$ is the temperature of the inner side of the cavity, conservatively assumed to be similar to that of the receiver tubes although in reality this would be lower as the tubes will block some of the radiation from solar and/or combustion.

4.2. Combustion-Only

For the Combustion-Only mode of operation, the combustion is assumed to be complete and the reactor is treated based on the presumption that it operates with sufficient momentum in the air and fuel stream to create a well-stirred furnace chamber similar to the model by Hottel [32,33]. On this basis, the thermal efficiency of the device is defined as the rate of energy absorbed by the HTF divided by the amount of power supplied by the fuel:

$$\eta_{comb\text{-}only} = \frac{\dot{Q}_{useful}}{\dot{Q}_{fuel,in}}. \quad (9)$$

The flame radiation from the combustion of the fuel is treated as an isothermal cylinder of gases so that flame and the combustion products are assigned a single temperature [34].

For this mode of operation, the useful power, $\dot{Q}_{useful}$ (which is set to 30 MW_{th}) from the flame to the HTF is adapted to be [26]:

$$\dot{Q}_{useful} = \dot{Q}_{HTF} = h_{RT\ to\ HTF} A_{RT} (T_{RT} - T_{HTF}) = (GS_1)_R \sigma \left(T_{gas}^4 - T_{RT}^4\right), \tag{10}$$

where the term $(GS_1)_R$ is defined as the total exchange area between the gas and tubes in radiative equilibrium (equal incoming and outgoing radiative heat flux) following the approach by Jenkins and Mullinger [26]:

$$(GS_1)_R = \frac{A_{int\ HSRC}}{\left[\frac{1}{\varepsilon_{gas}}\right] + \left[\frac{1}{C_s}\right] - 1}. \tag{11}$$

Natural gas is used as the fuel due to its ease of utilization and availability [31]. The pressure inside the HSRC during Combustion-Only mode is close to atmospheric pressure [20]. ε_{gas}, the gas emissivity, is estimated to be 0.3 (for a low emissivity flame) based on the Carbon to Hydrogen ratio of natural gas, typically in the region of ~4, following Jenkins and Mullinger [26] and C_s is the cold surface fraction, where

$$C_s = \frac{A_{RT}}{A_{int\ HSRC}}. \tag{12}$$

A_{RT} and $A_{int\ HSRC}$ are the total area of the receiver tubes and the internal surface of the HSRC, respectively.

The rate of energy supplied by the fuel is calculated using an energy balance (the power requirement from the fans and pumps, $\dot{W}_{fan+pump}$, is calculated separately as explained in Section 4.3):

$$\dot{Q}_{fuel,in} = \dot{Q}_{wall,loss} + \dot{Q}_{noz,loss} + \dot{Q}_{exhaust} + \dot{Q}_{useful} - \dot{Q}_{coldair,in}, \tag{13}$$

where $\dot{Q}_{wall,loss}$ and $\dot{Q}_{noz,loss}$ are found using the same approach as Section 4.1 while $\dot{Q}_{exhaust}$ and $\dot{Q}_{coldair,in}$ are defined below. The thermal input from the fuel is defined as

$$\dot{Q}_{fuel,in} = \dot{m}_{fuel} \times LHV_{fuel}. \tag{14}$$

The mass flow rate of fuel, $\dot{m}_{fuel}$, using Eq. (13), is found using an iterative process that solves for $\dot{Q}_{fuel,in}$, to achieve an energy balance for (12). In this way, the heat transfer to the tubes increases with the flame temperature, and hence also with temperature of the secondary air. The pump power requirement for the fuel is assumed to be negligible. The energy losses from the system are shown in Fig. 4 and consist of the nozzle opening losses, wall losses (both found using a similar approach to Section 4.1) and exhaust gases:

$$\dot{Q}_{exhaust} = \dot{m}_{exhaust} c_{p,exhaust} (T_{exhaust} - T_\infty). \tag{15}$$

The value of $T_{exhaust}$ can be found by performing an analysis of the HX in the HSRC. The approach used is the effectiveness-NTU method adapted from Bergman et al. [35]. Based on Fig. 1, the HX consists of 2 parts, i.e. a co-flow configuration and a counter-flow section. The co-flow to counter-flow ratio can be varied to determine the optimum configuration. The co-flow section provides strong cooling to the hottest part of the HX tubes where hot flue gases enter the HX, while the counter-flow section provides a high efficiency heat exchange for the lower temperature end of the exhaust gas stream [20]. Based on this, the model assumes a co-flow to counter-flow ratio of 5.67:1 to achieve a high HX effectiveness.

The initial internal energy transferred from the cold air into the device is defined by [36]:

$$\dot{Q}_{cold\ air,in} = \dot{m}_{cold\ air} u_{cold\ air}, \tag{16}$$

where $u_{cold\ air}$ is the specific internal energy of cold air blown into the device.

To estimate the effectiveness of the HX, the amount of sensible exhaust heat recovered as combustion air, $\dot{Q}_{sec,in}$, is calculated as:

$$\%_{sensible\ exhaust\ recovery} = \frac{\dot{Q}_{sec,in}}{\dot{Q}_{hot\ gas,out}}. \tag{17}$$

The rate of energy transferred to the secondary air in the HX is calculated by:

$$\dot{Q}_{sec,in} = \dot{m}_{cold\ air} C_{p,air} (T_{comb\ air} - T_\infty). \tag{18}$$

The remaining rate of energy from the gases after transferring heat to the HTF, before entering the HX, is defined by:

$$\dot{Q}_{hot\ gas,out} = \dot{m}_{exhaust} C_{p,flue\ gas} \left(T_{hot\ gas,out} - T_\infty\right), \tag{19}$$

The effectiveness-NTU method is applied when performing calculations for the HX. The effectiveness of a HX is defined as the actual amount of heat flux rate by the HX relative to the maximum possible heat flux rate. Hence this maximum heat flux rate needs to be determined by the following equation [35]:

$$\dot{Q}_{max} = C_{min} \left(T_{hot\ gas,out} - T_\infty\right), \tag{20}$$

where C_{min} is the lesser of the heat capacity rates, C_h and C_c, each defined by the following:

$$C_c = \dot{m}_{cold\ air} C_{p,c}, \tag{21}$$

$$C_h = \dot{m}_{hot\ gas,out} C_{p,h}. \tag{22}$$

Following this, the actual heat transfer rate for the co-flow and counter-flow configurations are:

$$\dot{Q}_{coflow} = \varepsilon_{coflow} \dot{Q}_{max} \tag{23}$$

$$\dot{Q}_{counterflow} = \varepsilon_{counterflow} \dot{Q}_{max} \tag{24}$$

where the definitions for the effectiveness for both cases, ε_{coflow} and $\varepsilon_{counterflow}$ are obtained from Bergman et al. [35].

The outlet temperatures of the flue gas (exhaust) can be found from overall energy balance equations, using an iterative process as the mass flow rates of the exhaust and cold air depends on the mass flow rate of fuel (mass balance):

$$T_{exhaust} = T_{hot\ gas,out} - \frac{\dot{Q}_{counterflow}}{\dot{m}_{exhaust} c_{p,h}}, \tag{25}$$

$$\dot{m}_{exhaust} = \dot{m}_{fuel} + \dot{m}_{cold\ air}. \tag{26}$$

Similarly, the temperature of the combustion air, $T_{comb\ air}$, was found using the approach as above.

4.3. Pressure drop and power requirement for fans and pumps

The pressure drop in all tubes is calculated following Bergman et al. [35]:

$$\Delta P = f \frac{\rho \left(u_{mean,fluid}\right)^2}{2D} (x_2 - x_1). \tag{27}$$

This formula takes into account the friction factor, f, which is defined as a dimensionless pressure drop for internal flow and this value can be obtained from Bergman et al. [27], density, ρ, and mean velocity, u_m of the heat transfer fluid or flue gas, and the length (the term $x_2 - x_1$ represents the overall length of the tube) as well as diameter, D of the tube. The power requirement for the fans and pumps is then estimated by multiplying the pressure drop with the volumetric flow rate of the heat transfer fluid or flue gas:

$$\dot{W}_{fan+pump} = (\Delta P) \dot{V}_{fluid}. \tag{28}$$

4.4. Estimating mass of HSRC

The weight of the entire device was calculated from the density of the material and the dimensions of the device, as per Table 1.

Table 1
Type of materials used for each component and its associated density.

Component	Material	Density (kg/m^3)
Tubes		
Receiver tubes	Inconel	8497
Heat exchanger tubes	Carbon steel	7850
Connector tubes	Carbon steel	7850
Molten salt	Sodium nitrate – 48% Potassium nitrate – 52%	1862
Shell		
Refractory	Ceramic fibre	130
Insulation	Clay	560
Steel casing	Stainless steel 310	7750

Another 10% of the overall weight of all the components was used to account for miscellaneous components.

5. Model validation

5.1. Solar-Only mode

The analytical model produced was validated for the Solar-Only mode, using a slightly different shape and configuration, adapted to match those of the solar cavity receiver of Li et al. [37]. These data corresponds to the Sandia National Laboratories' molten salt electric experiment (MSEE). The input data to the model for the validation study is shown in Table 2, while the results of the comparison are shown in Table 3. These show that the present model agrees with the values of Li et al. with a maximum deviation of 5.78%. This level of agreement provides confidence in the model.

5.2. Combustion-Only mode

For the Combustion-Only case, standard and well known heat transfer coefficients were adapted to suit the shape of the HSRC, as reported in Table 4. The equations have been verified by the indicated sources to be correct for each case.

6. Results and discussion

Fig. 5 presents the dependence of the thermal efficiency of the HSRC for the Combustion-Only mode as a function of the length to diameter ratio of the chamber, both for a fixed diameter of 3 m and for the case of a thermal output of 30 MW. Three sets of data are presented, corresponding to integral multiples of the length of the HX with respect to the cavity from 1 to 3. The cases in which the HX length is double or triple that of the cavity are representative of a range of alternative HX designs that could achieve more effective heat exchanger recovery, but that will come at the expense of increased pressure loss, weight and cost (as discussed later). Other configurations that could potentially offer a better trade-off in effectiveness, pressure drop and weight include dimpled or finned tube heat exchangers, but are not analysed here. The figure also presents the band of typical efficiency for a conventional boiler, which ranges from 65% to 85% [38]. Importantly, it can be seen that the overall efficiency of the HSRC in the Combustion-Only mode can match, or exceeded, that of the conventional boiler for values of $L_c/D_c > 3$, confirming the reliability of the economic analysis of Nathan et al. [19], provided that the reactions can be completed within the combustor volume. The fractional energy in the combustion products that is recovered through the HX is also shown for these three configurations. These results show that the recovery of about half of the sensible heat from the exhaust allows an overall efficiency of the device during the combustion mode to be greater than 80%.

Table 2
Parameters used in the Solar-Only mode validation assessment.

Solar input (kW)	100
Receiver area (m^2)	1
Thermal conductivity of receiver tubes (W/m K)	23.9
Temperature of molten salt in (°C)	290
Temperature of molten salt out (°C)	560
Aperture area (m^2)	0.4
Number of tubes	6

Table 3
Model validation data for Solar-Only mode of operation.

	Model from Li et al. [28]	Analytical model	Difference (%)
Convective heat loss (kW)	11.5	10.89	−5.30
Emissive heat loss (kW)	3.90	3.83	1.79
Reflective heat loss (kW)	4.50	4.76	5.78
Conductive heat loss (kW)	0.30	0.29	−3.33
Total heat loss (kW)	20.2	19.77	−2.13
Receiver efficiency	0.798	0.823	3.13

It is important to note that doubling the length of the HX for the case of $L_{HX}/L_C = 1$ from $L_c/D_c = 2$ to 4 results in an increase in efficiency from 58% to 77%. However the same increase in HX length by going from the case of $L_{HX}/L_C = 1$ to $L_{HX}/L_C = 2$ only increases the efficiency to about 69%. This is because the temperature of hot gases from combustion is greater for shorter lengths of the cavity (as the same amount of fuel is used for each case), which correspond to a higher exhaust temperature and lower heat recovery, lowering the overall thermal efficiency of the device.

Fig. 6 presents both the temperature of the receiver tubes, RT, and the corresponding thermal efficiency in Solar-Only mode as a function of the length of the chamber. The temperature of the RT in this mode is similar to that in the Combustion-Only mode because the model assumes the same heat flux to RT to ensure a similar thermal output of the HTF. According to Rodriquez et al. [39] three common materials used in solar thermal/molten salt applications are Incoloy Alloy 800H, Inconel 625LCF, and 316 stainless steel. Also shown in Fig. 6 are the limiting temperatures of these materials in the Solar-Only mode of operation as dotted lines [40,41]. Based on the figure, for safe operation of the HSRC, the L_c/D_c ratio of >4.5 is required if Incoloy Alloy 800H or Inconel 625LCF is used and an L_c/D_c ratio of >6 is needed if 316 Stainless Steel is used. The efficiency increases slightly with decreasing temperature of RT and peaks at $L_c/D_c \sim 4$.

Fig. 7 presents the outlet temperature from the two sides of the HX, namely of exhaust, $T_{exhaust}$, and of the pre-heated combustion air, T_{ca}, together with the HX effectiveness. As expected, η_{HX} increases with L_c/D_c due to the increased surface area for heat recovery. Importantly, high values of ε_{HX} necessarily correspond to high values of the combustion air temperature so that values of $T_{ca} > 400$ °C is to be expected and $T_{ca} > 600$ °C is desirable for efficient designs of the HSRC. This is higher than the typical combustion air temperature for boilers of 250 °C although it is typical of mid-temperature processes such as lime and significantly lower than high temperature processes such as cement and glass.

Fig. 8 presents the dependence both of the weight of the device and of the parasitic power requirements of the fan and pump relative to the overall thermal output (in this case 30 MW) as a function of L_c/D_c. As expected, the weight of the device increases linearly with L_c/D_c, and hence too, with L_{HX}. In contrast, the parasitic losses of the fan and pump power exhibit a minimum that occurs for $L_c/D_c \approx 4$. Importantly, the power requirements are relatively low, ranging between 0.6% and 2% of the useful thermal output for all cases. This is an acceptable value, and shows that the

Table 4
Heat transfer coefficients used for the Combustion-Only mode.

Interaction	Equations used	Sources
Molten salt to inner surface of RT	$Nu = 0.0243 \times Re^{0.8}_{molten\ salt} \times Pr^{0.4}_{molten\ salt}$	Fully developed, turbulent flow in a tube [22]
Combustion products to inner surface of HSRC shell	$Nu = 0.0243 \times Re^{0.8}_{combustion\ products} \times Pr^{0.4}_{combustion\ products}$	Fully developed, turbulent flow in a tube [36]
Outer surface of HSRC shell to surrounding	$Nu = C \times Re^{m}_{air} \times Pr^{1/3}_{air}$ If $Re_{air} = 40 - 4000$ $C = 0.683$ $m = 0.466$ If $Re_{air} = 4000 - 40,000$ $C = 0.193$ $m = 0.618$ If $Re_{air} = 40000 - 400000$ $C = 0.027$ $m = 0.805$	External flow of air around a cylinder [33]
Combustion products to inner surface HXT	$Nu = 0.0243 \times Re^{0.8}_{combustion\ products} \times Pr^{0.4}_{combustion\ products}$	Fully developed, turbulent flow in a tube [22]
Outer surface HXT to combustion air	$Nu = C \times Re^{m}_{air,max} \times Pr^{0.36}_{air} \times \left[\frac{Pr}{Pr_s}\right]^{1/4}$ Where for a staggered configuration of tubes, If $Re_{air,max} = 10^3 - 2 \times 10^5$ $C = 0.35$ $m = 0.6$ If $Re_{air,max} = 2 \times 10^5 - 2 \times 10^6$ $C = 0.022$ $m = 0.84$	External flow of air across banks of tubes (staggered arrangement) [33]

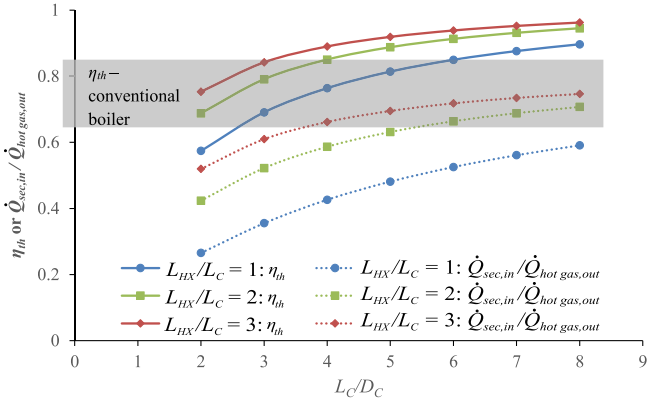

Fig. 5. Effect of varying L_c/D_c on the overall thermal efficiency and fraction of heat recovery from the hot combustion products for Combustion-Only mode for a thermal output of 30 MW. Results are reported for three values of heat exchanger length relative to the length of the chamber.

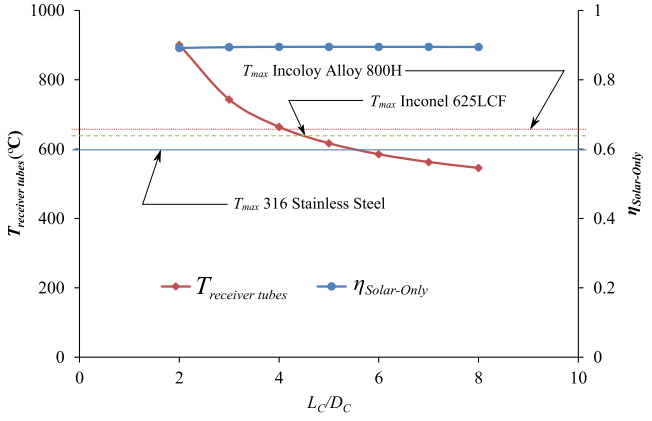

Fig. 6. Effect of L_c/D_c on the temperature of the receiver tubes and thermal efficiency for Solar-Only mode for a thermal input of 30 MW.

tubes chosen are sensibly sized. It should also be noted that separate calculations were performed which showed that the pressure drop through the HX is much greater than that through the receiver tubes, so that the fan power dominates the parasitic electrical power requirements for the system, as expected.

Fig. 9 presents the effect of changing the diameter of the heat exchanger tubes, OD_{HXT}, while keeping their thickness constant, on both the parasitic work and on the weight. This shows the trade-off, in that increasing OD_{HXT} decreases the pressure drop and fan power requirements, at the expense of increasing the weight, and hence also the cost of the tubes. A range of 1–5% total fan power with respect to the useful thermal output is deemed to be a reasonable parasitic loss and is expected to be near to the optimum for cost. Fig. 9 shows that this occurs for the $OD_{HXT} \approx 101$ mm for the case of a 2.1 mm wall thickness.

Table 5 reports the weight distribution of the HSRC for several configurations that achieve similar efficiencies both to a solar-only cavity receiver and a conventional boiler, in terms of weight in tonnes and percentage weight distribution, for a 30 MW thermal

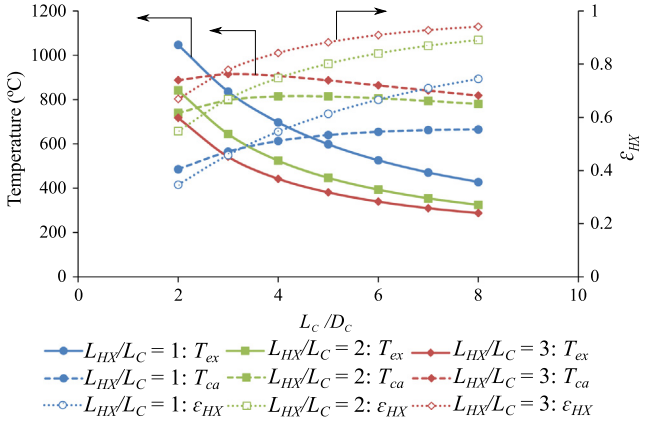

Fig. 7. Effect of varying L_c/D_c on the temperatures of the combustion air and of the exhaust gases leaving the HX for three lengths of HX, together with the HX effectiveness.

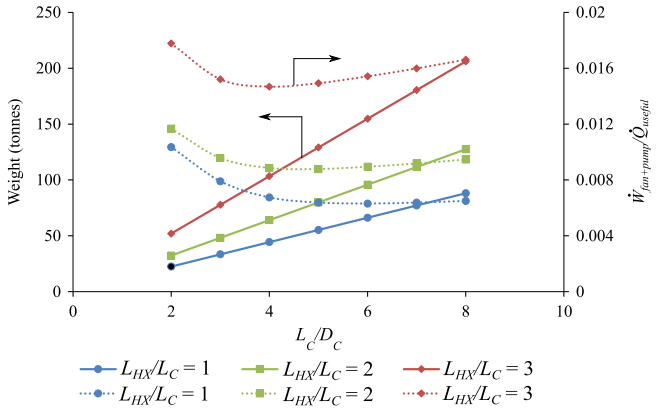

Fig. 8. Dependence on L_c/D_c of the overall estimated weight and of ratio of the fans & pumps power requirement relative to the thermal output of the device. The closed symbols represent the weight while the open symbols represent $\dot{W}_{fan+pump}/\dot{Q}_{useful}$.

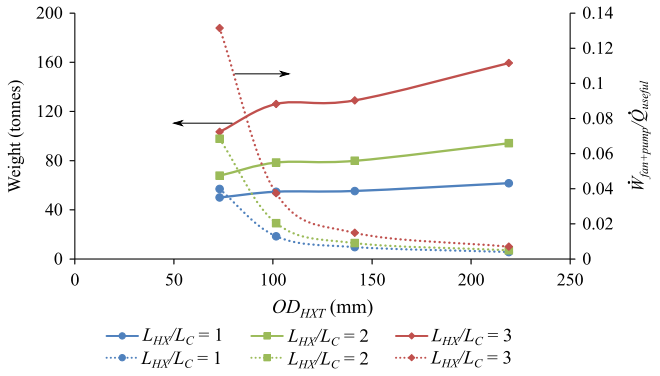

Fig. 9. Influence of the diameter of the HXT (at constant thickness) on the overall weight and on the ratio of the fans & pumps power requirement relative to the thermal output of the device. The closed symbols represent the weight while the open symbols represent $\dot{W}_{fan+pump}/\dot{Q}_{useful}$.

output. The device is also compared with an equivalent configuration of a solar-only receiver without the HX tubes and connector tubes which achieves a similar solar efficiency. The weight of the device is assumed to correlate with the subsequent cost of the device, in a first-order assessment of the validity of the assumptions by Nathan et al. [19]. The HSRC is divided into 6 main components, namely the receiver tubes, molten salt, heat exchanger tubes, external shell, connector tubes and miscellaneous items that include bolts, nuts, etc. Table 5 shows that:

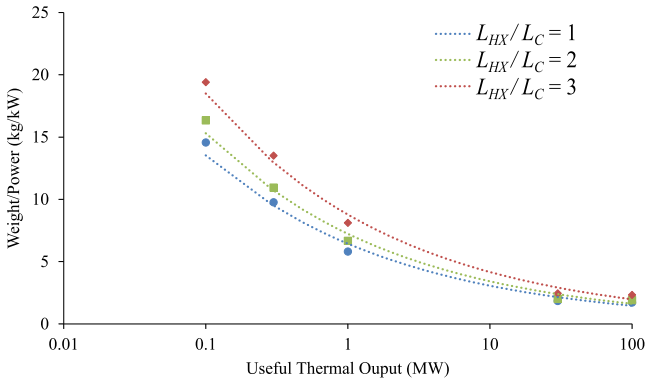

Fig. 10. Effects of the scale of useful thermal output power from the HSRC on the ratio of the overall estimated weight to thermal output power for constant $L_c/D_c \sim 5$ as a power law function.

- The weight of the HSRC ($L_{HX}/L_C = 1$) that achieves a similar efficiency to the solar-only device is heavier than it by a factor of ~2. This value provides support for the techno-economic assessment of Nathan et al. [18] who assumed that the HSRC is twice the cost of a regular solar cavity receiver.
- The weight of the HSRC depends strongly on the weight of the HXT, so that, the heat exchanger tubes' weight dominates the overall weight of the device in the case of $L_{HX}/L_C = 2$ and $L_{HX}/L_C = 3$. Hence, it is likely to be more cost-effective to use high heat transfer devices, such as dimples or fins, than to use several passes of the HXT.

It is also important to note that the shell itself, takes up a large percentage of the weight of the HSRC. The shell is greatly influenced by the thickness. When modelling, the shell is assumed to be made of 3 layers, a 75 mm refractory layer, a 30 mm insulation layer and a 2 mm steel casing. The thickness of each layer affects the weight of the shell significantly, and the layers chosen are relatively conservative in minimizing heat loss. Hence further reduction in weight, and potentially cost, is possible by optimising this aspect of the design.

Fig. 10 presents the effect on the weight to power ratio of changing the scale of the device as a power law function. The scale was varied at a constant value of $L_c/D_c \sim 5$. This shows that the weight/thermal output ratio increases as the scale decreases, which is consistent with the economies of scale that typically occur for thermal devices. However, importantly, this change is non-linear. Most of the advantage of scale is achieved for thermal outputs of order 1 MW, which means that the device is likely to be suited to small to medium scale installations as well as to larger scale devices.

Table 5
Weight and percentage weight distribution of HSRC.

Weight distribution	$L_{HX}/L_C = 1$		$L_{HX}/L_C = 2$		$L_{HX}/L_C = 3$		Solar receiver	
	Weight (tonnes)	Weight distribution (%)	Weight (tonnes)	Weight distribution (%)	Weight (tonnes)	Weight distribution (%)	Weight (tonnes)	Weight distribution (%)
Receiver tubes	9.63	17.41	8.67	12.04	8.03	7.46	8.03	29.41
Molten salt	9.94	17.97	8.95	12.43	8.29	7.69	8.29	30.35
Heat exchanger tubes	17.60	31.80	35.95	49.93	70.53	65.50	0.00	0.00
Shell	10.08	18.21	9.13	12.69	8.50	7.90	8.50	31.15
Connector tubes	3.05	5.52	2.75	3.82	2.55	2.36	0.00	0.00
Miscellaneous	5.03	9.09	6.55	9.09	9.79	9.09	2.48	9.09
Sum	55.34	100.00	72.00	100.00	107.68	100.00	27.30	100.00

7. Conclusions

The novel configuration of hybrid between a solar thermal tubular receiver and combustor has been presented and shown with an analytical steady-state model to be configurable to achieve the same efficiency as the solar-only and combustion-only counterparts. More specifically, the analysis has found that:

- The size and weight of the hybrid device is typically controlled by the heat transfer requirements of the combustor rather than that of the solar receiver, both because the heat flux that can be achieved by a solar concentrator is greater than that from combustion and because of the additional weight required for the heat exchanger to recover the heat from the combustion products.
- For the Solar-Only mode, the limiting factors are the heat transfer coefficient to the heat transfer fluid (molten salt) and/or the maximum operating temperature of the tubes.
- The design of the heat exchanger to recover heat from the combustion products is a critical element of the HSRC concept. It is necessary to recover at least 50% of this heat to achieve efficiencies similar to a conventional boiler. For the basic configuration of simple tubes assessed here, approximately 35% of the weight of the HSRC is associated with this component, although this could be reduced with more efficient HX components such as fins and dimples.
- It is possible to achieve an efficiency in the Combustion-Only mode that is similar to that of a conventional boiler with a suitably sized device. It is estimated that, to achieve this, the weight of the HSRC will be increased by a factor of approximately 2 over that of a solar-only device.

These calculations support the previous techno-economic analysis of Nathan et al. [19], which account only for the benefits of shared infrastructure. Further benefits can be expected when accounting for reduced start-up and shut-down losses.

Acknowledgements

The support of the Australian Research Council and of FCT Combustion and Vast Solar through the ARC Linkage scheme is gratefully acknowledged.

References

[1] Desideri U, Campana PE. Analysis and comparison between a concentrating solar and a photovoltaic power plant. Appl Energy 2014;113:422–33.
[2] Hoffschmidt B et al. Concentrating solar power. Compr Renew Energy 2012;3:595–636.
[3] Moore J, Apt J. Can hybrid solar–fossil power plants mitigate CO_2 at lower cost than PV or CSP? Environ Sci Technol 2013;47(6):2487–93.
[4] Mehos MS et al. Combustion system for hybrid solar fuel receiver. United States; 2004.
[5] Z'Graggen A, Steinfeld A. A two-phase reactor model for the steam-gasification of carbonaceous materials under concentrated thermal radiation. Chem Eng Process 2008;47(4):655–62.
[6] Piatkowski N et al. Solar-driven gasification of carbonaceous feedstock – a review. Energy Environ Sci 2011;4(1):73–82.
[7] Fork DK et al. Life estimation of pressurized-air solar-thermal receiver tubes. J Sol Energy Eng 2012;134(4). 041016-041016.
[8] Yamaguchi H et al. Solar energy powered Rankine cycle using supercritical CO_2. Appl Therm Eng 2006;26(17–18):2345–54.
[9] Lovegrove K et al. Realising the potential of concentrated solar power in Australia; 2012.
[10] Peterseim JH et al. Concentrated solar power hybrid plants, which technologies are best suited for hybridisation? Renew Energy 2013;57:520–32.
[11] Reilly HE, Kolb GJ. An evaluation of molten-salt towers including results of the solar two project. Albuquerque, New Mexico; 2001.
[12] Kolb GJ. Economic evaluation of solar-only and hybrid power towers using molten-salt technology. Sol Energy 1998;62(1):51–61.
[13] Ying Y, Hu EJ. Thermodynamic advantages of using solar energy in the regenerative Rankine power plant. Appl Therm Eng 1999;19(11):1173–80.
[14] Yang Y et al. An efficient way to use medium-or-low temperature solar heat for power generation – integration into conventional power plant. Appl Therm Eng 2011;31(2–3):157–62.
[15] Zoschak RJ, Wu SF. Studies of the direct input of solar energy to a fossil-fuelled central station steam power plant. Sol Energy 1975;17(5):297–305.
[16] Allani Y, Favrat D, Von SMR. CO_2 mitigation through the use of hybrid solar-combined cycles. Energy Convers Manage 1997;38(9999):S661–7.
[17] Kribus A et al. A solar-driven combined cycle power plant. Sol Energy 1998;62(2):121–9.
[18] Sargent & Lundy LLC Consulting Group. Assessment of parabolic trough and power tower solar technology cost and performance forecasts. NREL: Chicago, Illinois; 2003.
[19] Nathan GJ, Battye DL, Ashman PJ. Economic evaluation of a novel fuel-saver hybrid combining a solar receiver with a combustor for a solar power tower. Appl Energy 2014;113:1235–43.
[20] Nathan GJ et al. A hybrid receiver–combustor. A.R.I.P. Ltd.; 2013.
[21] Kitzmiller K, Miller F. Effect of variable guide vanes and natural gas hybridization for accommodating fluctuations in solar input to a gas turbine. J Sol Energy Eng 2012;134(4). 041008-041008.
[22] Kitzmiller K, Miller F. Thermodynamic cycles for a small particle heat exchange receiver used in concentrating solar power plants. J Sol Energy Eng Trans ASME 2011;133(3).
[23] Steinfeld A, Schubnell M. Optimum aperture size and operating temperature of a solar cavity-receiver. Sol Energy 1993;50(1):19–25.
[24] Jianfeng L, Jing D, Jianping Y. Heat transfer performance and exergetic optimization for solar receiver pipe. Renew Energy 2010;35(7):1477–83.
[25] Tian Y, Zhao CY. A review of solar collectors and thermal energy storage in solar thermal applications. Appl Energy 2013;104:538–53.
[26] Jenkins B, Mullinger P. Industrial and process furnaces. Butterworth Heinemann; 2008. p. 544.
[27] Wu S-Y, Xiao L, Li Y-R. Effect of aperture position and size on natural convection heat loss of a solar heat-pipe receiver. Appl Therm Eng 2011;31(14–15):2787–96.
[28] Xiao L, Wu S-Y, Li Y-R. Effect of cavity wall temperature and opening ratio on the natural convection heat loss characteristics of a solar cavity receiver. In: 2011 International conference on computer distributed control and intelligent environmental monitoring, CDCIEM 2011, February 19, 2011–February 20, 2011. Changsha, Hunan, China: IEEE Computer Society; 2011.
[29] Jilte RD, Kedare SB, Nayak JK. Natural convection and radiation heat loss from open cavities of different shapes and sizes used with dish concentrator. Mech Eng Res 2013;3(1):25–43.
[30] Leibfried U, Ortjohann J. Convective heat loss from upward and downward-facing cavity solar receivers: measurements and calculations. J Sol Energy Eng, Trans ASME 1995;117(2):75–84.
[31] Mills AF, Ganesan V. Heat transfer. 2nd ed. Pearson Education; 1999.
[32] Hottel HC. Radiant heat transmission. Heat Transm 1954;3.
[33] Hottel HC, Sarofim AF. Radiative transfer. McGraw-Hill; 1967.
[34] Baukal Jr CE. Heat transfer. In: The John Zink combustion handbook. John Zink Company LLC; 2001. p. 106.
[35] Bergman TL et al. Fundamentals of heat and mass transfer. 7th ed. John Wiley & Sons; 2011.
[36] Moran MJ et al. Fundamentals of engineering thermodynamics. John Wiley & Sons; 2010.
[37] Li X et al. Thermal model and thermodynamic performance of molten salt cavity receiver. Renew Energy 2010;35(5):981–8.
[38] CIBO. Boilers. In: Zeitz RA, editor. Energy efficiency handbook. Burke, Virginia: Council of Industrial Boiler Owners; 1997. p. 20.
[39] Rodriguez-Sanchez MR et al. Thermal design guidelines of solar power towers. Appl Therm Eng 2014;63(1):428–38.
[40] Bradshaw R, Goods S. Corrosion of alloys and metals by molten nitrates; 2003. p. 117–34.
[41] Miliozzi A et al. Fluido termovettore: dati di base della miscela di nitrati di sodio e potassio. ENEA report; 2007. ENEA/SOL/RD/2001/07.

Statement of Authorship

Title of Paper	Impact of start-up and shut-down losses on the economic benefit of an integrated hybrid solar cavity receiver and combustor
Publication Status	☑ Published ☐ Accepted for Publication ☐ Submitted for Publication ☐ Unpublished and Unsubmitted w ork w ritten in manuscript style
Publication Details	Lim, JH, Hu, E & Nathan, GJ 2016, 'Impact of start-up and shut-down losses on the economic benefit of an integrated hybrid solar cavity receiver and combustor', Applied Energy, vol. 164, pp. 10-20.

Principal Author

Name of Principal Author (Candidate)	Jin Han Lim		
Contribution to the Paper	Performed literature review. Responsible for the development of the pseudo-dynamic model required to calculate the benefits of the integrated hybrid solar cavity receiver and combustor. Took primary responsibility for responding to the reviewers.		
Overall percentage (%)	60		
Certification:	This paper reports on original research I conducted during the period of my Higher Degree by Research candidature and is not subject to any obligations or contractual agreements with a third party that would constrain its inclusion in this thesis. I am the primary author of this paper.		
Signature		Date	18/7/16

Co-Author Contributions

By signing the Statement of Authorship, each author certifies that:

i. the candidate's stated contribution to the publication is accurate (as detailed above);

ii. permission is granted for the candidate in include the publication in the thesis; and

iii. the sum of all co-author contributions is equal to 100% less the candidate's stated contribution.

Name of Co-Author	Associate Professor Eric Hu		
Contribution to the Paper	Supervised the work. Provided assistance in developing the pseudo-dynamic model. Assisted with editing the manuscript.		
Signature		Date	19/7/2016

Name of Co-Author	Professor Graham Nathan		
Contribution to the Paper	Supervised the work. Assisted in the development of the pseudo-dynamic model. Suggested methods for verification of model developed. Assisted with editing and finalising the manuscript.		
Signature		Date	19/7/16

CHAPTER 4

IMPACT OF START-UP AND SHUT-DOWN LOSSES ON THE ECONOMIC BENEFIT OF AN INTEGRATED HYBRID SOLAR CAVITY RECEIVER AND COMBUSTOR

Applied Energy 164 (2016) 10–20

Contents lists available at ScienceDirect

Applied Energy

journal homepage: www.elsevier.com/locate/apenergy

Impact of start-up and shut-down losses on the economic benefit of an integrated hybrid solar cavity receiver and combustor

Jin Han Lim *, Eric Hu, Graham J. Nathan

Centre for Energy Technology, School of Mechanical Engineering, The University of Adelaide, SA 5005, Australia

HIGHLIGHTS

- We present the benefits of integrating a solar cavity receiver and a combustor.
- The hybrid solar receiver combustor is compared with its equivalent hybrid.
- The start-up losses of the back-up boiler are calculated for a variable resource.
- Levelized cost of electricity is reduced by up to 17%.
- Fuel consumption is reduced by up to 31%.

ARTICLE INFO

Article history:
Received 8 May 2015
Received in revised form 18 November 2015
Accepted 26 November 2015

Keywords:
Concentrating solar-thermal energy
Hybrid solar receiver combustor (HSRC)
Resource variability

ABSTRACT

The impact of avoiding the start-up and shut-down losses of a solar thermal power plant by directly integrating the back-up boiler into a tubular solar-only cavity receiver is studied using a multiple time-step, piecewise-continuous model. A steady-state analytical model of the mass and energy flows through both this device and a solar-only cavity receiver reported previously are incorporated within a model of the solar power generating plant with storage. The performance of the Hybrid Solar Receiver Combustor (HSRC) is compared with an equivalent reference conventional hybrid solar thermal system employing a solar-only cavity receiver and a back-up boiler. The model accounts for start-up and shut-down losses of the boiler, threshold losses of the solar-only cavity receiver and the amount of trace heating required to avoid cooling of the heat transfer fluid. The model is implemented for a 12 month/five year time-series of historical Direct Normal Irradiation (DNI) at 1 h time-steps to account for the variability in the solar resource at four sites spanning Australia and the USA. A method to optimize the size of the heliostat field is also reported, based on the dumped fraction of solar power from the heliostat field. The Levelized Cost of Electricity (LCOE) for the HSRC configuration was estimated to be reduced by up to 17% relative to the equivalent conventional hybrid solar thermal system depending on the cost of the fuel, the storage capacity and the solar resource, while the fuel consumption was estimated to be reduced by some 12–31%.

1. Introduction

The need to mitigate greenhouse gas emissions is driving the development of technologies to harness renewable energy sources such as solar and wind, which are abundant in nature [1]. However, these forms of energy are also diffuse and intermittent. Two of the potential solutions to manage cost effectively the intermittent nature of the renewable resources are storage technologies and hybrids with combustion technologies [2–4]. Of the various types of storage technologies, thermal energy storage (TES) is often the most desirable due to its high performance in energy storage density and energy conversion efficiency [5]. When coupled to a solar thermal plant, TES also allows electricity to be dispatched at times when the solar resource is unavailable. However, it is presently only cost-effective to address some of the variability this way [6], that is, it is unlikely to be economic to store enough energy to cover for periods of extended cloud [7]. Hybrids with fossil fuel systems are attractive in the short term because renewable energy provides a means to reduce CO_2 emissions, while fossil fuels inherently contain stored chemical energy readily available at a low cost [8]. For these reasons a combination of thermal energy storage and hybrid systems offers the potential to provide some CO_2 mitigation at moderate cost, together with a continuous electricity output [9]. In the longer term, the combustion source could be provided from

* Corresponding author at: The University of Adelaide, 5005, Australia. Tel.: +61 425748780.
E-mail address: jin.lim@adelaide.edu.au (J.H. Lim).

http://dx.doi.org/10.1016/j.apenergy.2015.11.028
0306-2619/

Nomenclature

$\widetilde{C}$	concentration ratio
A	area (m^2)
I	solar irradiation (W/m^2)
Q	energy (J)
$\dot{Q}$	heat transfer rate (W)
$\dot{W}$	work rate = power output (W)

Greek symbols

σ	Stefan-Boltzmann constant
η	efficiency
χ	fraction

Abbreviations

CST	Concentrating Solar Thermal
DNI	Direct Normal Irradiation
EPGS	Electrical Power Generating System
HSRC	Hybrid Solar Receiver Combustor
IEA	International Energy Agency
LCOE	Levelized Cost of Electricity
PBR	Power Block Ratio
SGH	Solar Gas Hybrid
TES	Thermal Energy Storage

Subscripts

ap	aperture
boil	boiler
cap	capacity
comb	combustion
crit	critical or threshold value
dump	dumped
DN	Direct Normal
elec	electrical
exh	exhaust
gen	generator
helio	heliostat
min	minimum
noz	nozzle opening
rec	solar receiver
salt	molten salt
sec	secondary air
sol	solar
stm	steam
sto	storage
t	time (years)
th	thermal output
trace	trace heating
use	useful

biomass or other forms of low-carbon-intensive fuel. In light of this, there is a need for hybrid thermal energy systems to complement renewable energy sources.

One recently proposed hybrid technology concept utilising energy storage is the Hybrid Solar Receiver Combustor (HSRC), of Nathan et al. [10]. Their preliminary economic evaluation found that, relative to the nearest equivalent system with a separate solar-only cavity receiver and a boiler, termed the solar gas hybrid (SGH), the HSRC reduces the capital cost of the overall power system, which includes the storage tanks, steam generator, Electrical Power Generating System (EPGS) and backup boiler (for the SGH) system, by up to 18% and overall LCOE by up to 11% for a 100 MW_{th} receiver size [11]. However, that assessment was based only on annually averaged performance of the plant and did not consider the influence of the variability of the solar resource. Lim et al. has recently developed an analytical model consisting of heat transfer and energy balance equations, which can be used to model performance of the HSRC at each time-step in a data string of solar resource. That model was used to determine the dimensions of the HSRC required to achieve similar efficiencies to that of a solar-only cavity receiver and a conventional boiler, and to estimate the subsequent weight of the device relative to a solar-only device [12]. The assessment confirmed that configurations can be found for which the combustion-only model of the HSRC achieves similar performance to the stand-alone boiler for a weight that is approximately double that of a solar-only device, justifying a key assumption in the economic assessment of Nathan et al. [11]. However, the economic study by Nathan et al. also did not consider the further potential benefits associated with avoiding the start-up and shut-down losses of a boiler and the trace heating required to maintain the temperature of the working fluid (here molten salt) for the solar-only cavity receiver. In addition, the minimum threshold of solar flux required for the HSRC is expected to be lower than that of the SGH, the benefits of which was also not analysed in their assessment. Hence, there is a need to account for the effects of resource variability both on the actual differences in operation and on the influence of start-up and shut-down losses on the potential additional benefits of the integrated HSRC device over the SGH.

For a conventional SGH to be run continuously, it is necessary to operate the boiler in "stand-by" mode for periods. This requires maintaining the boiler at a sufficiently high temperature, and/or starting it up before the steam is needed, to allow the boiler to be brought on line when required during periods of low solar insolation. For this reason, both start-up and shut-down losses are incurred during the transitions between solar-only and combustion-only operation, which leads to additional fuel consumption. In addition, the rate at which the boiler can be heated up is limited by the thermal stresses on the walls of the boiler [13]. Hence, the heat-up time for a boiler is set by the manufacturer's specification. Furthermore, the minimum capacity of a conventional boiler is also limited, with a typical turndown ratio of the maximum to minimum throughput being in the range of 3–4 [14]. The HSRC offers the potential to avoid most of these losses because it replaces the two units with a single device that is kept warm continuously by either Concentrating Solar Thermal (CST) or combustion. However, the magnitude of these potential benefits depends both on the start-up and shut-down requirements of the boiler and on the solar resource variability (seasonal, diurnal and weather-based), so that they can only be evaluated reliably by a model that accounts for all of these factors. Hence the present paper also aims to compare the influence of start-up and shut-down losses from the two types of hybrid system.

In a conventional SGH as with any solar power tower system, a trace-heating system is needed to maintain above its freezing point the temperature of the heat transfer fluid within the piping system [15,16]. The current state-of-the-art heat transfer fluid in solar thermal systems around in the world is molten salt, although other fluids are also being considered [17]. The need for electrical trace heating brings significant challenges. For example, non-uniform

trace heating of the pipes during the installation of the Solar Two Project caused a five month delay and required extensive replacement and reinstallation of the whole system, resulting in unnecessary expenditure [15]. In addition, the use of electrical trace heating imposes a significant energy penalty because the conversion of heat to electricity invokes the losses of the Rankine cycle, which is typically only some 30–40% efficient [15]. In contrast, the HSRC operates continuously, which offers potential to avoid or greatly reduce the need for trace heating. However, the extent of these benefits also depends on the intermittent nature of the resource, which is also difficult to evaluate without a dynamic model. While the impact on the capital cost of the amount of trace heating required is difficult to evaluate without a detailed design of both the receiver and the associated piping network, the power consumption can be estimated on the basis of the resource and published data on power consumption. Hence a further aim of the present investigation is to estimate the potential benefits in terms of avoided trace heating on the net power consumption of the HSRC relative to the SGH.

In light of the above background, the first aim of this paper is to develop a piecewise-continuous (i.e. pseudo-dynamic) model of the power plant for a novel hybrid solar receiver combustor, the HSRC, employing molten salt as the heat transfer fluid. The second aim is to compare the power consumption both from combustion and trace heating for the HSRC relative to the SGH, for the scenario in which continuous power output is to be maintained throughout one or more years of historical solar DNI data. This paper also aims to calculate the solar fraction from both systems and estimate the relative change in overall LCOE for both systems, and so to more reliably estimate the economic benefits of the HSRC relative to the SGH.

2. Methodology

The model developed extends the work of Lim et al. [12] to also include the storage tanks, a steam generator and an EPGS, using MATLAB as a programming tool. The pseudo-dynamic performance is then calculated for both the SGH and the HSRC by assuming steady state operation at each time-step from a time-series of hourly DNI data from the National Solar Radiation Database and Bureau of Meteorology (BOM) at selected sites from the USA and Australia respectively. The majority of cases are assessed for the full 12 months of the year 2000 for USA sites and the year 2002 for Australia sites to account for seasonal variation in solar heat flux. For key results, in particular for the LCOE calculations, data that spans five years (years 2000–2004) is used to account for year-to-year variability in solar heat flux. The sites chosen are Daggett (USA), Prescott Love Field (USA), Darwin (AUS) and Mildura (AUS), each of which has a high annual solar radiation [7].

2.1. Schematic diagram

Fig. 1 shows the schematic diagram for the reference SGH system, the terminology for which is presented in the Nomenclature section. Note that the boiler is coupled into the system in such a way that it can provide heat to the EPGS, when the heat is not available from the solar resource either directly, from the receiver, or indirectly from the storage tank following the work of Kueh et al. [7]. The concentrated solar radiation from the heliostat field, $\dot{Q}_{helio}$, is introduced into the cavity receiver, heating the working fluid through the tubes. The useful heat from the receiver, $\dot{Q}_{rec,out}$ is stored in the hot storage tank, to be used by the steam generator when needed. When the hot storage tank has reached its storage limit, the excess power is dumped ($\dot{Q}_{tank(hot),dump}$). The value of $\dot{Q}_{rec,out}$ is set to a constant value of 100 MW_{th} for all scenarios considered here to provide a consistent basis for comparison, although other scenarios are also possible.

Fig. 2 presents a schematic diagram of the HSRC system. The main difference between this system and the SGH (Fig. 1) is the integration of the boiler within the solar-only cavity receiver, as described by Lim et al. [12]. Similar to the SGH system, the thermal power output from the HSRC, $\dot{Q}_{HSRC,out}$, is set to a constant value of 100 MW_{th}. From this, a direct comparison between the SGH and HSRC can be performed.

2.2. Logic control diagram

Fig. 3 presents the logic diagram for the control of the SGH system in response to the solar variability. Here, $\dot{Q}_{helio}$ is directed into the solar-only cavity receiver, where it is used if it exceeds the minimum threshold for which the gains exceed the losses. Below this threshold the trace heating system is turned on and the molten salt is heated to prevent solidification. The value of $\dot{Q}_{helio}$ is then compared with the maximum allowable thermal output from the solar-only cavity receiver, $\dot{Q}_{rec,max}$. If it exceeds this, the surplus is dumped. The useful heat from the receiver, $\dot{Q}_{rec,out}$, is then used to fill the hot storage tank unless it is already full, and the boiler is operated only if the power obtained from the hot storage tank, $\dot{Q}_{tank(hot)}$ is insufficient to meet the demand of the EPGS. In this SGH system, it is assumed that the boiler is operated optimally

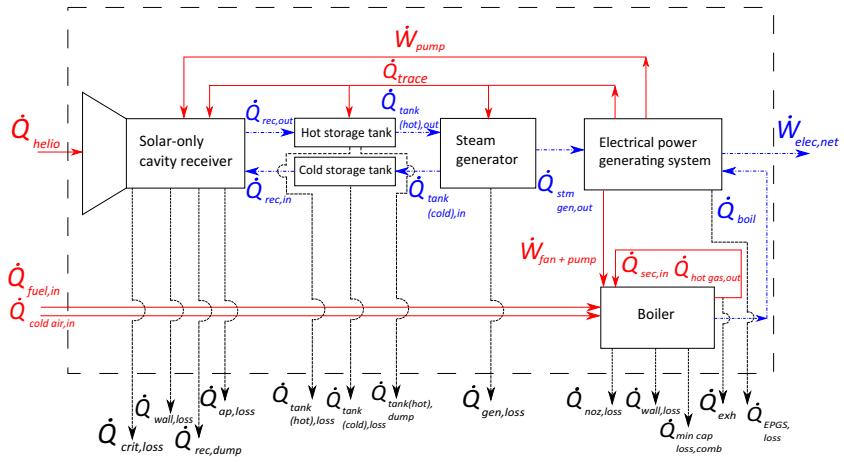

Fig. 1. Schematic diagram of the power flows through the solar gas hybrid, SGH, system.

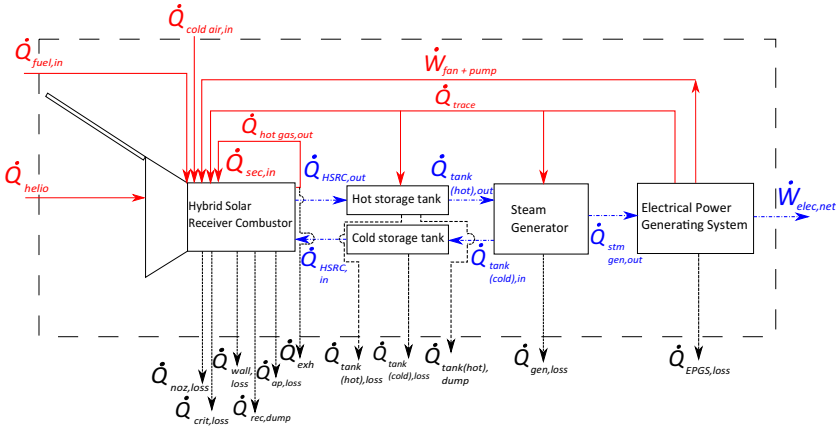

Fig. 2. Schematic diagram of the power flows through the hybrid solar receiver combustor, HSRC, system.

for start-up. That is, when power from the boiler is required, fuel consumption is calculated to account for the heat up based on the number of hours the boiler has been out of operation and for the power required to meet the thermal load. This would require good forecasting to be achieved.

Fig. 4 presents the logic diagrams for the control of the HSRC system. The system is similar to that of the SGH, except for the absence of a separate boiler. This, in turn, eliminates the need to start-up the boiler. Supplementary fuel is introduced into the HSRC to keep the receiver warm and meet the power demand. The thermal output from the receiver was set to be 100 MW_{th} for each system.

2.3. Heliostat field size

The area of the mirrors in the heliostat field, A_{helio}, was varied systematically, together with the rated capacity of the hot storage tank, $\dot{Q}_{tank(hot),max}$, for power block ratios (PBR) of 0.4, 0.6 and 0.8 times the maximum capacity of the solar-only cavity receiver or HSRC following Kueh et al. [7], as follows:

$$\text{PBR} = \frac{\dot{Q}_{tank(hot),max}}{\dot{Q}_{rec,max} \text{ or } \dot{Q}_{HSRC,max}}, \quad (1)$$

where $\dot{Q}_{HSRC,max}$ is the maximum allowable thermal output from the HSRC. The value of $\frac{\dot{Q}_{tank(hot),dump}}{\dot{Q}_{tank(hot),max}}$, was calculated and set to avoid more than 5% dumping of the total power output from the hot storage tank, $\dot{Q}_{tank,hot(out)}$, where $\dot{Q}_{tank(hot),dump}$ is the net amount of solar heat flux dumped from the hot storage tank.

2.4. Solar input threshold

The lower threshold for solar input is defined as the minimum solar radiation to the HSRC/solar-only cavity receiver needed to exceed the convective and radiant losses from it.

To determine threshold of solar input for HSRC, the total losses are calculated as follows:

$$\dot{Q}_{loss,total} = \dot{Q}_{noz,loss} + \dot{Q}_{ap,loss} + \dot{Q}_{wall,loss}. \quad (2)$$

These losses are all calculated with the cavity at its design temperatures, to achieve an output temperature of the molten salt of 565 °C, following the details described in our previous study [12]. Briefly, $\dot{Q}_{noz,loss}$ represents the total radiative and convective losses through the nozzle (burner) openings, $\dot{Q}_{ap,loss}$ are the total losses through the aperture and $\dot{Q}_{wall,loss}$ represents the total losses from the walls.

To determine the threshold of solar input for a solar-only cavity receiver [7]:

$$1 - \eta_{helio} = 1 - \frac{\sigma T_{rec}^4}{I_{DN}\widetilde{C}}, \quad (3)$$

where η_{helio} is the optical efficiency of the heliostat field, σ is the Stefan–Boltzmann constant, T_{rec} is the average temperature of the cavity receiver, I_{DN} is the incoming DNI and $\widetilde{C}$ is the concentration ratio. The concentration ratio was assumed to be $\widetilde{C}$ = 1000, which is a typical value for CST systems with a solar-only cavity receiver, similar to the approach by Kueh et al. [7].

2.5. Start-up times for the boiler and HSRC

The start-up time for a conventional boiler depends strongly on the duration for which the boiler is out of operation. These have been calculated following Li et al., as per Table 1 [18]. In addition, the turndown ratio of the boiler is assumed to be 3.333 [14].

For the case of the HSRC, it is assumed that the same trace-heating system employed to maintain the temperature of the heat transfer fluid above its freezing point will also keep the cavity of the HSRC warm when the plant is operated from stored thermal energy. This results in additional electrical power consumption but eliminates the need to start-up the HSRC ahead of the time when fuel is needed for operation. In all other instances, the HSRC will be in operation using either solar energy, combustion or a combination of both.

2.6. Trace heating

To calculate the amount of trace heating required to prevent solidification of the heat transfer fluid, the following formula was used:

$$\dot{Q}_{trace} = 1.1 \times \left(\dot{Q}_{trace,perpipe} \times \text{no.pipe} \times (\text{length}_{pipe,salt} + (\text{tower height} \times 2))\right). \quad (4)$$

Here the value $\dot{Q}_{trace,perpipe}$ was obtained following Rodriguez-Garcia et al. [16], the number and length of the pipes carrying the working fluid was determined from Lim et al. [12] and the tower height was assumed to be 120 m based on a similar ratio of height to total thermal output to that of the Gemasolar tower,

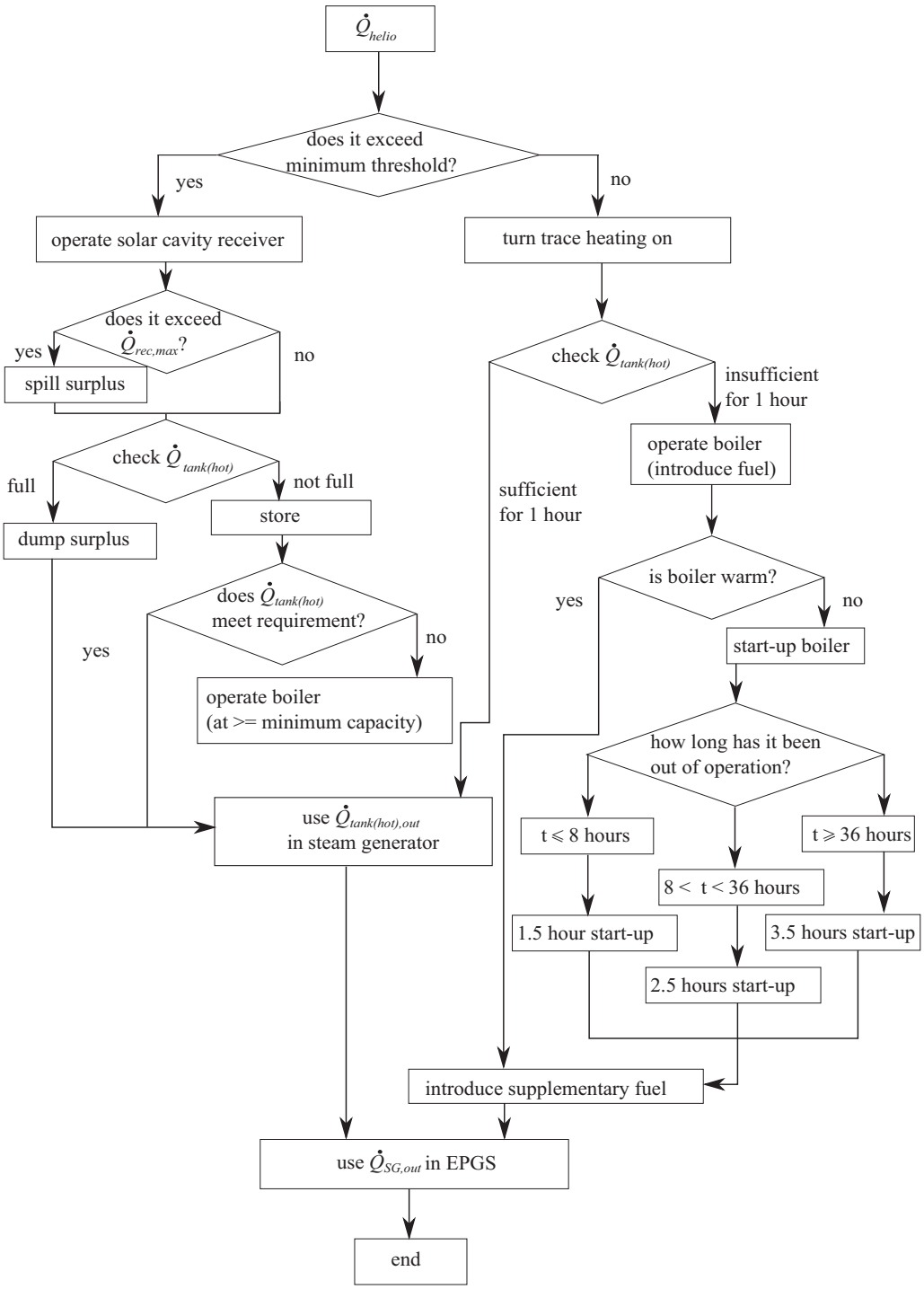

Fig. 3. Logic diagram used to control the SGH system in response to solar resource variability.

which is 145 m tall with a 120 MW thermal output [20]. The additional 10% is added to the overall power to account for the need to heat miscellaneous components and the storage system.

2.7. Solar fraction

The definition of solar fraction for a period t (e.g. one year), $\chi_{solar,t}$, is as follows:

$$\chi_{solar,t} = \frac{\dot{Q}_{helio,t}}{\dot{Q}_{rec,out,t} + \dot{Q}_{boil,t} \text{ or } \dot{Q}_{HSRC,out,t}}, \quad (5)$$

where

$\dot{Q}_{helio,t}$ represents the total amount of solar power introduced into either the SGH or HSRC system for year t, while $\dot{Q}_{rec,out,t}$ is the total thermal output from the solar-only cavity receiver for year t and $\dot{Q}_{boil,t}$ is the total thermal output from the boiler for year t. $\dot{Q}_{HSRC,out,t}$ is the total thermal output from the HSRC for year t.

2.8. Levelized cost of electricity

The levelized cost of electricity (LCOE) was calculated using parameters defined in Table 2 to enable a reasonable comparison of the relative merit of the HSRC in comparison with the SGH, to

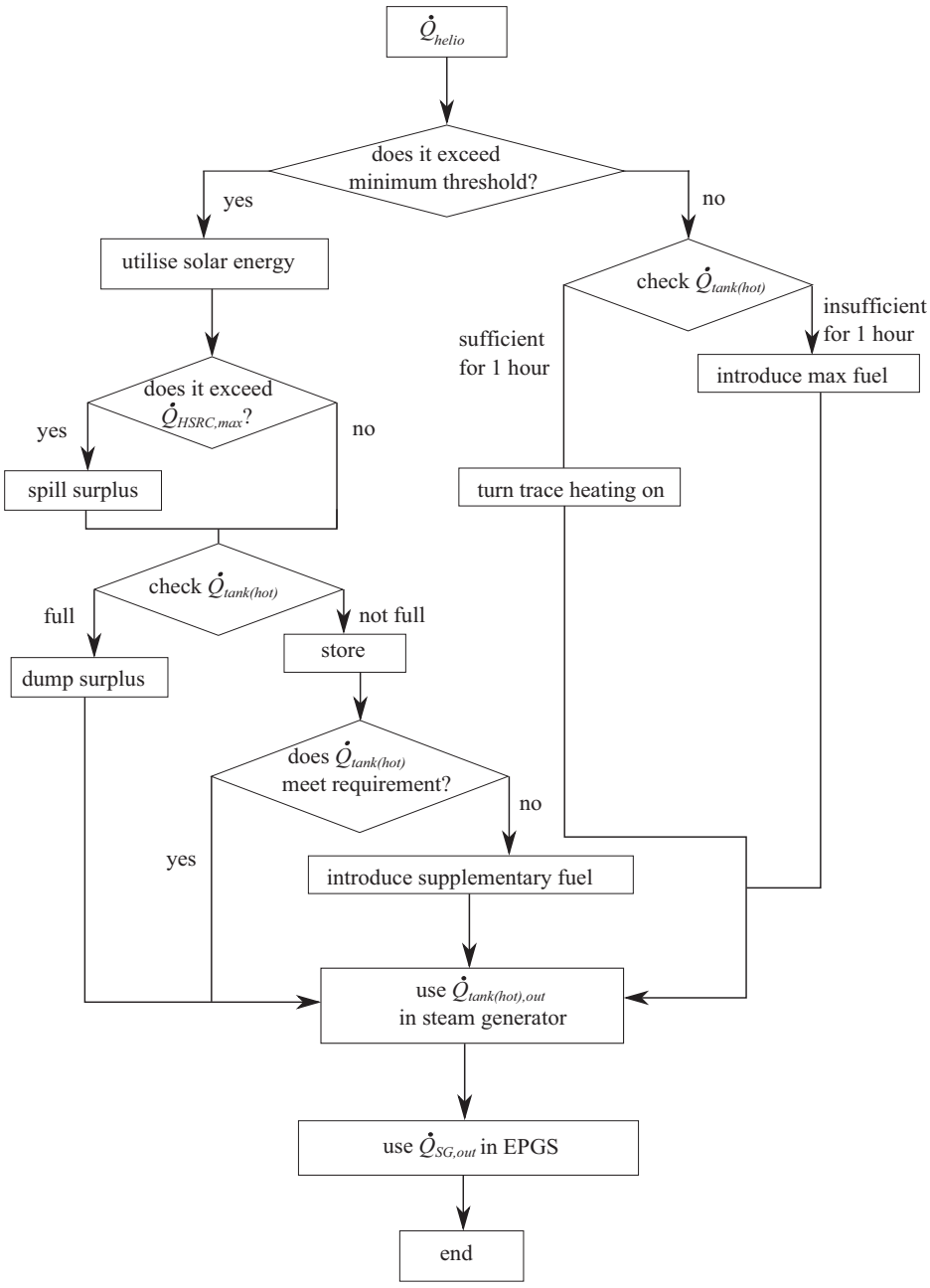

Fig. 4. Logic diagram used to control the HSRC system in response to solar resource variability.

Table 1
The required time to start-up a boiler as a function of the time for which it has been out of operation, following Li et al. [19]. The average start-up time was used in the piecewise-continuous model.

Time out of operation (h)	Range of start-up time (h)	Average start-up time (h)
⩽8	1–2	1.5
8–36	2–3	2.5
⩾36	2–5	3.5

avoid the challenge of obtaining absolute values for a particular location. Hence we have followed Nathan et al. [11] in selecting the values and correlations of cost from Sargent and Lundy [21].

The LCOE was calculated with the following formula obtained from International Energy Agency (IEA) [22]:

$$\mathrm{LCOE}_{\mathrm{overall}} = \frac{\sum_t \left((\mathrm{Investment}_t + O\&M_t + \mathrm{Fuel}_t + \mathrm{Carbon}_t + \mathrm{Decommissioning}_t) * (1+r)^{-t}\right)}{\sum_t \left(\mathrm{Electricity}_t * (1+r)^{-t}\right)} \quad (6)$$

Here t represents the year, $\mathrm{Investment}_t$ is the cost of investment in year t, $O\&M_t$ is the operations and maintenance costs for year t, Fuel_t is the fuel costs for year t, Carbon_t is the total cost of carbon emissions for year t (e.g. from a carbon tax), $\mathrm{Decommissioning}_t$ is the decommissioning cost for year t, r in the term $(1+r)^{-t}$ is the discount factor for year t, and $\mathrm{Electricity}_t$ is the amount of electricity produced in year t. Also following Nathan et al., the life of the plant was assumed to be 30 years, while the present comparison conservatively ignores the costs of carbon emissions and decommissioning as well as inflation [11]. The discount factor is assumed to be equivalent to the assumed internal rate of return of 10% over the project

Table 2
Correlations and values used in the present LCOE calculations (US dollars).

Component cost	Correlation/value	Unit	References
Heliostats	216	$/m^2	[21]
Salt-cooled receiver	3.52 $\dot{Q}_{rec,max}^{0.44}$	$M	[21]
Tower	0.0305 $\dot{Q}_{rec,max}$ + 0.961	$M	[21]
Thermal storage	0.0153 Q_{sto} + 0.502	$M	[21]
Steam generator	0.212 $\dot{Q}_{SG,out,max}^{0.7}$	$M	[21]
EPGS	1.84 $\dot{Q}_{SG,out,max}^{0.7}$	$M	[21]
Gas-fired boiler	1.69 $\dot{Q}_{boil,max}^{0.7}$	$M	[24]
Operation & maintenance			
Solar field	1.88 A_{helio} + 0.189	$M/yr	[21]
Plant	0.0151 $\dot{W}_{elec,net}$ + 2.92	$M/yr	[21]
Fuel cost (Natural gas)	2–15	$/GJ	[21]
Levelized cost calculation parameters			
Internal rate of return	5–20%		
Plant life	30 years		

life for most of the calculations done. A sensitivity study of the discount factor was also performed for ranges between 5% and 20%.

Table 2 shows the correlations used in the LCOE calculations. Correlations for the gas-fired boiler and EPGS are based on data obtained from literature where a capacity scaling exponent of 0.7 was applied based on the thermal input. The cost of the HSRC is assumed to be twice of that of the solar cavity receiver to account for the additional fans and combustion system. This is consistent with the assessment done by Lim et al. who found that the weight of the HSRC is twice of that of a solar cavity receiver, subsequently doubling its cost [12]. The costs of all other components of the systems are obtained from Sargent and Lundy and Bemis and DeAngelis [21,24].

According to IEA, the cost of fuel is a key component of the overall cost of electricity generation for systems utilising fossil fuels [22]. Most of the calculations were performed for the reference scenario in which the cost of natural gas is at a relatively low value of $USD3/GJ (to allow a direct comparison with the earlier assessment of Nathan et al. [11]). This is only slightly below the current average price of natural gas in the USA of approximately $USD3.8/GJ, but within the range at which the price fluctuates [25]. However, the current price of natural gas in Australia is approximately $USD4/GJ while Europe is higher at $USD8/GJ. The import price of natural gas in Asia is as high as $USD15/GJ [25]. Hence, the influence of the price of fuel was assessed by a sensitivity analysis of the LCOE for gas prices between $USD2/GJ and $USD15/GJ.

2.9. System component efficiencies

Table 3 presents the assumed efficiency for the other system components used in the model to calculate the annual electricity produced.

The efficiency of the HSRC in solar-only and combustion-only mode was defined by an analytical model of the device developed by Lim et al. where the following equations were used [12]:

$$\eta_{\text{sol-only}} = \frac{\dot{Q}_{\text{HSRC,out}}}{\dot{Q}_{\text{helio}}} \tag{7}$$

Table 3
System components and their efficiencies.

System component		HSRC	SGH	References
Solar cavity receiver	%	(7)	0.89	[23]
Storage tanks	%	0.99	0.99	[15]
Electricity Power Generating System (EPGS)	%	0.41	0.41	[15]
Boiler (for SGH)	%	(8)	0.86	[11]

and $$\eta_{\text{comb-only}} = \frac{\dot{Q}_{\text{HSRC,out}}}{\dot{Q}_{\text{fuel,in}}}. \tag{8}$$

Here $\dot{Q}_{\text{HSRC,out}}$ and $\dot{Q}_{\text{helio}}$ have previously been defined and $\dot{Q}_{\text{fuel,in}}$ is the total power from the combustion of fuel (assumed to be natural gas).

In the mixed-mode of operation, a similar approach was used to calculate the efficiency of the device and is defined by the following equation:

$$\eta_{\text{mix}} = \frac{\dot{Q}_{\text{HSRC,out}}}{\dot{Q}_{\text{helio}} + \dot{Q}_{\text{fuel,in}}}. \tag{9}$$

Because this study only compares the relative performance of the HSRC to the SGH, it is not necessary to model the other system components, i.e. storage tanks and EPGS, in detail.

3. Model verification

The heat transfer within the HSRC is calculated using the validated analytical model of Lim et al. [12]. The pseudo-dynamic modelling approach adopts the same procedure as Kueh et al. [7]. A verification process has also been performed whereby the trends of the SGH and HSRC systems were analysed and checked to ensure that the flows of power are consistent with expectation. The total power input has to be equivalent to the sum of the total power output and power losses.

Figs. 5 and 6 present two short-term time series of power flows through the SGH and HSRC systems, respectively, for periods of 4 days. Both were also conducted for the case at which the PBR is 0.8 and for the site of Daggett (USA). It can be seen that the total power input matches the total power output and losses. For example, as $\dot{Q}_{\text{helio}}$ increases at t = 10, 32, 60, 85 h, the value of $\dot{Q}_{\text{tank(hot),out}}$ also increases, until the storage tank reaches its maximum capacity, after which the remainder is dumped ($\dot{Q}_{\text{tank(hot),dump}}$). When $\dot{Q}_{\text{helio}}$ is below the threshold, the boiler or HSRC is used to produce thermal power, resulting in an increase in $\dot{Q}_{\text{boil}}$ or $\dot{Q}_{\text{HSRC,out(comb)}}$ respectively. The value of $\dot{Q}_{\text{tank(hot),dump}}$ becomes positive when the hot storage tank is full and there is excess of solar power from the heliostats.

4. Results and discussion

Fig. 7 presents the distribution of power inputs and losses for both the HSRC and SGH for the cases of 1, 5 and 10 h of thermal storage capacity, for the configurations in which the PBR = 0.4, 0.6 and 0.8 at the site of Daggett. This site was chosen as the reference site based on the analysis of Kueh et al. [7], who found that, of the six sites they assessed, it has the lowest vulnerability to unscheduled reduction in output due to solar resource variability for a solar-only plant. The figure shows that the power required for trace heating is low (0.077 GW_{th}/year) for the HSRC system with a low storage capacity (i.e. 1 h) because the working fluid in the device is continuously heated. In contrast, the power required for trace heating of the equivalent SGH case is still significant (65.01 GW_{th}/year) owing to the need to heat the system electrically during periods of low insolation. This difference results in significant power savings for the HSRC. As the storage capacity is increased, the power required for trace heating power decreases because the trace heating is required only when power is withdrawn from the storage tank. It is also important to note that the trace heating power reported in this figure is the electrical heat required, which is sourced from the EPGS. That is, the gross power consumption required for trace heating is approximately 2.4 times

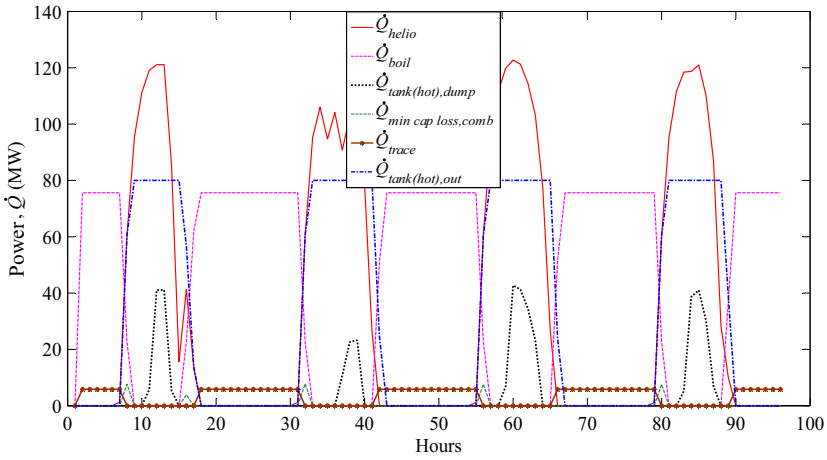

Fig. 5. Short-term time series of the power flows through the HSRC system to provide qualitative verification of the performance of the model for the dates 01.01.2000–04.01.2000 at the site of Daggett. The power block ratio, PBR = 0.8.

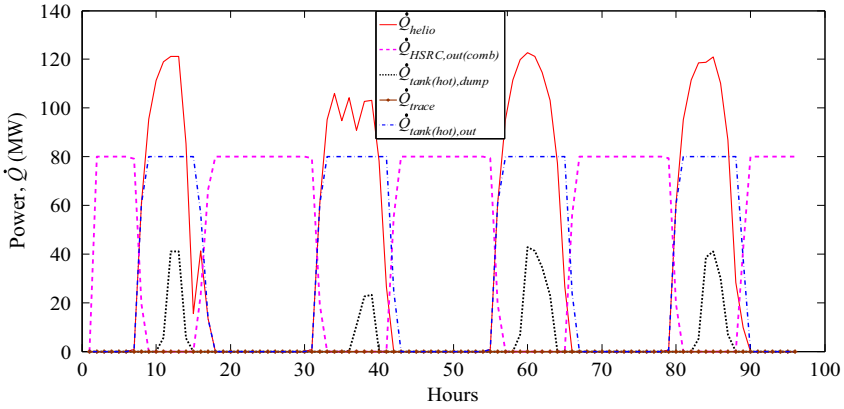

Fig. 6. Short-term time series of the power flows through the SGH system to provide qualitative verification of the performance of the model for the dates 01.01.2000–04.01.2000 at the site of Daggett. The power block ratio, PBR = 0.8.

greater, because the thermal efficiency of the EPGS is assumed to have a typical value of 42%.

The power consumption required for combustion is higher for the SGH than for the equivalent HSRC by values of 12%, 17% and 31%, for storage capacities of 1, 5 and 10 h, respectively. This is due to the need to start-up the boiler for the SGH case, which is not required for the HSRC. In addition, in some instances the limited turndown of the boiler results in some occasions for which the minimum output from the boiler exceeds the requirement of the SGH system, which results in an additional loss (contributing to approximately 10% of the increased fuel consumption). The percentage difference in the power generated from the combustion process increases with the storage capacity. For the largest storage capacity of 10 h, the percentage difference in fuel consumption is 31%, even though the total fuel consumption decreases as the storage capacity is increased. The threshold losses are also lower for the HSRC than for the SGH. However, the magnitude of these losses is small relative to the other losses. The trends are consistent for all cases of normalized power block capacity.

Fig. 8 presents the solar fraction calculated for all cases of 1, 5 and 10 h of thermal storage capacity, for the configurations in which the PBR = 0.4, 0.6 and 0.8, also for the site of Daggett. As expected, the solar fraction increases with the size of the storage capacity since storage increases the time over which the solar power is utilised. However, in addition, the solar fraction of the HSRC can be seen to be some 0.5–1.7% higher than for the equivalent SGH. This is because the HSRC utilises more solar radiation at lower thresholds than does the SGH, which also results in more fuel savings for the HSRC system.

Fig. 9 presents the sensitivity to the selection of the site of the distribution of power through the two systems for the cases of 1, 5 and 10 h of thermal storage capacity, for the configurations in which the PBR = 0.4, 0.6 and 0.8, for the locations of Daggett, Prescott Love Field (PLF), Mildura, and Darwin following Kueh et al. [7]. This shows that the solar contribution differs at every site, with Daggett having the highest solar input (301 GW_{th}/year for the case of the HSRC with 1 h of thermal storage) followed by PLF (278 GW_{th}/year), Darwin (241 GW_{th}/year) and Mildura (235 GW_{th}/year). The results are consistent with the known differences in DNI at each location and with the trends from the previous analysis of Kueh et al. [7]. Similarly, the amount of trace heating required increases from 0.077 GW_{th}/year at Daggett to 0.154 GW_{th}/year at Mildura for the case of the HSRC with 1 h of thermal storage, owing to the increased need to maintain the heat of the heat transfer fluid when solar is unavailable. Also, the power required from combustion is around 400 GW_{th}/year for the case of the HSRC with 1 h of thermal storage in Daggett, while it is higher at 466 GW_{th}/year in Mildura. All these results are consistent for all systems and storage capacities.

Fig. 10 presents the solar fraction calculated for a power block of 0.8, for all four locations. Similar to the previous analysis, the solar fraction is higher for larger storage capacities. As expected,

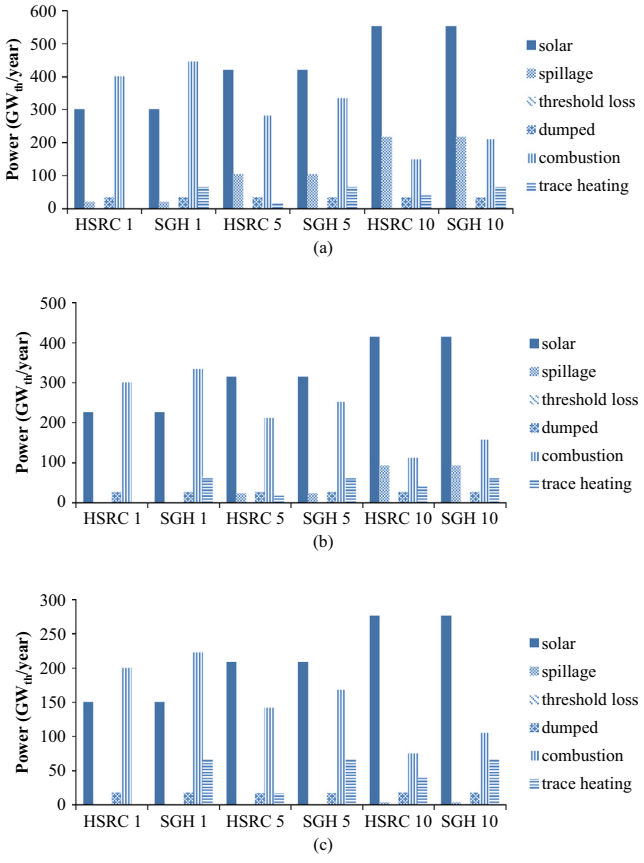

Fig. 7. Annually averaged distribution of power inputs and losses for both the Hybrid Solar Receiver Combustor (HSRC) and Solar Gas Hybrid (SGH) for the cases of 1, 5 and 10 h of thermal storage capacity at the site of Daggett. Data are reported for the configurations in which the normalized capacity of the power blocks relative to the peak solar input, PBR is: (a) 0.8, (b) 0.6 and (c) 0.4. Note that all data are reported as gross thermal power to and from the EPGS.

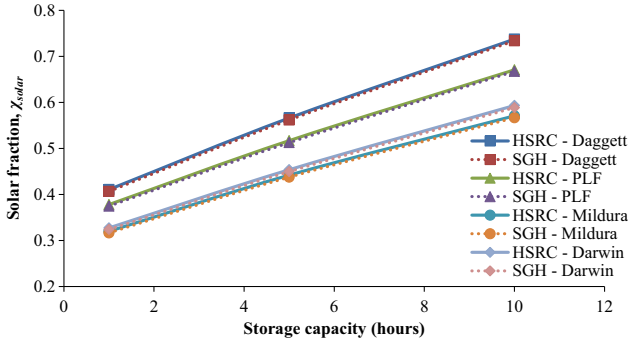

Fig. 8. The solar fraction based on the fraction of input power sources for the two types of hybrid at various capacities of normalized power block size at the site of Daggett.

the solar share is highest for Daggett, which has the highest average DNI. Significantly, the value of the solar share for these systems, all of which achieve full baseload output, for the case of 12 h storage spans the range of 0.73 for the DNI of Daggett to 0.57 for the sites of Mildura and Darwin, which have a similar solar share even though Darwin has a higher average DNI. This difference is because the heliostat field area is different for each, being optimized to achieve a similar fraction of power dumped, as discussed above. Prescott Love Field has an intermediate value solar fraction at 0.66. For each location, the solar fraction of the HSRC

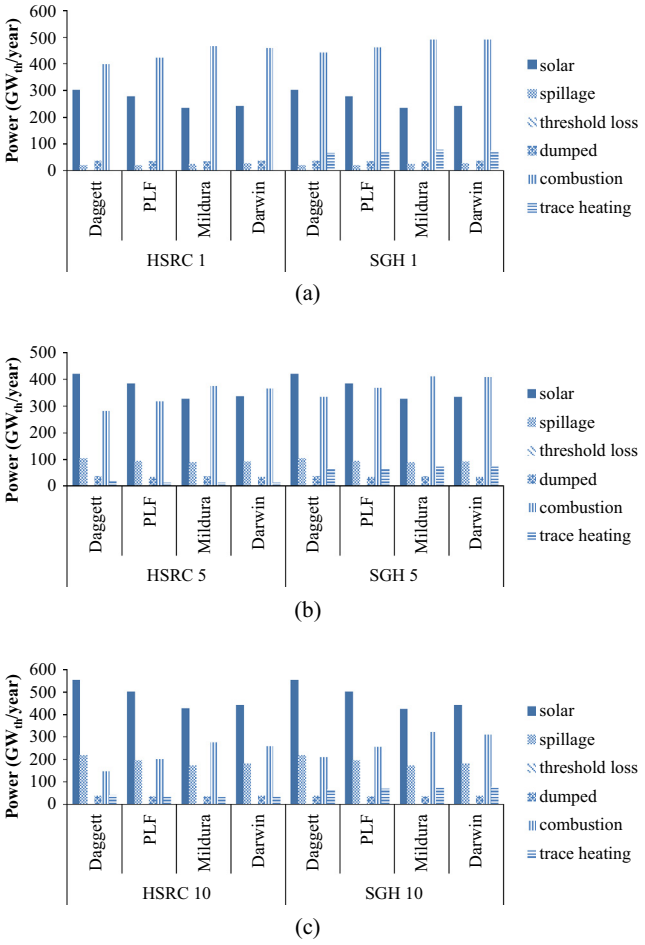

Fig. 9. Annually averaged distribution of power inputs and losses for both the Hybrid Solar Receiver Combustor (HSRC) and Solar Gas Hybrid (SGH) for the cases of (a) 1, (b) 5 and (c) 10 h of thermal storage capacity at the sites of Daggett, PLF, Mildura and Darwin. Data are reported for the configurations in which the normalized capacity of the power block relative to the peak solar input, PBR = 0.8. Note that all data are reported as gross thermal power to and from the EPGS.

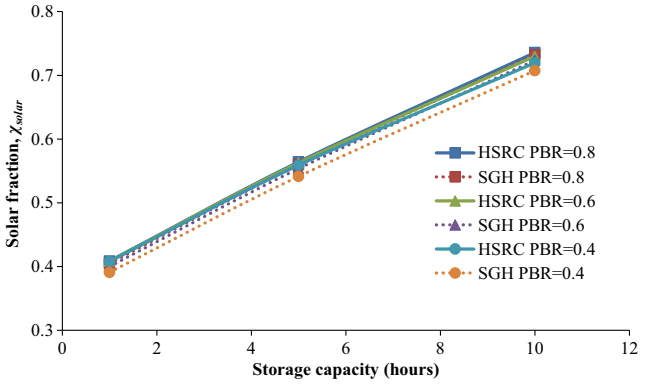

Fig. 10. The solar fraction based on the fraction of input power sources for the two types of hybrid for the same normalized capacity of the power block relative to the peak solar input, PBR = 0.8 at various locations.

system is up to 1.7% higher than that of the SGH, consistent with the previous analysis.

The results of LCOE calculations are presented in Fig. 11. It can be seen that the trends in LCOE calculation are consistent with those of Nathan et al. [11], which gives further confidence in the

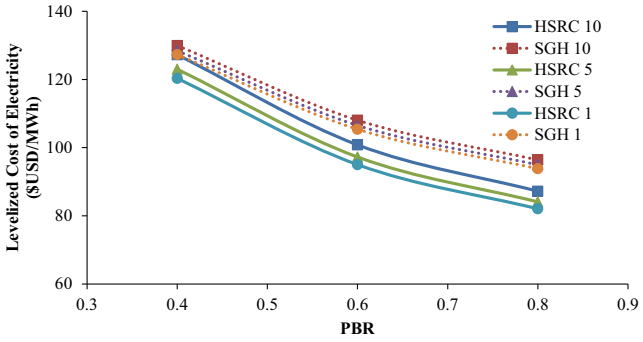

Fig. 11. The Levelized Cost of Electricity (LCOE) with differing power blocks relative to the peak solar input, PBR, for both the Hybrid Solar Receiver Combustor (HSRC) and the Solar Gas Hybrid (SGH) for the cases of 1, 5 and 10 h of thermal storage capacity at the site of Daggett.

model given that similar correlations have been used for the assessment. The overall LCOE is approximately 5–13% lower for the HSRC relative to the SGH for values of PBR between 0.4 and 0.8, respectively for all storage capacities. This percentage difference in LCOE is higher for larger scales due to the increase in fuel consumption which results in more savings for the HSRC system. The LCOE of both systems also decreases with increasing scale for all cases (consistent with the finding of Nathan et al. [11]). This can also be seen from the graph with the LCOE decreasing as the size of the power block increases. It is expected that more significant savings will be made with the HSRC system with increasing power block size.

Fig. 12 presents the sensitivity of LCOE to variations in gas price. As expected, the LCOE is calculated to increase with the price of gas and to increase more steeply for the SGH than for the HSRC owing to the higher fuel consumption of the former. For systems with thermal storage capacity of one hour, the percentage difference in LCOE between the SGH and HSRC relative to the SGH increases from 12% to 14% with the price of gas, while for systems with thermal storage capacity of 10 h, this percentage difference increases from 9% to 17%. This shows that the benefits of employing the HSRC are greater with higher fuel prices as the percentage difference of LCOE between the SGH and HSRC increases, for different sizes of thermal storage capacity.

Fig. 13 presents the sensitivity of LCOE to variations in the discount factor for each of the systems analysed. It can be observed that the LCOE increases linearly with the discount factor for each system, as expected. However, importantly, the relative difference between the LCOE of the two systems is only weakly dependent on

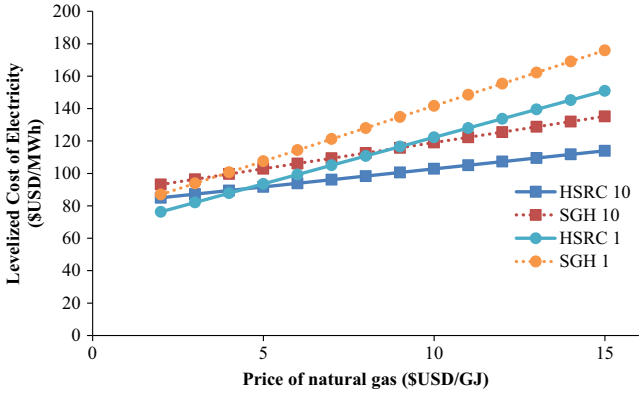

Fig. 12. The dependence of the Levelized Cost of Electricity (LCOE) on natural gas price for the Hybrid Solar Receiver Combustor (HSRC) and the Solar Gas Hybrid (SGH) for the cases of 1 and 10 h of thermal storage at the site of Daggett for the same normalized capacity of the power block relative to the peak solar input, PBR = 0.8.

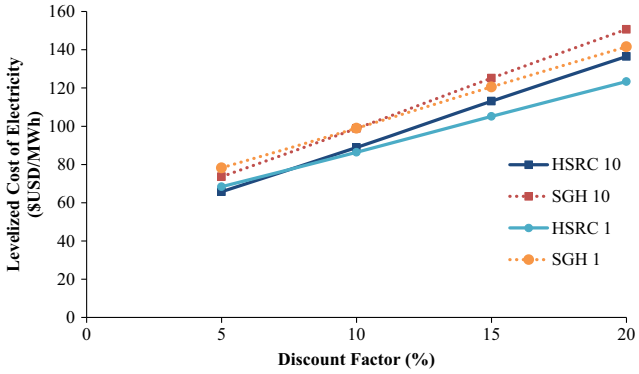

Fig. 13. The dependence of the Levelized Cost of Electricity (LCOE) on discount factor for the Hybrid Solar Receiver Combustor (HSRC) and the Solar Gas Hybrid (SGH) for the cases of 1 and 10 h of thermal storage at the site of Daggett for the same normalized capacity of the power block relative to the peak solar input, PBR = 0.8.

this ratio. For systems with a thermal storage capacity of 10 h, the percentage difference in LCOE between the SGH and HSRC relative to the SGH varies only between 9% and 11% for discount factors over the range of 5–20%, while it is independent of the discount factor at 13% over this entire range for a thermal storage capacity of 1 h.

5. Conclusion

The impact of direct integration of a combustion system into a cavity receiver on LCOE has been calculated more reliably than previously by accounting for solar resource variability and for the effects of start-up and shut-down using a piecewise-continuous (pseudo-dynamic) model. This has found that, for sites with high annual average DNI (reference case of Daggett, USA):

- The Hybrid Solar Receiver Combustor, HSRC, reduces the net fuel consumption relative to the equivalent solar gas hybrid, SGH, by between 12% for the case of 1 h of thermal storage to 31% for the case of 12 h of thermal storage. Approximately 90% of this reduction is achieved by eliminating the power required to start the boiler after it has been switched off during transient operation in the conventional hybrid system. Some further benefits (approximately 10% of fuel savings) accrue from avoiding the losses associated with the minimum output from the boiler exceeding the requirement of the SGH system.
- The HSRC also increases the net electrical power output relative to the SGH by between 9%, for the case of 1 h of thermal storage, and 3.5% for the case of 10 h of thermal storage. This increase is a result of the reduced need for electrical trace-heating of the heat transfer fluid.
- The HSRC system achieves higher solar fractions relative to the SGH of between 0.5% for the case of 1 h of thermal storage to 1.7% for the case of 10 h of thermal storage as solar insolation at lower thresholds are utilised by the HSRC.
- The HSRC system decreases the cost of the overall LCOE by up to 14% for the case of 1 h of thermal storage and up to 17% for the case of 10 h of thermal storage compared to the SGH for fuel (natural gas) prices ranging from $USD2/GJ to $USD15/GJ.

Acknowledgements

The authors would like to acknowledge the support of the Australian Research Council and of FCT Combustion and Vast Solar through the ARC Linkage Grant LP110200060.

References

[1] International Renewable Energy Agency. Concentrating solar power; 2013.
[2] Pasamontes M et al. Hybrid modeling of a solar-thermal heating facility. Sol Energy 2013;97:577–90.
[3] Fath HES. Technical assessment of solar thermal energy storage technologies. Renew Energy 1998;14.
[4] Hu E et al. Solar thermal aided power generation. Appl Energy 2010;87(9):2881–5.
[5] Tian Y, Zhao CY. A review of solar collectors and thermal energy storage in solar thermal applications. Appl Energy 2013;104:538–53.
[6] Zhang HL et al. Concentrated solar power plants: review and design methodology. Renew Sustain Energy Rev 2013;22:466–81.
[7] Kueh K, Nathan GJ, Saw WL. Storage capacities required for a solar thermal plant to avoid unscheduled reductions in output. Solar Energy 2015 [accepted 16/04/15].
[8] Ordorica-Garcia G, Delgado AV, Garcia AF. Novel integration options of concentrating solar thermal technology with fossil-fuelled and CO_2 capture processes. Energy Proc 2011;4:809–16.
[9] Powell KM, Edgar TF. Modeling and control of a solar thermal power plant with thermal energy storage. Chem Eng Sci 2012;71:138–45.
[10] Nathan GJ et al. A hybrid receiver-combustor. A.R.I.P. Ltd; 2013.
[11] Nathan GJ, Battye DL, Ashman PJ. Economic evaluation of a novel fuel-saver hybrid combining a solar receiver with a combustor for a solar power tower. Appl Energy 2014;113:1235–43.
[12] Lim JH et al. Analytical assessment of a novel hybrid solar tubular receiver and combustor. Appl Energy 2016;162:298–307.
[13] Kruger K, Franke R, Rode M. Optimization of boiler start-up using a nonlinear boiler model and hard constraints. Elsevier Ltd.; 2004.
[14] Eoff D. Understanding fuel savings in the boiler room. ASHRAE J 2008;50(12):38–43.
[15] Reilly HE, Kolb GJ. An evaluation of molten-salt towers including results of the solar two project. New Mexico: Albuquerque; 2001.
[16] Rodriguez-Garcia M-M, Herrador-Moreno M, Zarza Moya E. Lessons learnt during the design, construction and start-up phase of a molten salt testing facility. Appl Therm Eng 2014;62(2):520–8.
[17] Medrano M et al. State of the art on high-temperature thermal energy storage for power generation. Part 2 – Case studies. Renew Sustain Energy Rev 2010;14(1):56–72.
[18] Yang D, Chen T. HGSSP – a computer program for simulation of once-through boiler start-up behavior. Heat Transfer Eng 2001;22(5):50–60.
[19] Li B, Chen T, Yang D. DBSSP – a computer program for simulation of controlled circulation boiler and natural circulation boiler start up behavior. Energy Convers Manage 2005;46(4):533–49.
[20] Romero M, Gonzalez-Aguilar J. Solar thermal CSP technology 2013.
[21] Sargent & Lundy LLC Consulting Group. Assessment of parabolic trough and power tower solar technology cost and performance forecasts. Chicago, Illinois: NREL; 2003.
[22] IEA. Projected costs of generating electricity; 2010.
[23] Hathaway BJ, Lipiski W, Davidson JH. Heat transfer in a solar cavity receiver: design considerations. 325 Chestnut St, Suite 800, Philadelphia, PA 19106, United States: Taylor and Francis Inc.; 2012.
[24] Bemis GR, DeAngelis M. Levelized cost of electricity generation technologies. Contemporary Policy Issues. VIII; 1990.
[25] NAB Group Economics. Natural gas market update – August 2014. N.A.B. Limited; 2014.

Statement of Authorship

Title of Paper	Assessment of the potential benefits and constraints of a hybrid solar receiver and combustor operated in the MILD combustion regime
Publication Status	☐ Published ☐ Accepted for Publication ☑ Submitted for Publication ☐ Unpublished and Unsubmitted w ork w ritten in manuscript style
Publication Details	Lim, JH, Chinnici, A, Dally, BB & Nathan, GJ 2016, 'Assessment of the potential benefits and constraints of a hybrid solar receiver and combustor operated in the MILD combustion regime', Energy (manuscript number: EGY-D-16-02149)

Principal Author

Name of Principal Author (Candidate)	Jin Han Lim		
Contribution to the Paper	Performed literature review. Developed the analytical model required for analysis. Wrote the manuscript. Responsible for submission process.		
Overall percentage (%)	60		
Certification:	This paper reports on original research I conducted during the period of my Higher Degree by Research candidature and is not subject to any obligations or contractual agreements with a third party that would constrain its inclusion in this thesis. I am the primary author of this paper.		
Signature		Date	18/7/16

Co-Author Contributions

By signing the Statement of Authorship, each author certifies that:

i. the candidate's stated contribution to the publication is accurate (as detailed above);

ii. permission is granted for the candidate in include the publication in the thesis; and

iii. the sum of all co-author contributions is equal to 100% less the candidate's stated contribution.

Name of Co-Author	Dr Alfonso Chinnici		
Contribution to the Paper	Assisted in developing analytical model of MILD hybrid solar receiver and combustor. Assisted with editing the manuscript.		
Signature		Date	18/07/16

Name of Co-Author	Professor Bassam Dally		
Contribution to the Paper	Supervised the work. Provided suggestions and recommendations to improve modelling approach. Assisted with editing the manuscript.		
Signature		Date	18/7/16

Name of Co-Author	Professor Graham Nathan		
Contribution to the Paper	Supervised the work. Suggested different approaches to analytical modelling. Assisted with editing and finalising the manuscript.		
Signature		Date	19/7/16

CHAPTER 5

ASSESSMENT OF THE POTENTIAL BENEFITS AND CONSTRAINTS OF A HYBRID SOLAR RECEIVER AND COMBUSTOR OPERATED IN THE MILD COMBUSTION REGIME

Energy 116 (2016) 735–745

Contents lists available at ScienceDirect

Energy

journal homepage: www.elsevier.com/locate/energy

Assessment of the potential benefits and constraints of a hybrid solar receiver and combustor operated in the MILD combustion regime

Jin Han Lim*, Alfonso Chinnici, Bassam B. Dally, Graham J. Nathan

Centre for Energy Technology, School of Mechanical Engineering, The University of Adelaide, SA 5005, Australia

ARTICLE INFO

Article history:
Received 12 May 2016
Received in revised form
5 October 2016
Accepted 5 October 2016

Keywords:
Concentrating solar-thermal energy
Hybrid solar receiver combustor (HSRC)
MILD combustion
Levelized cost of electricity

ABSTRACT

A novel configuration of a Hybrid Solar Receiver and Combustor (HSRC) operated in the Moderate and Intense Low oxygen Dilution (MILD) combustion regime, termed the MILD HSRC is reported. This combustion regime is chosen because of its potential to lower NO_x emissions, while increasing the magnitude and uniformity of heat transfer relative to alternative combustion systems, but has not previously been assessed with the HSRC concept. An analytical model is used to identify configurations of the MILD HSRC that achieve the conditions required for MILD combustion. The preferred configuration was then incorporated into a multiple time-step, piecewise-continuous model to evaluate the potential savings in fuel and hence, overall Levelized Cost of Electricity (LCOE) for the MILD HSRC in an electrical power plant. This revealed that there is potential to reduce fuel consumption and LCOE by up to 41% and 4% respectively, relative to the HSRC operating with conventional combustion for a receiver size of $30MW_{th}$. The reduction in LCOE increases up to 6% for a receiver size of $100MW_{th}$ due to economies of scale. This justifies further work to develop detailed designs and evaluate specific technical and economic performance through demonstration and scale-up.

1. Introduction

Environmental concerns and government regulations are motivating the search for alternative energy sources to those from fossil fuels, such as wind, solar and tidal [1]. One of the technologies expected to play an important role in low-carbon-intensity energy systems is solar thermal energy, owing to its potential to achieve low cost energy storage, so that many solar thermal plants are now being deployed across Europe and the USA [2]. Nevertheless, despite the value of storage, managing the intermittency and variability across the entire year with sensible or latent storage alone would require an excessively large storage capacity and a large over-sizing of the heliostat field to enable a power plant to operate continuously without any backup [3]. The quest for firm and dispatchable source of power has therefore motivated the development of hybrid solar thermal devices that integrate the energy from both concentrated solar energy and combustion as a means to lower the cost of energy systems with a high penetration of renewable energy [4]. On this basis, the present paper aims to evaluate a new configuration of a recently proposed hybrid concept that offers both continuous supply of energy and low pollutant emissions during those periods of operation for which combustion is utilised.

The Hybrid Solar Receiver Combustor, HSRC, combines the functions of a solar cavity receiver and boiler in a single device [5–8]. This device has been proposed to enable the supply of continuous power, or firm supply, through the combustion of fuels, either fossil or renewable, despite seasonal and weather-based variability of the solar resource, which is difficult to achieve with sensible or latent heat storage alone. A comparison of the HSRC with other hybrid devices has been reported previously [5]. To the best knowledge of the authors, the only other device that integrates the use of combustion and solar is that proposed by Mehos et al. [9]. However, the combustor for this device was proposed to be mounted on the back of the cavity receiver, i.e. the device has two separate chambers for the combustor and solar receiver. In contrast, the HSRC uses the same chamber for both combustion and solar heating. This device enables operation in three modes, namely Solar-Only, Combustion-Only and Mixed-mode [7]. It has been shown, with analytical modelling, that the device can be configured to achieve similar efficiencies to that of either a solar–only cavity receiver or a conventional boiler in their stand-alone modes of

* Corresponding author.
E-mail address: jin.lim@adelaide.edu.au (J.H. Lim).

http://dx.doi.org/10.1016/j.energy.2016.10.017
0360-5442/

Nomenclature

$\dot{Q}$	heat transfer rate (W)
$\dot{W}$	work rate = power output (W)

Greek symbols

η	efficiency

Abbreviations

EPGS	Electrical Power Generating System
HSRC	Hybrid Solar Receiver Combustor
HTI	Heat Transfer Improvement
LCOE	Levelized Cost of Electricity
MILD	Moderate and Intense Low oxygen Dilution
SGH	Solar Gas Hybrid

Subscripts

air	air from surrounding
ap	aperture
boil	boiler
cap	capacity
comb-air	combustion air
conv	conventional
crit	critical or threshold value
decom	decommissioning
dump	dumped
elec	electric al
ex	exhaust
gas	hot gases from combustion
gen	generator
helio	heliostat
int	internal
invest	investment
min	minimum
noz	nozzle opening losses
rec	solar receiver
recir	recirculated
salt	molten salt
sec	secondary air
self-ig	self-ignition
sol	solar
stm	steam
sto	storage
t	time (years)
th	thermal output
trace	trace heating
use	useful
wall	wall losses

operation under steady-state conditions [7]. However, when accounting for the variability of the solar resource, the HSRC has been estimated to lower the cost of LCOE compared with a reference Solar Gas Hybrid (SGH) that uses a separate solar-only cavity receiver and a backup boiler, by up to 17% for a 100MW_{th} receiver size depending on the price of fuel and thermal storage capacity. Nevertheless, no previous assessment has considered the need to incorporate low-NO_x technology, which will be necessary to avoid the otherwise high emissions from conventional combustion that contributes to acid rain and photochemical smog [10]. Low NO_x technology is particularly important for the HSRC because its heat recovery system generates higher temperatures than a boiler in both the Combustion-Only and the Mixed-modes of operation [6,7]. Therefore, it is desirable to develop a configuration of the HSRC with low NO_x emissions.

The process of integrating combustion into a solar receiver will inevitably increase the weight of the device, since the HSRC incorporates an additional heat exchanger to recover heat from the combustion products, together with the combustion equipment. Furthermore, the addition of a conventional flame into a cavity receiver will increase its length due to the lower heat transfer from a flame relative to concentrated solar radiation [7]. For example, previous analysis has found that the optical length to cavity diameter ratio, $L_C/D_C \approx 5$ to 6 for a conventional flame, which is near double that for a solar-only device [7]. This leads to a relatively high cost in construction when accounting for both the HSRC and the tower relative to a stand-alone solar system, although this is more than offset by the avoidance of a boiler [5]. Nevertheless, it is desirable to develop a configuration of a more compact HSRC without significantly affecting the overall efficiency and thermal performance.

A potential approach to address the aforementioned issues is to employ MILD combustion within the HSRC. MILD combustion is a rapidly developing technology, which is based on the principles of heat and flue gas recirculation. This innovative combustion process has been widely shown to offer many significant potential benefits over conventional combustion [11–19]. These are a reduction in NO_x emissions by up to 70% relative to conventional combustion, high thermal efficiency, increased thermal field uniformity, enhanced combustion stability and broad fuel flexibility [12,14]. For these reasons, this combustion regime also offers the potential to increase the compactness of the combustor and fuel savings. However, no previous assessment of the potential benefits of incorporating MILD combustion into the HSRC has yet been reported. The aim of the present paper is therefore to meet this need.

Several groups have reported that MILD combustion produces a higher heat flux than a conventional flame counterpart [14–17,20]. Nevertheless, the extent to which this effect is general is not yet known because the heat transfer from a flame depends on many parameters, particularly on the amount of soot that typically dominates the emissivity of the flame, but depends non-linearly on the turbulent mixing parameters that control composition, strain and residence time. Weber et al. has reported that their MILD combustion system approached a well-stirred reactor for oxygen concentrations in the furnace of 2%–3% [16]. The authors note that this uniformity in heat flux is often desirable and often cannot be met with a conventional combustion configuration. Cavaliere and de Joannon [14] deduced that the radiative heat transfer in MILD combustion can be significantly different from a conventional combustion process due to the dilution of the gases containing carbon dioxide and water. These species increase the infrared radiative flux, which contributes to higher heat transfer in the oxidation zone [14]. Similarly, Tsuji et al. claimed that in MILD combustion the radiation heat transfer increases by more than 30% under the conditions of high preheated air temperatures of around 1270 K [17]. It has also been reported that MILD combustion achieves a higher thermal efficiency relative to conventional combustion, that can result in a 25% reduction in the physical size of a furnace [17]. This was attributed to the more uniform furnace temperatures that reduce the irreversible losses associated with a conventional combustion process [20]. Although the peak temperature of MILD combustion is lower than conventional

combustion, MILD combustion has been reported to enable a smaller furnace due to the higher irradiative heat transfer [17]. Based on the broad consensus that MILD combustion offers the potential to increase heat transfer over conventional combustion, it is therefore desirable to develop HSRC configurations that can achieve this combustion regime.

For the reasons described above, the aim of the present investigation is to assess the potential advantages and disadvantages of the use of MILD HSRC technology over conventional combustion within a hybrid solar thermal-combustion system. In particular, it aims to compare the technical and economic performance of this device against the HSRC operating with conventional combustion and the SGH based on the assumption that the detailed configuration of the device can be optimised to achieve the performance of MILD combustion reported elsewhere in the literature.

2. Device configuration

The proposed configuration of the MILD HSRC is shown in Fig. 1. This device incorporates a tubular solar cavity receiver, integrated with a combustor and air preheater to achieve the MILD combustion regime. Concentrated solar radiation, when it is available at sufficient intensity, enters the device via the aperture and heats the receiver tubes carrying a heat transfer fluid. In the present analysis, the heat transfer fluid is assumed to be molten salt because it is used widely in the CSP industry [21] and its properties are well known [22]. Here we analyse the case in which the heat is used to generate electricity, although it could also be used for other applications. When the solar flux is below its minimum useful threshold, the aperture of the MILD HSRC can be closed to enable the device to operate in the Combustion-Only mode. The device can also be operated in a Mixed-Mode, in which both solar and MILD combustion are used simultaneously. A counter-flow heat exchanger, HX, system is incorporated into the device to recover sensible heat from the hot combustion products. The same device is also used to recirculate a fraction of the hot combustion products to achieve both a high temperature and strong dilution of the air. Fig. 2 shows the HSRC operating with conventional combustion. The main difference between the two configurations is in the heat recovery section of the device. The HSRC operating with conventional combustion sends all of the hot exhaust through the HX while, for the MILD HSRC, some of the combustion products are directly mixed with the heated combustion air to further preheat and dilute the combustion air prior to directing it to the combustor. In the present study, both configurations employ only a counter-flow HX configuration (in contrast to previously reported configurations [6,7]), to ensure that the comparison of the two combustion modes is performed with the same configuration of HX.

3. Methodology

The present model employed to analyse performance is an extension of the previously developed analytical models of Lim et al. [7,8], which employ multiple time-steps in a piecewise-continuous time series. The previous analytical model was validated to first order accuracy in the Solar-Only and Combustion-Only modes of operation by adapting the model to match those of the solar cavity receiver of Li et al. [23] and employed standard and well known heat transfer coefficients that were adapted to suit the shape of the HSRC [7]. The model was also verified to ensure that the flows of power during dynamic operation are consistent with expectation [8]. This model has been adapted for the Combustion-Only mode to accommodate MILD combustion. Although the heat transfer coefficients for MILD combustion have not been reported previously and are also expected to depend on the details of the configuration, it is reasonable to assume that the heat transfer for MILD combustion is not worse than that of conventional combustion based on previous experimental measurements cited above [17]. Various authors reported that the heat transfer improved when operating in the MILD regime for certain furnace configurations by up to 30% [12,14,17]. On this basis, the influence of heat transfer coefficients was assessed by a sensitivity study that varied the extent of the heat transfer improvement (HTI) due to MILD combustion over the range of 0%–30%.

The total thermal output from the heat transfer fluid within the HSRC was set to be 30MW_{th} on the basis that this is the typical

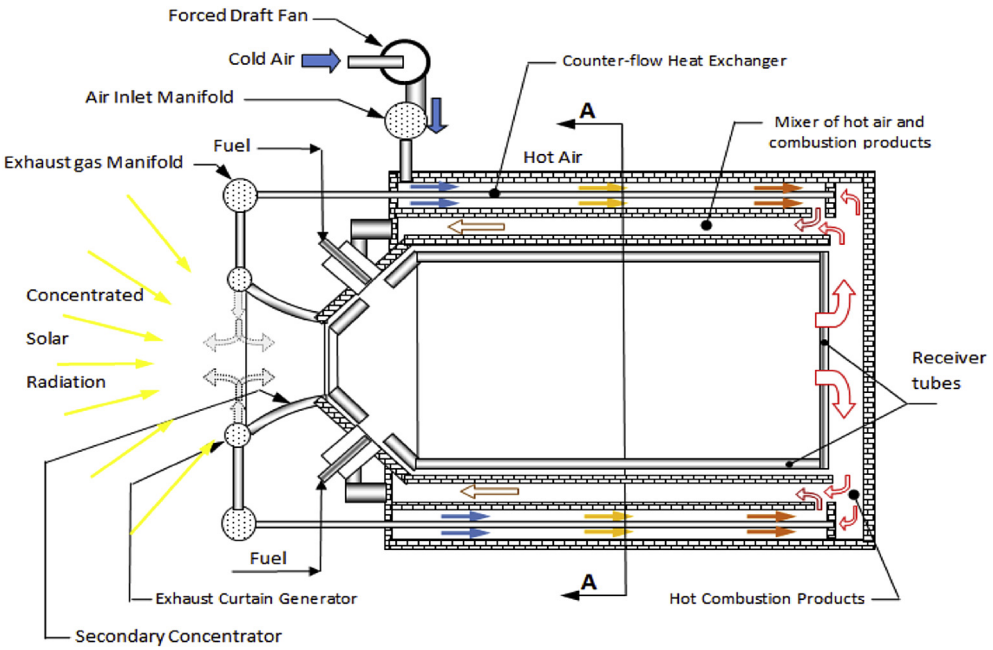

Fig. 1. The Hybrid Solar Receiver Combustor (HSRC) configured to operate in the MILD combustion regime, with a counter-flow heat exchanger for the combustion air.

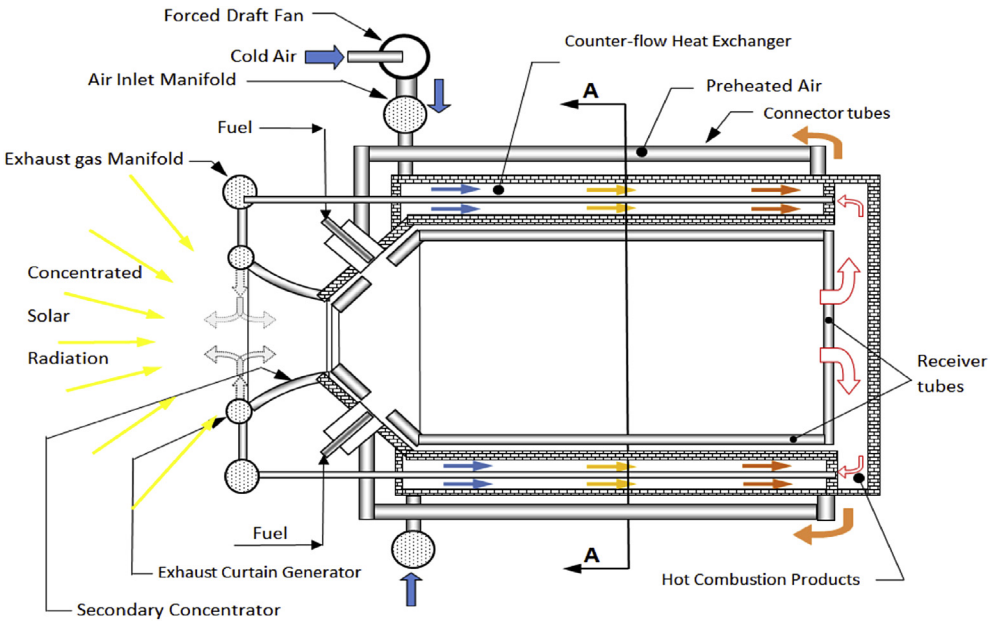

Fig. 2. Configuration of the Hybrid Solar Receiver Combustor operating with conventional combustion and a heat exchanger for the combustion air that operates only in the counter-flow direction, in contrast to previously reported configurations [7].

value of the largest scale that is realistic for a cavity receiver, following Lim et al. [7].

The recirculation of hot combustion products may impose limitations on the materials used to construct the HSRC, in particular for the tubes carrying the hot combustion products. The typical maximum operating temperature of materials varies. For these reasons, a systematic assessment was performed of the use of different types of widely employed high temperature materials [24] as shown in Table 1.

3.1. Criteria to define MILD combustion regime

A study was performed to ensure that the conditions required to achieve MILD combustion can be met with the proposed configuration of HSRC, based on the definition of Cavaliere and de Joannon [14]. In particular, MILD combustion occurs when the inlet temperature of the reactant mixture, T_{inlet}, is higher than the mixture self-ignition temperature, $T_{self-ig}$ [14,17]. Here, we consider the case in which natural gas is used as the fuel, so that $T_{self-ig} = 810$ KK [25]. In addition, it is required that the reacting mixture is highly diluted (to below the flammability limits), i.e. the local oxygen concentration is lower than 10% (typically 3–5%) by volume [11]. Another parameter required to be achieved for MILD combustion is that the maximum allowable temperature increase with respect to the inlet temperature, $\Delta T = T_{flame} - T_{comb-air}$, during combustion is lower than T_{self}. This is one of the most widely accepted criteria for MILD combustion, for the case where the furnace is assumed to be a well-stirred reactor for the mixture of preheated air diluted with hot combustion products (from the HX) and the fuel [11,16,26,27]. The analytical model adopts this assumption and it also assumes that the fuel-air jet momentum ratio is sufficiently high to achieve MILD combustion [12,16]. These assumptions are made following the work of Weber and Dugue whose furnace configurations have distinct similarities to that of the HSRC in that they employ vitiated air at high temperature as the oxidant stream, have a similar furnace shape, and employ similar arrangements for the inlet and outlet streams [16,28]. Table 2 summarizes the parameters required for MILD combustion to occur.

3.2. Model development

The present model was used to calculate the heat transfer, mass flow rates and energy into and out from a series of control volumes at steady state for each time-step in a time-series. Each term is described with a mathematical equation with a mass and energy balance calculated for the Combustion-Only mode of operation. The model for the Solar-Only mode of operation is unchanged from that reported previously [7].

Figs. 3 and 4 present the energy flows for the MILD HSRC and the HSRC operating with conventional combustion in the Combustion-Only mode of operation. The thermal inputs comprise the fuel and air, $\dot{Q}_{fuel,in}$ and $\dot{Q}_{air,in}$, which react to heat the receiver tubes containing the heat transfer fluid (molten salt) with the aperture shutter closed to avoid unnecessary losses. The gaseous combustion products are then passed through a HX, which recovers a fraction of the sensible exhaust heat, $\dot{Q}_{gas,out}$, by preheating the

Table 1
Selected high temperature materials assessed for potential use in the heat exchanger for the combustion air within the Hybrid Solar Receiver Combustor [24].

Material	Highest operating temperature (K)
Incoloy800	1366
SS304	1173
Inconel600	1485

Table 2
Parameters required to achieve Moderate and Intense Low oxygen Dilution (MILD) Combustion based on previous work.

Parameters required for MILD combustion	Value	Reference
Local oxygen concentration in furnace	3%–10%	[11]
$\boldsymbol{T_{inlet}}$	$>T_{self-ig}$	[14,17]
$\boldsymbol{\Delta T = T_{flame} - T_{comb}}$	$<T_{self-ig}$	[14]

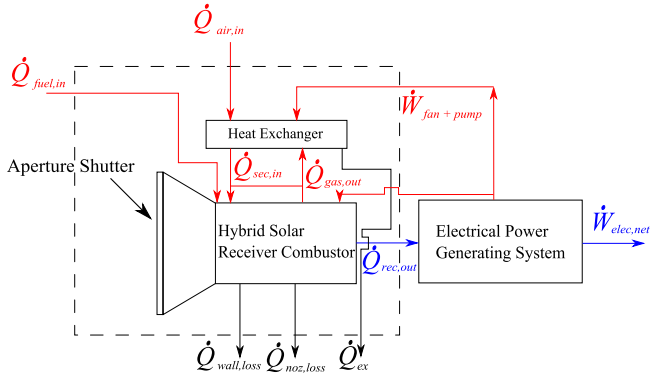

Fig. 3. Energy balance for the MILD HSRC (Combustion-Only mode) with boundary of the control volume.

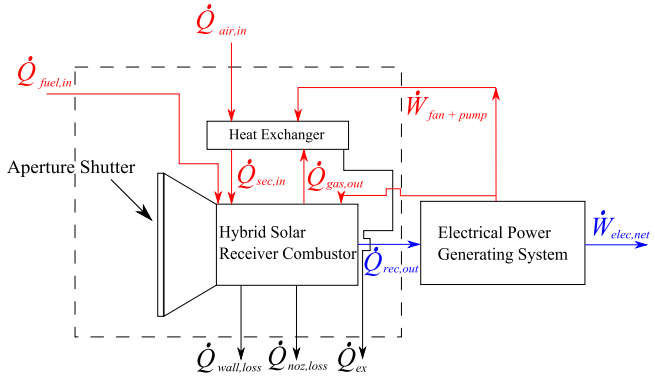

Fig. 4. Energy balance for the HSRC operating with conventional combustion (Combustion-Only mode) with boundary of the control volume [7].

combustion air, termed, $\dot{Q}_{sec,in}$, by an amount that depends on the effectiveness of the HX (refer to Section 2 for HX configuration). The losses from the system are assumed to comprise a radiant and a convective term through the burner nozzle, $\dot{Q}_{noz,loss}$, wall losses, $\dot{Q}_{wall,loss}$, sensible heat in the exhaust, $\dot{Q}_{ex}$, and the parasitic losses required to operate the pumps and fans, $\dot{W}_{fan+pump}$. The heat from the heat transfer fluid, $\dot{Q}_{rec,out}$, is transferred to the electrical power generating system to produce electricity, $\dot{W}_{elec,net}$.

The total amount of power supplied by the fuel is calculated as follows:

$$\dot{Q}_{fuel,in} = \dot{Q}_{rec,out} + \dot{Q}_{wall,loss} + \dot{Q}_{noz,loss} + \dot{Q}_{ex} - \dot{Q}_{air,in}, \quad (1)$$

where further details of the definitions of the terms $\dot{Q}_{wall,loss}$, $\dot{Q}_{noz,loss}$, $\dot{Q}_{ex}$, and $\dot{Q}_{air,in}$ can be found in the investigation of Lim et al. [7]. Here, $\dot{Q}_{rec,out}$ is the total thermal output, which is fixed at 30MW$_{th}$[7]:

$$\dot{Q}_{rec,out} = (GS_1)_R \sigma \left(T_{gas}^4 - T_{RT}^4\right). \quad (2)$$

The term $(GS_1)_R$ is defined as the total exchange area between the combustion gases and the receiver tubes in radiative equilibrium (for which the incoming and out-going radiative heat fluxes are equal) [29]:

$$(GS_1)_R = \frac{A_{int\ HSRC}}{\left[\frac{1}{\varepsilon_{gas}}\right] + \left[\frac{1}{C_s}\right] - 1} \quad (3)$$

Natural gas was assumed to be used as the fuel due to its wide availability [30]. The pressure inside the HSRC during Combustion-Only mode was assumed to be close to atmospheric pressure [6]. The gas emissivity, ε_{gas}, was calculated as a function of the gas temperature and partial pressures of O_2 and CO_2 following Modest [31], while C_s is the cold surface fraction [32], where

$$C_s = \frac{A_{tube,rec}}{A_{int\ HSRC}}. \quad (4)$$

Here, $A_{tube,rec}$ and $A_{int\ HSRC}$ are the total area of the receiver tubes and the internal surface of the HSRC, respectively.

A split ratio, S, which is defined by the ratio of the mass flow rate of hot gaseous combustion products recirculated to the combustion mixture, to the mass flow rate of hot gaseous combustion products to the exhaust outlet via the HX, is introduced:

$$split\ ratio\ (S) = \frac{\dot{m}_{recir}}{\dot{m}_{ex}} \quad (5)$$

Calculations were made to ensure that the level of dilution achieves the MILD parameters stated. In the analysis performed, the value of S was varied systematically ranging from 50:50, 60:40, 75:25, and 90:10 to determine if MILD combustion can be achieved, and how this value affects the performance of the device.

The split ratio affects the mass flow rates of the fuel, air and combustion products in the device. An iteration process was performed to ensure that the mass flow in the device is balanced:

$$\dot{m}_{gas,out} = \dot{m}_{recir} + \dot{m}_{ex} = \dot{m}_{fuel} + \dot{m}_{air} \quad (6)$$

$\dot{m}_{fuel}$ is found from using $\dot{Q}_{fuel,in}$ calculated from (1), with the following equation:

$$\dot{Q}_{fuel} = \dot{m}_{fuel} \times LHV_{fuel}, \quad (7)$$

where LHV_{fuel} is the lower heating value of the fuel, assumed to be natural gas [33].

To calculate the mass flow rate of fuel and the oxygen concentration in the device, the chemical equation of the reaction of natural gas and air is first listed as follows (assuming complete combustion):

$$C_{1.16}H_{4.32} + 2.24O_2 + 8.42N_2 \rightarrow 1.16CO_2 + 2.16H_2O + 8.42N_2 \quad (8)$$

Based on this equation, the percentage of oxygen can be estimated from the known mass flow rate of fuel. An excess air of 11% was assumed in the model, to fix the equivalence ratio, $\phi = 0.9$. The stoichiometric air to fuel ratio and subsequent air to fuel ratio was found following Turns et al. [34]:

$$(A/F)_{stoic} = \left(\frac{\dot{m}_{air}}{\dot{m}_{fuel}}\right)_{stoic} = \frac{4.76a}{1}\frac{MW_{air}}{MW_{fuel}}, \quad (9)$$

$$\left(\frac{A}{F}\right) = \left(\frac{A}{F}\right)_{stoic} \Big/ \phi \quad (10)$$

where MW_{air} and MW_{fuel} represents the molecular weight of air and fuel respectively, $a = x + y/4$, where $x = 1.16$ and $y = 4.32$ from equation (7).

The mass flow rate of air, $\dot{m}_{air,in}$ was calculated from the air to fuel ratio above.

The overall thermal efficiency of the HSRC was then calculated from the equation:

$$\eta_{th} = \frac{\dot{Q}_{rec,out}}{\dot{Q}_{fuel,in}}, \tag{11}$$

where $\dot{Q}_{rec,out}$ and $\dot{Q}_{fuel,in}$ are defined above.

The effectiveness-NTU method was applied when performing calculations for the HX component in the HSRC, similar to the previous work by Lim et al. [7]. This method is required for the exhaust gas temperature, T_{ex}, to be calculated as follows:

$$T_{ex} = T_{gas,out} - \frac{\dot{Q}_{HX}}{\dot{m}_{ex} c_{p,h}}, \tag{12}$$

where $\dot{Q}_{HX}$ is the heat transfer rate for the fully counter-flow HX and is defined as:

$$\dot{Q}_{HX} = \varepsilon_{HX} \dot{Q}_{max}. \tag{13}$$

The term ε_{HX} in equation (13) is the effectiveness of the HX, obtained from Bergman et al. [32], while $\dot{Q}_{max}$ is defined as the maximum heat flux rate:

$$\dot{Q}_{max} = C_{min}\left(T_{hot\ gas,out} - T_{\infty}\right), \tag{14}$$

where C_{min} is the lesser of the heat capacity rates, C_h and C_c, both defined as follows:

$$C_c = \dot{m}_{air,in} C_{p,c}, \tag{15}$$

$$C_h = \dot{m}_{gas,out} C_{p,h}. \tag{16}$$

Similarly, the temperature of the combustion air, $T_{comb-air}$, was found using the approach as above. The temperature of the HX, T_{HX}, was calculated as the average between the temperature of $T_{comb-air}$ and T_{ex}.

Another factor that needs to be considered is the pressure drop through all the tubes in the device, which was calculated following Bergman et al. [35]:

$$\Delta P = f \frac{\rho\left(u_{mean,\ fluid}\right)^2}{2D}(x_2 - x_1). \tag{17}$$

This formula accounts for the friction factor, f, a dimensionless pressure drop for internal flow and can be obtained from Bergman et al. [32], density, ρ, and mean velocity, u_m of the heat transfer fluid or flue gas, and the length (the term $x_2 - x_1$ represents the overall length of the tube) and diameter, D of the tube. The calculated pressure drop was used to estimate the parasitic power requirement for the fans and pumps. This was done by multiplying the pressure drop with the volumetric flow rate of the heat transfer fluid or flue gas [32]:

$$\dot{W}_{fan+pump} = (\Delta P)\dot{V}_{fluid}. \tag{18}$$

Both analytical models were then extended to include other components of a power plant such as hot and cold storage tanks, a steam generator, and an electrical power generating system. Fig. 5 presents a schematic diagram for the SGH system. The boiler provides heat to the Electrical Power Generating System, at times when heat is unavailable from either the solar resource or the storage tank, following the work of Kueh et al. [3]. Concentrated solar radiation from the heliostat field, $\dot{Q}_{helio}$, is introduced to the solar cavity receiver providing heat to the heat transfer fluid. The heat from the receiver $\dot{Q}_{rec,out}$ is stored in the hot storage tank and utilised by the steam generator when required. If the amount of heat exceeds the storage limit, the remainder is dumped, the value of which is denoted $\dot{Q}_{tank(hot),dump}$.

Fig. 6 presents a schematic diagram of the HSRC device implemented into a power plant system. The main difference between this system and the SGH (Fig. 5) is the integration of the solar-only cavity receiver and boiler.

3.3. Economic analysis

The economic analysis follows that of Lim et al. [8]. The Levelized Cost of Electricity (LCOE) was calculated for both HSRC concepts as implemented in a power plant, relative to a reference case termed the Solar Gas Hybrid (SGH), which is a system with a separate solar-only cavity receiver and a boiler backup for the electrical power generating system.

The LCOE was calculated using the following formula from International Energy Agency (IEA):

$$LCOE_{overall} = \frac{\sum_t ((Invest_t + O\&M_t + Fuel_t + Carbon_t + Decom_t)*(1+r)^{-t}}{\sum_t \left(Elec_t*(1+r)^{-t}\right)} \tag{19}$$

where t represents the year; $Invest_t$ is the investment cost in year t; $O\&M_t$ represents the operations and maintenance costs for year t; $Fuel_t$ is the cost of fuel for year t; $Carbon_t$ is the cost of carbon emissions (e.g. from a carbon tax) for year t; $Decom_t$ represents the decommissioning cost of the power plant for year t; r in the term $(1+r)^{-t}$ is the discount factor for year t; and $Elec_t$ is the amount of electricity produced in year t. The life of the plant was assumed to be 30 years, following Nathan et al. [5] and Lim et al. [8,35]. In addition, the present comparison ignores the costs of carbon emissions and decommissioning as well as inflation [5]. The discount factor was assumed to be equivalent to the assumed internal rate of return of 10% over the project life [8].

Table 3 presents the values and correlations used in the cost estimations. Since the assessment is only a relative comparison between the HSRC concepts and the SGH, the values used are reasonable and also avoid the challenge of obtaining absolute values for a particular site.

One of the cases studied by Lim et al. was repeated for the MILD HSRC, the details of which are listed in Table 4[8].

4. Results and discussion

Fig. 7 presents the dependence of the oxygen concentration (by

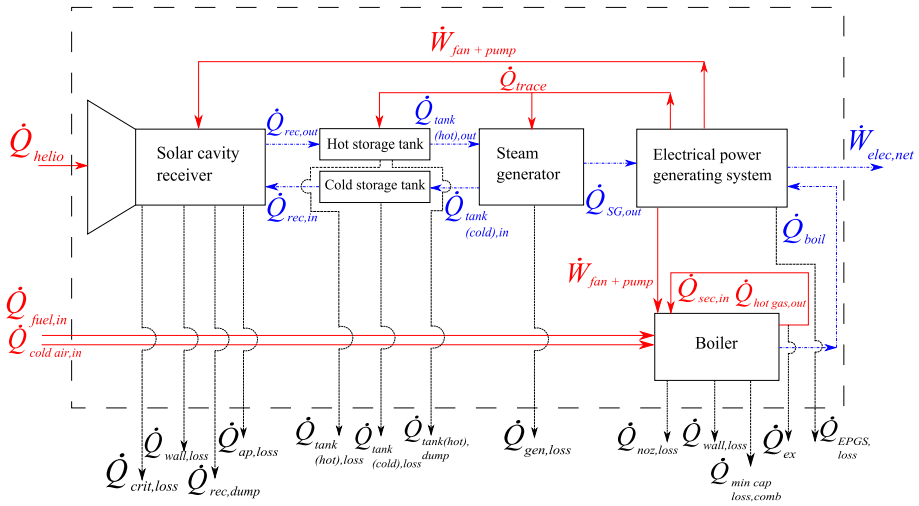

Fig. 5. Schematic diagram of the power flows through the Solar Gas Hybrid, SGH, system [8].

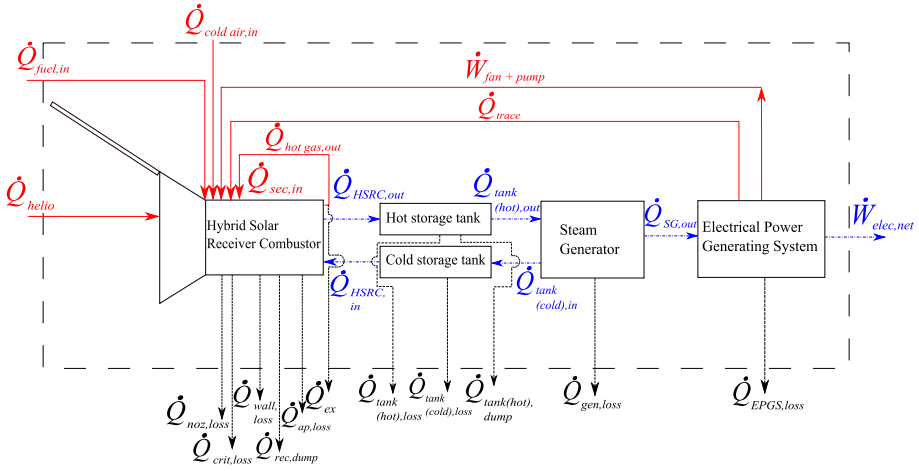

Fig. 6. Schematic diagram of the power flows through the Hybrid Solar Receiver Combustor, HSRC, system [8].

Table 3
Values and correlations used to calculate the Levelized Cost of Electricity, LCOE (US dollars).

Component cost	Correlation/value	Unit	Reference
Heliostats	216	$/m^2	[21]
Salt-cooled receiver	$3.52\ \dot{Q}_{rec,max}^{0.44}$	$M	[21]
HSRC	$2 \times 3.52\ \dot{Q}_{rec,max}^{0.44}$	$M	[7]
Tower	$0.0305\ \dot{Q}_{rec,max} + 0.961$	$M	[21]
Thermal storage	$0.0153\ \dot{Q}_{sto} + 0.502$	$M	[21]
Steam generator	$0.212\ \dot{Q}_{SG,out,max}^{0.7}$	$M	[21]
Electrical power generating system	$1.84\ \dot{Q}_{SG,out,max}^{0.7}$	$M	[21]
Gas-fired boiler	$1.69\ \dot{Q}_{boil,max}^{0.7}$	$M	[36]
Operation & Maintenance			
Solar field	$1.88\ A_{helio} + 0.189$	$M/yr	[21]
Plant	$0.0151\ \dot{W}_{elec,net} + 2.92$	$M/yr	[21]
Fuel cost (Natural gas)	3	$/GJ	[37]
Levelized cost calculation parameters			
Internal rate of return	10%		
Plant life	30 years		

volume) within the HSRC on the value of the split ratio, *S*. The oxygen concentration was found to be one of the main parameters that changes with *S*. It was found that, for MILD combustion to occur, at least 50% of the exhaust gases need to be recirculated (S = 50:50) to avoid oxygen concentrations higher than the upper limit of 10%, while a value higher than ~90% exhaust gas

Table 4
Parameters for the case study performed for the conventional and MILD HSRC concepts relative to the reference Solar Gas Hybrid, SGH.

Parameters	
Location	Daggett
Year	2000
Hours of storage	5
Power block ratio, $\frac{\dot{Q}_{tank(hot),out}}{\dot{Q}_{rec,max}}$ or $\dot{Q}_{rec,max}$	0.8

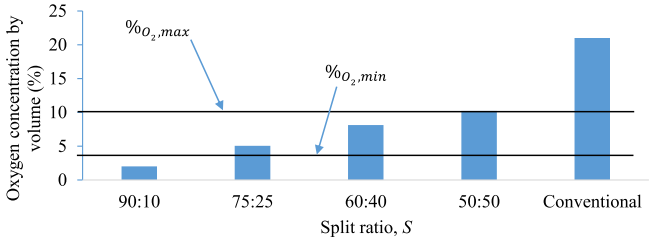

Fig. 7. The dependence of the oxygen concentration (% by volume) on the split ratio (the ratio of hot exhaust gases to the combustion mixture to the ratio of hot exhaust gases to the exhaust outlet via the heat exchanger) for the MILD HSRC for an overall output of 30MW$_{th}$. Also shown is the maximum and minimum oxygen concentration required for MILD combustion.

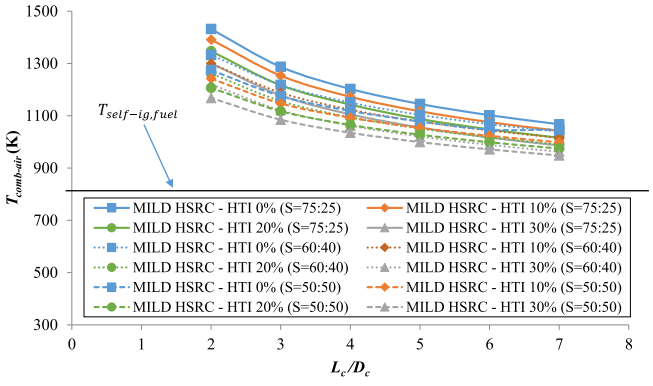

Fig. 8. Effect of varying L_C/D_C on the combustion air temperatures for an overall output of 30MW$_{th}$. Results are reported for the MILD HSRC configuration (HTI 0% represents heat transfer improvement of 0%) for split ratios of S = 75:25, S = 60:40 and S = 50:50. $T_{self-ig,fuel}$ represents the self-ignition temperature of the fuel, i.e. natural gas.

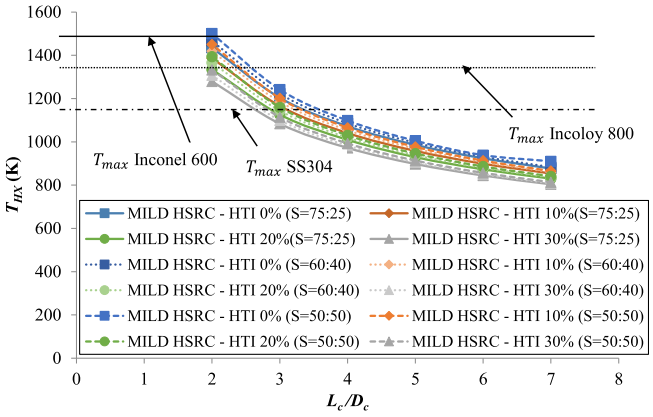

Fig. 9. The effect of varying the L_C/D_C on the estimated temperature of the heat exchanger (T_{HX}). Also shown is the maximum operating temperature of selected high temperature materials. Results are reported for the MILD HSRC configurations (HTI 0% represents heat transfer improvement of 0%) for split ratios of S = 75:25, S = 60:40 and S = 50:50.

recirculation (S = 90:10) will result in the oxygen concentration being less than the lower limit of 3% [12]. Hence, for all the following results presented, the MILD HSRC is assumed to be operating with a split ratio of either 75:25, 60:40 or 50:50.

Fig. 8 presents the combustion air temperatures for all the cases of MILD HSRC with and without HTI as a function of the length to diameter ratio of the chamber, L_C/D_C, for the cases of S = 75:25, S = 60:40 and S = 50:50. For a fixed cavity diameter, D_c, of 3 m, it can be seen that the combustion air temperatures are higher than the mixture self-ignition temperature for all scenarios. The lowest combustion air temperature of around 948 K is calculated to occur for the MILD HSRC – HTI 30% case at an L_C/D_C ratio of 7 and S = 50:50, which is still higher than $T_{self-ig}$ = 810 K for natural gas. Therefore, this shows that the configuration of the device satisfies this requirement to achieve MILD combustion for all cases of L_C/D_C and for S = 75:25, S = 60:40 and S = 50:50.

Fig. 9 presents the effect of varying L_C/D_C on the calculated mean operating temperature of the HX component, T_{HX} in the HSRC, relative to the maximum operating temperature of selected high temperature materials for the cases of S = 75:25, S = 60:40 and S = 50:50. The value of S has a modest, but significant, influence on T_{HX}, which is calculated to be the highest for the case of S = 50:50, followed by S = 60:40 and S = 75:25 due to the higher mass flow rate of the exhaust gases. In general, it is evident that, for the cases of L_C/D_C>2.2 and L_C/D_C>2.5, T_{HX} does not exceed the maximum temperatures of Inconel 600 and Incoloy 800, respectively, while for the case of L_C/D_C > 3.5, SS304 is safe to be used, for all cases of HTI. It is also important to note that the external walls of the device are assumed to be heavily insulated with ceramic fibre and clay, as per the previous work by Lim et al. [7]. These materials are able to withstand very high temperatures of up to 1500 K and 2050K respectively, which are both considerably higher than the wall temperatures estimated in the device. It is also worth noting that the tubes have been configured to account for thermal expansion of the different materials.

Fig. 10 presents the maximum calculated increase in temperature from the MILD reaction process, ΔT, which must be lower than the mixture self-ignition temperature, $T_{self-ig}$, to achieve MILD combustion. This is shown for all the cases of MILD HSRC with and without HTI as a function of L_C/D_C for the cases of S = 75:25, S = 60:40 and S = 50:50. From the results shown in Fig. 9, this is

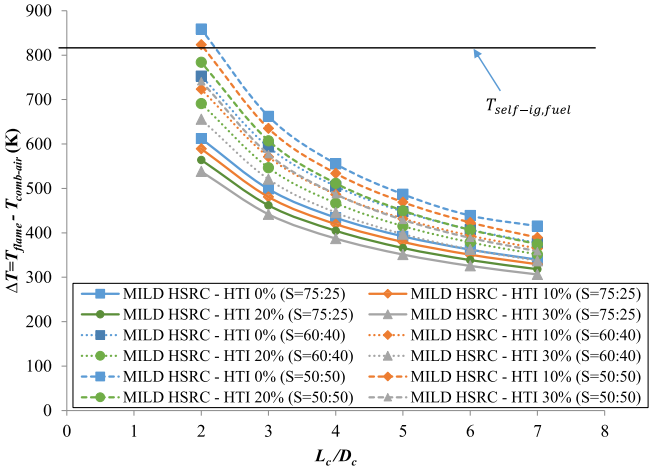

Fig. 10. Effect of varying L_C/D_C on the maximum allowable temperature increase with respect to the inlet temperature, ΔT, for an overall output of 30MW$_{th}$. Results are reported for the MILD HSRC configurations (HTI 0% represents heat transfer improvement of 0%) for split ratios of S = 75:25, S = 60:40 and S = 50:50. $T_{self-ig,fuel}$ represents the self-ignition temperature of the fuel, i.e. natural gas.

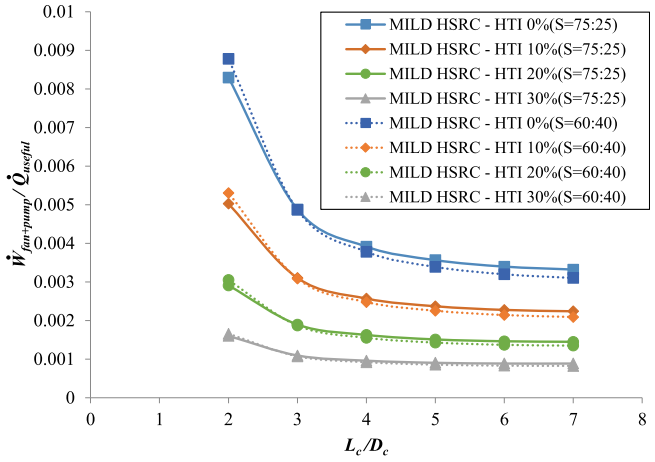

Fig. 11. The effect of varying *Lc*/*Dc* on the parasitic power requirements for the fan and pump with the MILD HSRC configuration, for an overall output of 30MW$_{th}$. The Heat Transfer Improvement (HTI) from the MILD combustion regime is systematically varied for split ratios of $S = 75{:}25$ and $S = 60{:}40$.

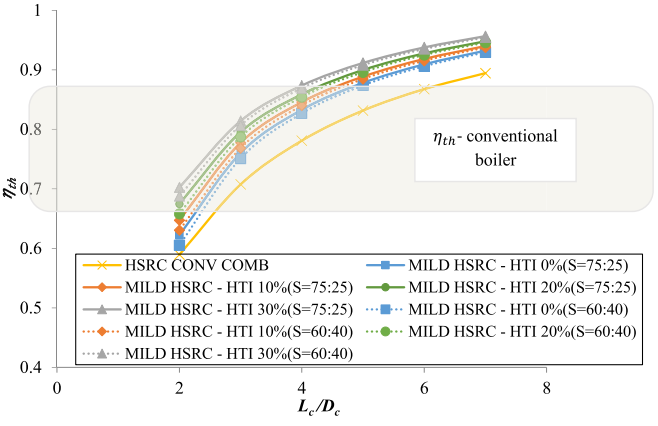

Fig. 12. Effect of varying L_C/D_C on the overall thermal efficiency for an overall output of 30MW$_{th}$. Results are reported for both the Hybrid Solar Receiver Combustor (HSRC) configurations (HTI 0% represents heat transfer improvement of 0%) for split ratios of $S = 75{:}25$ and $S = 60{:}40$.

true for almost all the cases except for MILD HSRC − HTI 0% and MILD HSRC − HTI 10% at an L_C/D_C ratio of 2 and $S = 50{:}50$. It is also evident that ΔT is lowest for the case of $S = 75{:}25$ followed by $S = 60{:}40$ and $S = 50{:}50$. Following this, further assessments only consider the cases of $S = 75{:}25$ and $S = 60{:}40$.

Fig. 11 presents the dependence of the parasitic power requirements for the fan and pump, to operate the device in the MILD combustion regime, as a function of L_C/D_C for the case of $S = 75{:}25$ and $S = 60{:}40$. It can be observed that this power decreases with an increase in L_C/D_C, with a larger gradient from $L_C/D_C = 2$ to $L_C/D_C = 3$ for all cases of HTI. More importantly, these power requirements calculated are relatively low, ranging from 0.1% to 1% of the overall useful thermal output of the device for all cases of heat transfer improvement. This also means that the size of the tubes chosen for the HX and heat transfer fluid are reasonable (HX tubes are 101.6 mm with a thickness of 4.2 mm while the heat transfer fluid tubes are 60 mm with a thickness of 5.5 mm). These pipe sizes are therefore chosen as a reference case for all of the following analysis.

Fig. 12 presents the efficiency achieved with both the HSRC configurations as a function of the length of the chamber for the cases $S = 75{:}25$ and $S = 60{:}40$. In general, the efficiency of the

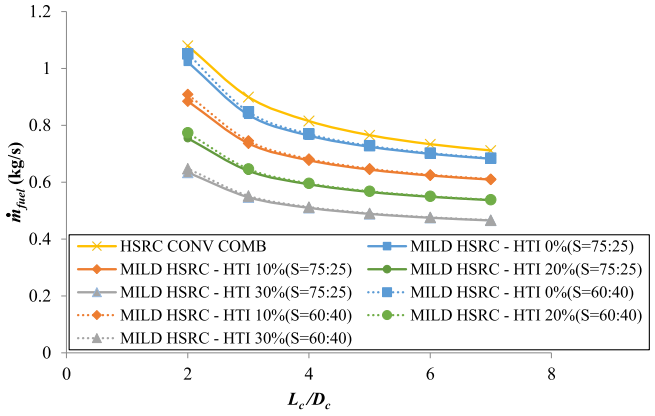

Fig. 13. Effect of varying L_C/D_C on the mass flow rate of fuel for an overall output of 30MW$_{th}$. Results are reported for both the Hybrid Solar Receiver Combustor (HSRC) concepts (HTI 0% represents heat transfer improvement of 0%).

device increases for all cases with an increase in L_C/D_C. For the HSRC operating with conventional combustion, the efficiency ranges from 59% to 89% for L_C/D_C ratios of 2–7 with a constant chamber diameter of 3 m. Significantly, even for the MILD HSRC with HTI = 0%, it can be seen that MILD combustion increases the thermal efficiency due to its lower mass flow rates of exhaust gases. It is also evident that the thermal efficiency for the case of $S = 75{:}25$, is slightly higher than that for $S = 60{:}40$ for the same reason. As the heat transfer performance is increased, less fuel is required to achieve the target thermal output. This results in a higher efficiency for the MILD HSRC than for the conventional case by up to 19% for the lower L_C/D_C ratios. Both the HSRC devices achieve thermal efficiencies similar to that of a conventional boiler for L_C/D_C ratios between 3 and 4.

Fig. 13 presents the total mass flow rate of fuel required to achieve the required thermal output. In general, the mass flow rate of fuel decreases with an increase in L_C/D_C because the efficiency and heat recovery increases with length. The percentage difference between the mass flow rate of fuel also increases with an increase in L_C/D_C, by up to 41% for the case which HTI = 30% for MILD combustion.

Table 5 presents the parameters of the selected configuration of the MILD HSRC based on the previous analysis used in the following economic analysis.

The MILD HSRC with $L_C/D_C = 4$ was selected for further analysis of the economic benefits of this device relative to the HSRC operating with conventional combustion and also with the reference case of SGH. This length is consistent with the analysis from Lim et al. who found that the L_C/D_C ratio of device should be ~4 in the Solar-Only mode of operation to avoid exceeding the temperature

Table 5
Parameters employed for the economic analysis of the selected configuration of the MILD HSRC.

Parameters	Value
Length of cavity, L_C	12 m
Diameter of cavity, D_C	3 m
L_C/D_C	4
Size of HX pipes	
Outer diameter	101.6 mm
Thickness	4.2 mm
Size of pipes carrying working fluid	
Outer diameter	60 mm
Thickness	5.5 mm
Split ratio, S	75:25

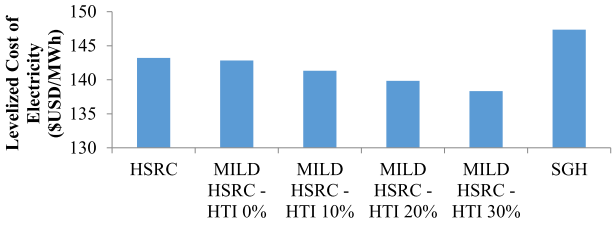

Fig. 14. The overall Levelized Cost of Electricity (LCOE) for both the Hybrid Solar Receiver Combustor (HSRC) concepts, i.e. HSRC configured for conventional combustion and the MILD HSRC, and the Solar Gas Hybrid (SGH) for the case of 5 h of thermal storage capacity at the site of Daggett for a receiver size of $30MW_{th}$.

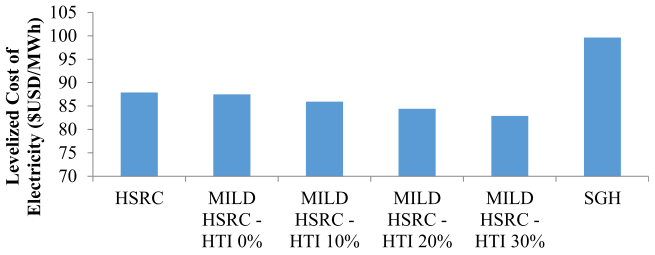

Fig. 15. The overall Levelized Cost of Electricity (LCOE) for both the Hybrid Solar Receiver Combustor (HSRC) concepts, i.e. HSRC operating with conventional combustion and the MILD HSRC, and the Solar Gas Hybrid (SGH) for the case of 5 h of thermal storage capacity at the site of Daggett for a receiver size of $100MW_{th}$.

limitation of the receiver tubes [7]. Exceeding this length will increase both the weight and cost of the device [7,8].

Fig. 14 presents the LCOE of all the HSRC concepts analysed here. It can be seen that the MILD HSRC decreases the LCOE by up to 3.5% more than the HSRC relative to the conventional hybrid, depending on the magnitude of the HTI achieved in practice. Relative to the equivalent SGH system, the MILD HSRC reduces the overall LCOE by up to 6%. The comparison between the HSRC and the SGH are consistent with those reported by Lim et al. [8], noting that their data were reported for a receiver size of $100MW_{th}$.

The same analysis was repeated for a receiver size of $100MW_{th}$ as per Fig. 15 at constant L_C/D_C following the previous work of Lim et al. [8]. It can be seen that the LCOE of MILD HSRC is lower by up to 6% relative to the HSRC operating with conventional combustion, and up to 17% relative to the reference case SGH. Also important to note is that the overall LCOE for all the systems analysed are lower than that of the $30MW_{th}$ which confirms that the technology takes advantage of economies of scale, as reported by both Nathan et al. [5] and Lim et al. [8].

5. Conclusions

The economic performance of a direct hybrid between a solar cavity receiver and a combustor is found to be improved with the use of MILD combustion instead of conventional combustion. The key findings from the analytical assessment are as follows:

- A configuration of MILD HSRC has been identified that can achieve the requirements needed to establish the MILD combustion regime. That is, it can achieve (assuming complete mixing between natural gas and air), average oxygen concentrations lower than 10% by volume (and typically 3–8%) and local temperature greater than the self-ignition temperature of natural gas;
- The split ratio, i.e. the ratio of hot exhaust gases directed towards the combustion mixture to the ratio of hot exhaust gases directed towards the exhaust outlet via the HX, is a key parameter that influences the level of dilution (and hence, the oxygen concentration) and the temperature of the preheated air/combustion products stream prior to entering the device. The optimal value of the split ratio, S, to achieve an oxygen concentration of 5–8% by volume, was found to be in the range of approximately 75:25 to 60:40;
- The length of the cavity relative to its diameter, L_C/D_C, was found to be able to be reduced relative to the conventional combustion case by some 25%. A value of $L_C/D_C \approx 4$ was found to achieve a high thermal efficiency, which is comparable to that of a conventional boiler, for the present configuration and scale of $30MW_{th}$. This ratio also allows standard materials to be used (SS304), instead of special high temperature materials. It is also worth noting that the optimal range of L_C/D_C will also depend on the nature of the fuel.

The key potential benefits of the MILD HSRC are estimated to be as follows:

- Fuel savings of up to 41% relative to the HSRC operating with conventional combustion, depending on the magnitude of the heat transfer improvement (HTI) relative to conventional combustion (noting that this range of improvement is based on experimentally reported values). This corresponds to an estimated reduction in LCOE of up to 4% for a receiver size of $30MW_{th}$. When compared with the reference Solar Gas Hybrid (which employs a separate boiler), the LCOE is reduced by up to 6%. For a receiver size of $100MW_{th}$, the percentage reduction in LCOE is greater, corresponding to up to 6% and 17% relative to the HSRC operating with conventional combustion and SGH respectively. These percentage reductions in LCOE will increase with the price of fuel.

These results justify the on-going development of the MILD HSRC configuration.

Acknowledgements

The authors acknowledge the support of the Australian Research Council and of FCT Combustion and Vast Solar through the ARC Linkage Grant LP110200060.

References

[1] International Renewable Energy Agency. Concentrating solar power. 2013.
[2] Zhang HL, et al. Concentrated solar power plants: review and design methodology. Renew Sustain Energy Rev 2013;22:466–81.
[3] Kueh KC, Nathan GJ, Saw WL. Storage capacities required for a solar thermal plant to avoid unscheduled reductions in output. Sol Energy 2015;118:209–21.
[4] Jamel MS, Abd Rahman A, Shamsuddin AH. Advances in the integration of solar thermal energy with conventional and non-conventional power plants. Renew Sustain Energy Rev 2013;20(0):71–81.
[5] Nathan GJ, Battye DL, Ashman PJ. Economic evaluation of a novel fuel-saver hybrid combining a solar receiver with a combustor for a solar power tower. Appl Energy 2014;113:1235–43.
[6] Nathan GJ, et al. A hybrid receiver-combustor. A.R.I.P. Ltd.; 2013.
[7] Lim JH, et al. Analytical assessment of a novel hybrid solar tubular receiver and combustor. Appl Energy 2016;162:298–307.
[8] Lim JH, Hu E, Nathan GJ. Impact of start-up and shut-down losses on the economic benefit of an integrated hybrid solar cavity receiver and combustor. Appl Energy 2016;164:10–20.
[9] Mehos MS, et al. Combustion system for hybrid solar fuel receiver. United States. 2004.
[10] Baukal Jr CE. Heat transfer. In: The John Zink combustion handbook. John Zink Company LLC; 2001. p. 106.
[11] Mancini M, et al. On mathematical modelling of flameless combustion. Combust Flame 2007;150(1–2):54–9.
[12] Li PF, et al. Progress and recent trend in MILD combustion. Sci China Technol Sci 2011;54(2):255–69.

[13] Rafidi N, Blasiak W, Gupta AK. High-temperature air combustion phenomena and its thermodynamics. J Eng Gas Turbines Power 2008;130(2).
[14] Cavaliere A, de Joannon M. Mild combustion. Prog Energy Combust Sci 2004;30(4):329–66.
[15] Dally BB, et al. On the burning of sawdust in a MILD combustion furnace. Olentangy River Road, P.O. Box 3337, Columbus, OH 43210-3337, United States: American Chemical Society; 2010. p. 2540.
[16] Weber R, et al. Combustion of natural gas with high-temperature air and large quantities of flue gas. Proc Combust Inst 2000;28(1):1315–21.
[17] Tsuji H, et al. Boca paton. High Temperature Air Combustion: CRC Press; 2003.
[18] Sabia P, et al. Dynamic behaviors in methane MILD and oxy-fuel combustion. Chemical effect of CO2. Energy & Fuels 2015;29(3):1978–86.
[19] De Joannon M, et al. Optimal post-combustion conditions for the purification of CO 2-rich exhaust streams from non-condensable reactive species. Chem Eng J 2012;211:318–26.
[20] Som SK, Datta A. Thermodynamic irreversibilities and exergy balance in combustion processes. Prog Energy Combust Sci 2008;34(3):351–76.
[21] Sargent, Lundy LLC, Consulting Group. Assessment of parabolic trough and power tower solar technology cost and performance forecasts. Chicago, Illinois: NREL; 2003.
[22] Sohal MS, et al. Engineering database of liquid salt thermophysical and thermochemical properties. Idaho National Laboratory; 2010. p. 2.
[23] Li X, et al. Thermal model and thermodynamic performance of molten salt cavity receiver. Renew Energy 2010;35(5):981–8.
[24] Qu W. Progress works of high and super high temperature heat pipes. INTECH Open Access Publisher; 2011.
[25] New World Encyclopedia. Natural gas [cited 2016 28 Sept]. 2014. Available from:, http://www.newworldencyclopedia.org/entry/natural_gas.
[26] Sabia P. Experimental and numerical studies of mild combustion processes in model reactors. Università degli Studi di Napoli Federico II; 2006.
[27] Evans M, et al. Classification and lift-off height prediction of non-premixed MILD and autoignitive flames. In: Proceedings of the combustion institute; 2016.
[28] Weber R, Dugué J. Combustion accelerated swirling flows in high confinements. Prog Energy Combust Sci 1992;18(4):349–67.
[29] Jenkins B, Mullinger P. Industrial and process furnaces. Butterworth Heinemann; 2008. p. 544.
[30] Mills AF, Ganesan V. Heat transfer. second ed. Pearson Education; 1999.
[31] Modest MF. Radiative heat transfer. Academic press; 2013.
[32] Bergman TL, et al. Fundamentals of heat and mass transfer. seventh ed. John Wiley & Sons; 2011.
[33] Wang M. The greenhouse gases, regulated emissions, and energy use in transportation (greet) model: version 1.5. Center for Transportation Research, Argonne National Laboratory; 2008.
[34] Turns SR. Combustion and thermochemistry. In: An introduction to combustion: concepts and applications. McGraw Hill; 2012.
[35] Lim JH, et al. Techno-economic assessment of a hybrid solar receiver and combustor. AIP Conf Proc 2016;1734(1):070020.
[36] Bemis GR, DeAngelis M. Levelized cost of electricity generation technologies. Contemp Policy Issues 1990;VIII.
[37] NAB Group Economics. In: Limited NAB, editor. Natural gas market update – August 2014; 2014.

Statement of Authorship

Title of Paper	Techno-economic evaluation of modular hybrid concentrating solar power systems
Publication Status	☐ Published ☐ Accepted for Publication ☑ Submitted for Publication ☐ Unpublished and Unsubmitted w ork w ritten in manuscript style
Publication Details	Lim, JH, Dally, BB, Chinnici, A & Nathan, GJ 2016, 'Techno-economic evaluation of modular hybrid concentrating solar power systems', Energy (manuscript number: EGY-D-16-02670).

Principal Author

Name of Principal Author (Candidate)	Jin Han Lim		
Contribution to the Paper	Performed literature review. Developed the pseudo-dynamic required for Levelized Cost of Electricity (LCOE) calculations. Wrote the manuscript. Responsible for submission process.		
Overall percentage (%)	60		
Certification:	This paper reports on original research I conducted during the period of my Higher Degree by Research candidature and is not subject to any obligations or contractual agreements with a third party that would constrain its inclusion in this thesis. I am the primary author of this paper.		
Signature		Date	18/7/16

Co-Author Contributions

By signing the Statement of Authorship, each author certifies that:

i. the candidate's stated contribution to the publication is accurate (as detailed above);

ii. permission is granted for the candidate in include the publication in the thesis; and

iii. the sum of all co-author contributions is equal to 100% less the candidate's stated contribution.

Name of Co-Author	Professor Bassam Dally		
Contribution to the Paper	Supervised the work. Provided suggestions and ideas to improve modelling approach. Assisted with editing the manuscript.		
Signature		Date	18/7/16

Name of Co-Author	Dr Alfonso Chinnici		
Contribution to the Paper	Supervised the work. Assisted in developing pseudo-dynamic model. Assisted with editing the manuscript.		
Signature		Date	18/07/16

Name of Co-Author	Professor Graham Nathan		
Contribution to the Paper	Supervised the work. Provided suggestions regarding modelling scenarios. Assisted with editing and finalising the manuscript.		
Signature		Date	19/7/16

CHAPTER 6

TECHNO-ECONOMIC EVALUATION OF MODULAR HYBRID CONCENTRATING SOLAR POWER SYSTEMS

Techno-economic evaluation of modular hybrid concentrating solar power systems

Jin Han Lim, Bassam B. Dally, Alfonso Chinnici, Graham J. Nathan

Keywords: hybridisation; working fluid; sodium; molten salt; modularisation;

Techno-economic evaluation of modular hybrid concentrating solar power systems

Jin Han Lim, Bassam B. Dally, Alfonso Chinnici, Graham J. Nathan

Centre for Energy Technology, School of Mechanical Engineering

The University of Adelaide, SA 5005, Australia

Abstract

This paper assesses the influence on techno-economic performance of modularising hybrid Concentrating Solar Power (CSP) systems with fossil fuel backup for both a Hybrid Solar Receiver Combustor (HSRC), which integrates a combustor into a solar cavity receiver, and a Solar Gas Hybrid (SGH) system with a similar cavity receiver and a back-up boiler. It was found that the energy losses in a system of small-sized modules, which employs molten salt as its heat transfer fluid (HTF), are dominated by trace heating owing to the increased piping over their larger receiver counterpart. However, this can be reduced significantly by using alternative HTFs with a lower melting point such as sodium. In addition, for modularisation to be cost effective requires it to also enable access to alternative, lower-cost manufacturing methods. That is, the benefit of standard learning rates is insufficient to lower the LCOE on its own. For a plant with 30 units of $1MW_{th}$ modules the LCOE is competitive, relative to a single unit of $30MW_{th}$, after ~10 plants are installed if the modularised components (i.e. heliostats, receivers and towers) can be decreased by >80% and >40% for molten salt and sodium as the HTF, respectively.

Nomenclature

$\dot{Q}$	heat transfer rate (W)
$\dot{W}$	work rate = power output (W)

Greek Symbols

ε	experience parameter

Abbreviations

CSP	Concentrating Solar Power
EPGS	Electrical Power Generating System
HSRC	Hybrid Solar Receiver Combustor
HTF	Heat Transfer Fluid
IEA	International Energy Agency
LCOE	Levelized Cost of Electricity
SG	Steam Generator
SGH	Solar Gas Hybrid

Subscripts

air	air from surrounding
ap	aperture
boil	boiler
cap	capacity
comb	combustion air

conv	conventional
crit	critical or threshold value
cum	cumulative
decom	decommissioning
dump	dumped
elec	electrical
exh	exhaust
gas	hot gases from combustion
gen	generator
helio	heliostat
int	internal
invest	investment
mat	material
max	maximum
min	minimum
mod	modular
Na	liquid sodium
noz	nozzle opening losses
rec	solar receiver

salt	molten salt
sec	secondary air
sol	solar
stm	steam
sto	storage
t	time (years)
th	thermal output
trace	trace heating
use	useful
wall	wall losses

1.0 Introduction

There is a growing interest in modular electrical power systems with distributed and off-grid power generation as a potential method to lower the cost of renewable electrical energy generation and thereby increase its penetration [1]. Smaller modules of solar power generation also tend to be particularly attractive for off-grid applications, where fossil fuelled systems lose the comparative advantage associated with economies of scale [1]. One of the renewable energy technologies under development is Concentrating Solar Power (CSP) technologies, which offer the comparative advantage of low cost energy storage, owing to the lower cost of thermal storage over electrical storage [2]. However, to provide a firm, continuous supply of electricity throughout the year, the size of storage becomes very large, with one study estimating up to 10 days capacity, even for sites with high average annual solar resource [3]. The cost of such large thermal storage capacities is expected to be prohibitive [4]. As a result,

hybridization of solar thermal power systems with combustion is likely to offer a lower cost approach to maintaining supply, with the fuel coming from fossil resources in the short term and alternative low-net-CO_2 in the longer term. However, little information is available of the economics of modular hybrid CSP systems.

One hybrid technology of interest is the Hybrid Solar Receiver Combustor (HSRC), recently proposed by Nathan et al. [5]. The HSRC concept is based on combining the functions of a solar-only cavity receiver and a combustor into a single component. This integration was found for a single tower system to reduce the overall LCOE relative to its nearest equivalent system, the Solar Gas Hybrid (SGH), by up to 17% depending on the price of fuel, for a 100MW_{th} receiver size [6]. This estimate was based on an analytical model of heat transfer with energy balance equations [7], together with a piecewise-continuous (i.e. pseudo-dynamic) model that accounts for solar variability on performance [6]. Lim et al also found that of the HSRC reduces the net fuel consumption relative to the SGH by 12% to 31% depending on the size of thermal storage capacity, predominantly due to the HSRC avoiding the start-up and shut-down losses of the backup boiler for the SGH [6, 8]. Since this technology is particularly robust and can potentially be configured in different sizes [9], it is of interest to analyse the techno-economic implications of modularising the HSRC system relative to its equivalent SGH. Hence, this paper aims to estimate the LCOE of several modular units of the HSRC as compared with a single unit of the HSRC for the same power block size comparing these systems to their equivalent counterparts.

Modular systems are being introduced in power generation technologies including wind turbines, solar PV, CSP [1, 10] and nuclear reactors [11, 12]. This is driven by the potential to lower the cost by mass production of standardized components of much smaller scale. Other advantages are claimed with the use of lower-cost materials [13], which offers the potential for additional options to identify the economic optimum in LCOE. The complexity and technical

challenges of construction are also lower for smaller/modular CSP systems [14]. In addition, for a large power plant with multiple modules, there is no need to shut down the entire plant in the event where there is a problem with one of the modules. This provides greater flexibility when operating a power plant. Another potential advantage is that the power station can be constructed in stages, therefore allowing cash-flow to be generated in stages [15]. Nevertheless, these potential advantages must be compared against the disadvantages that include an increase in operations and maintenance (O&M) costs, an increase in the number of components, and an increase in the thermal and parasitic losses due to an increase in surface area to volume ratio associated with reduced thermal scale of the components. However, to our knowledge, no assessment of the direct economic merit of modularisation of hybrid CSP plants has been reported. Therefore, the paper aims to evaluate the trade-off between the aforementioned pros and cons for modular hybrid CSP systems.

In light of the discussion above, the first aim of the present investigation is to extend the pseudo-dynamic model of the HSRC and SGH developed previously for the evaluation of modules of different sizes. The next aim is to estimate the dominant losses associated with both types of modular hybrid CSP systems. The third aim is to assess the economic trade-off between these losses and lower manufacturing costs due to improved learning/cheaper materials for both modular HSRC and SGH systems.

2.0 Methodology

The pseudo-dynamic model of by Lim et al. [6], written in Matlab, was extended to assess the modularisation of selected components in the HSRC and SGH systems. It calculates the pseudo-dynamic performance of each system by assuming steady-state operation at each time-step from a time-series of hourly Direct Normal Irradiation data. The model developed has been previously verified to show that the dynamic response of the system to various time-series is consistent with expectation [6].

2.1 Site Selection

The pseudo-dynamic model uses data from the National Solar Radiation Database and Bureau of Meteorology at selected sites from the USA and Australia respectively for the year 2000 to 2004. In particular, the sites selected are Daggett (USA), Prescott Love Field (USA), Darwin (AUS) and Mildura (AUS) because of their have high average annual solar radiation [3]. Of these sites, Daggett has the lowest vulnerability to unscheduled reduction in output due to the variability in solar resource. Hence, this site was selected as a reference case for all of the calculations performed in this paper.

2.2 System Components for Modularisation

Figs. 1 and 2 present schematic diagrams of the modules of heliostat field and receiver that are combined to power a central power block for the HSRC and SGH power systems, respectively. The total number of modules, n_{mod}, is varied over the range of one to 30. The HTF is also used as the thermal storage medium, with a hot and a cold storage tank. Power is assumed to be generated by a Rankine Cycle. A steam generator is used to transfer heat from the HTF to the steam, while the Rankine Cycle is simplified into an Electrical Power Generating System (EPGS).

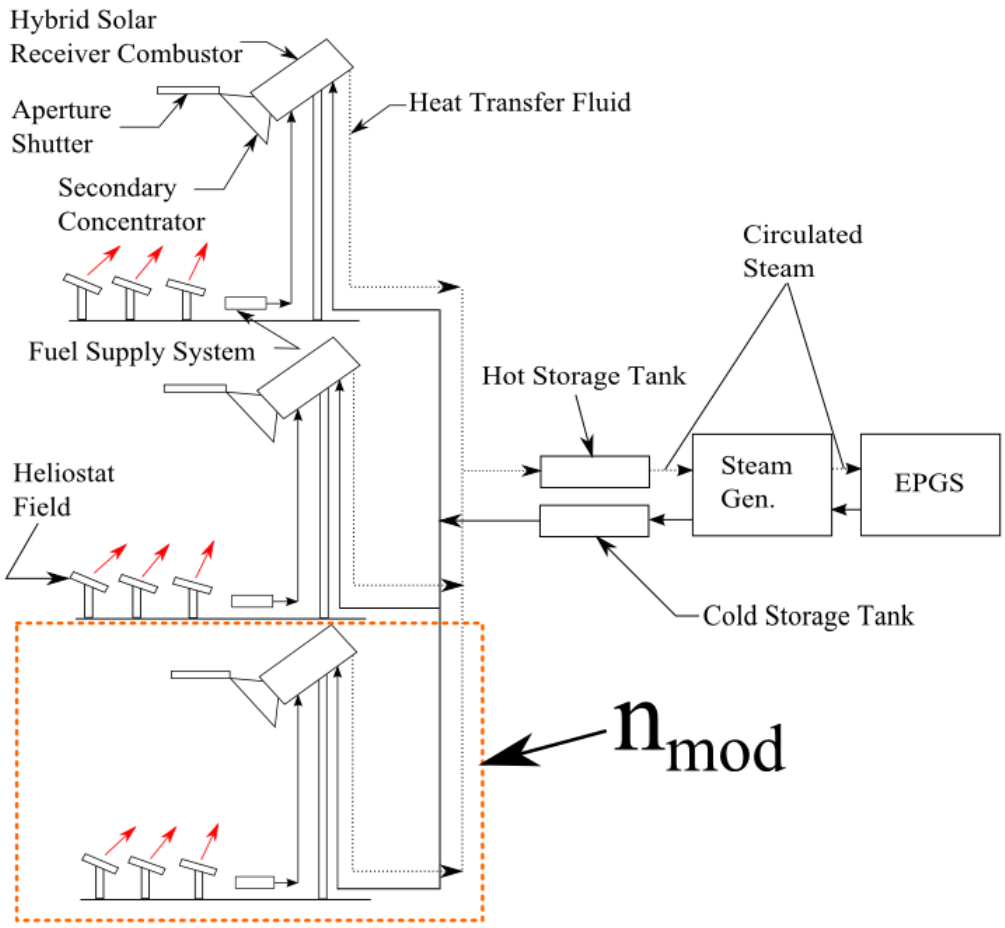

Fig.1. Schematic diagram a modular system of the Hybrid Solar Receiver Combustor (HSRC) mounted on a solar power tower in a typical Concentrating Solar Power system. Here, EPGS is the Electrical Power Generating System.

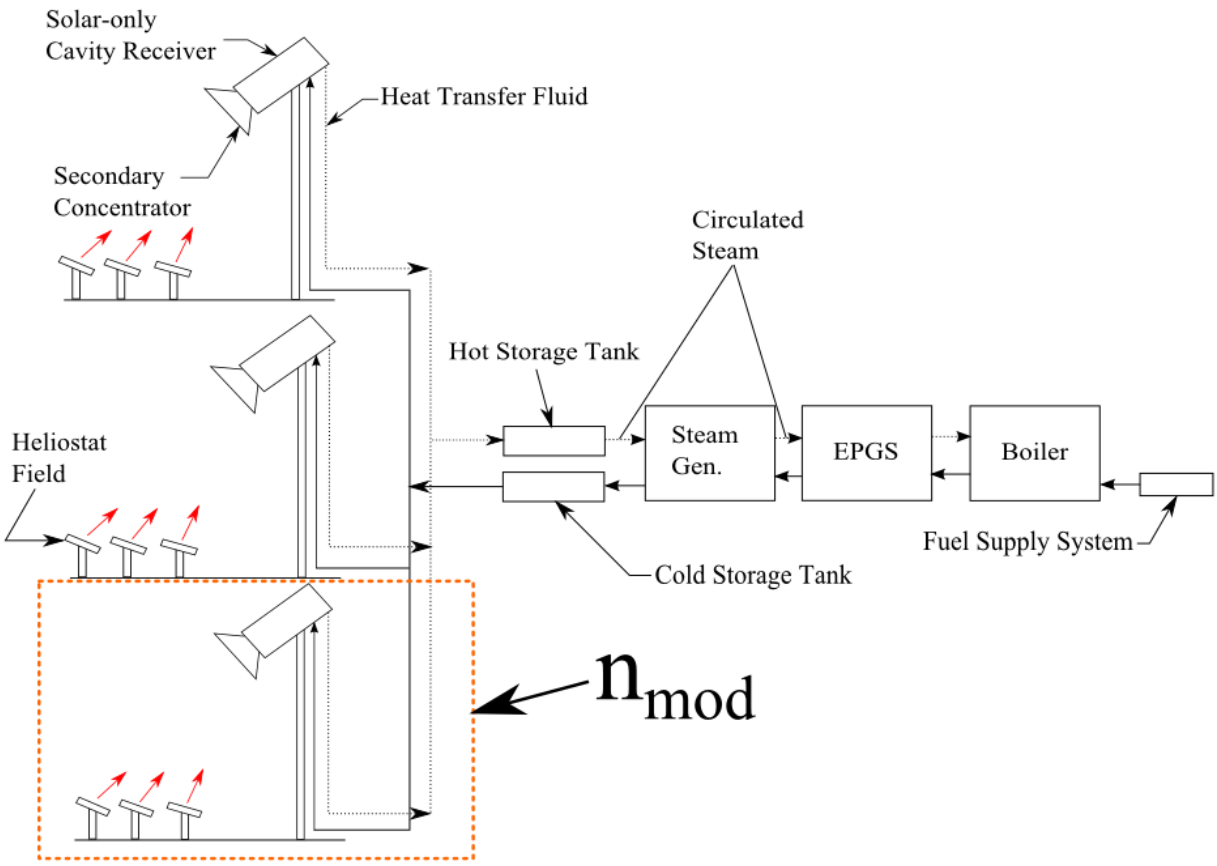

Fig.2. Schematic diagram of a modular system of the reference Solar Gas Hybrid (SGH) case, where EPGS is the Electrical Power Generating System.

2.3 Heat Transfer Fluid

The reference heat transfer fluid (HTF) chosen for most assessments of both the HSRC and SGH systems was molten salt, because its properties are well known [16] and that the fluid is currently state-of-the-art and widely employed in the CSP industry [17]. However, molten salt is known to have undesirable properties which include a high melting temperature of ~220°C. To avoid the problems associated with solidification, electrical trace heating is typically used, resulting in significant parasitic losses. Hence, assessments were also performed with sodium as an alternative HTF, which has a melting temperature of ~97°C [18].

2.4 Pseudo-Dynamic Model

Fig. 3 presents a schematic diagram of the modular HSRC system. Solar power is concentrated from the heliostat field, $\dot{Q}_{helio}$, to the HSRC, which heats the HTF. The useful heat from the device, $\dot{Q}_{HSRC,out}$, is then stored in a hot storage tank, to be used in the steam generator when required. When the hot storage tank has reached its limit, the excess power is dumped ($\dot{Q}_{tank(hot),dump}$). This system differs from those in previous assessments on single-tower systems in the use of a long pipe transferring fluid between the receiver and the tank.

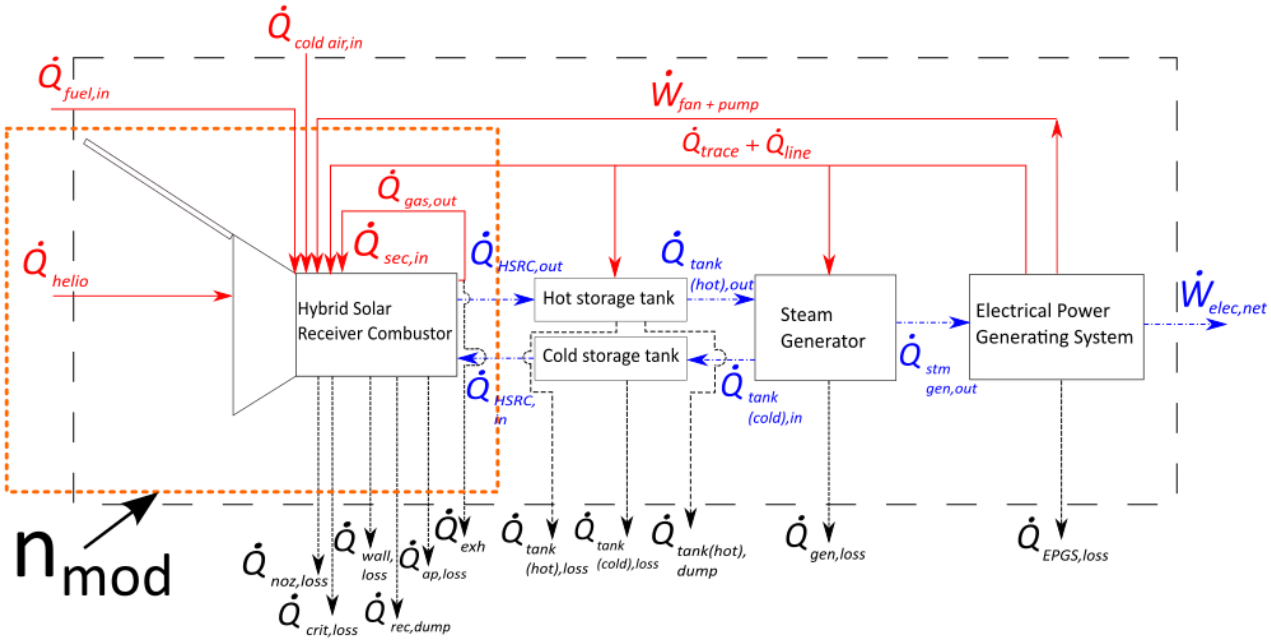

Fig.3. The flow of power through the Hybrid Solar Receiver Combustor, HSRC, system where n_{mod} represents the number of modules.

Fig. 4 presents a schematic diagram of the reference modular SGH system. The main difference between this system and the HSRC system is that the backup boiler is coupled into the system to provide heat to the Electricity Power Generating System (EPGS), when heat is not available from the hot storage tank.

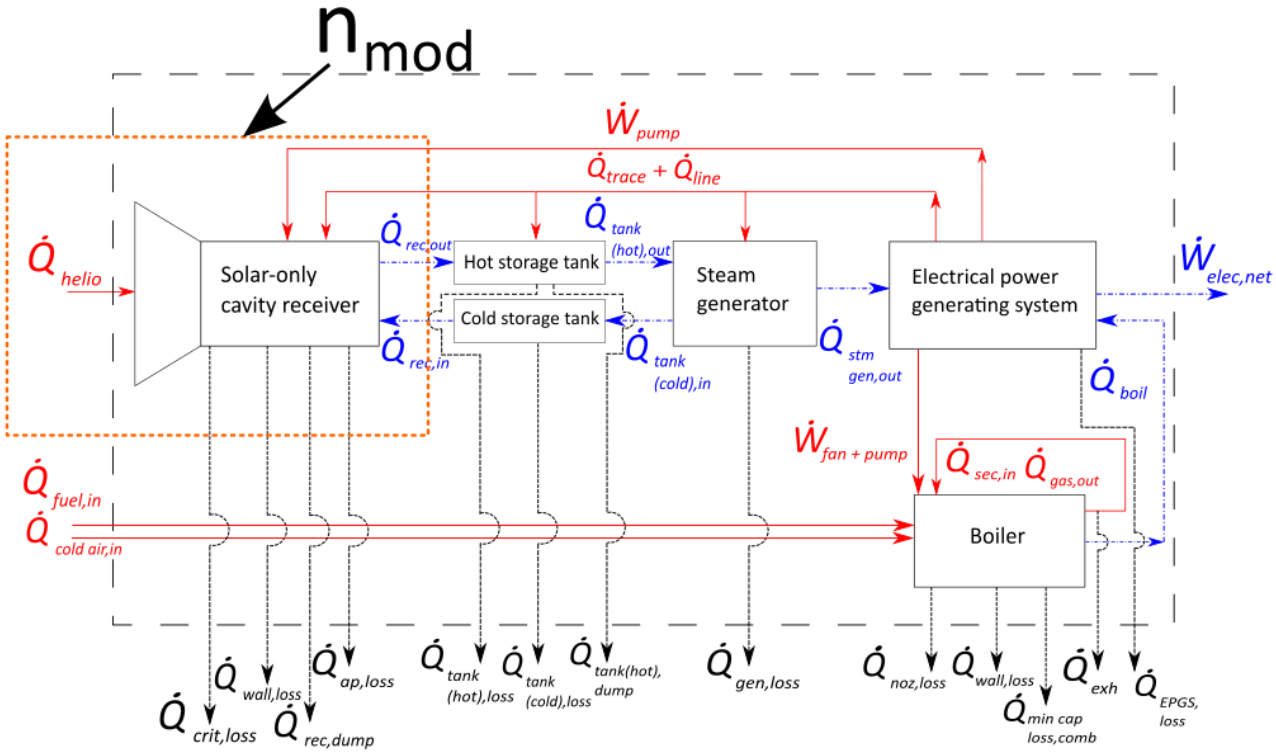

Fig.4. The flow of power through the Solar Gas Hybrid, SGH, system where n_{mod} represents the number of modules.

The design of HSRC was optimised separately for each of the scales selected assuming a constant length to diameter of cavity ratio, L_C/D_C, of five and constant velocity scaling to achieve a similar thermal performance to its 30MW$_{th}$ counterpart [7] following previous work by Weber and Breussin, and Hsieh et al [19, 20]. The trade-offs of scaling are accounted for by the correlations used in the economic assessment, which is presented in Section 2.7. Another parameter kept constant was the power block ratio, defined as the rated capacity of the hot storage tank to the receiver, $PBR = \frac{\dot{Q}_{tank(hot),max}}{\dot{Q}_{HSRC,max}} = 0.8$ for the HSRC system and $PBR = \frac{\dot{Q}_{tank(hot),max}}{\dot{Q}_{rec,max}} = 0.8$ for the reference case SGH. Also, the heliostat field was sized for each system based on the ratio of $\frac{\dot{Q}_{tank(hot),dump}}{\dot{Q}_{tank(hot),max}}$ which was set to avoid more than 5% dumping of

the total power output from the hot storage tanks, as per the previous work by Lim et. al [6]. In addition, the capacity of the backup boiler for the SGH was set to 24MW_{th}, operating with an efficiency of 80% [21]. This information is summarized in Table 1.

Table 1. List of all the variables that were fixed in the assessments of modularisation.

Fixed Variables	**Values**
L_C/D_C ratio of solar-only cavity receiver and backup boiler	5
Heliostat size based on the ratio $\frac{\dot{Q}_{tank(hot),dump}}{\dot{Q}_{tank(hot),max}}$	<5%
Power block ratio, $PBR = \frac{\dot{Q}_{tank(hot),max}}{\dot{Q}_{rec\ or\ HSRC,max}}$	0.8
Backup boiler capacity (for SGH)	24MW_{th}
Efficiency of back-up boiler	80%

2.5 Scenarios

Table 2 presents the key information for each of the systems analysed, all of which were fixed to produce a constant overall thermal output of 30MW_{th}. It should be noted that the receivers were scaled over the range of 1MW_{th} to 30MW_{th} because this range is most likely to offer economies of scale [7]:

Table 2. A summary of the cases analysed.

System	**Receiver size, $\dot{Q}_{rec}$ (MW_{th})**	n_{mod}	**Description**
SGH	30	1	solar-only cavity receiver with 24MW_{th} backup boiler
HSRC	30	1	HSRC
SGH	10	3	solar-only cavity receiver with 24MW_{th} backup boiler
HSRC	10	3	HSRC
SGH	3	10	solar-only cavity receiver with 24MW_{th} backup boiler
HSRC	3	10	HSRC
SGH	1	30	solar-only cavity receiver with 24MW_{th} backup boiler
HSRC	1	30	HSRC

Three thermal storage capacities of all the assessed systems, $\dot{Q}_{sto}$, listed in Table 1 were considered, that is 1, 5 and 10 hours of storage.

2.6 Plant Layout

Fig. 5 shows the plant layouts that were assumed for the scenarios analysed. The layouts were selected based on the only modular CSP system, to our knowledge, currently in operation, which is in Jemalong, New South Wales, Australia [22].

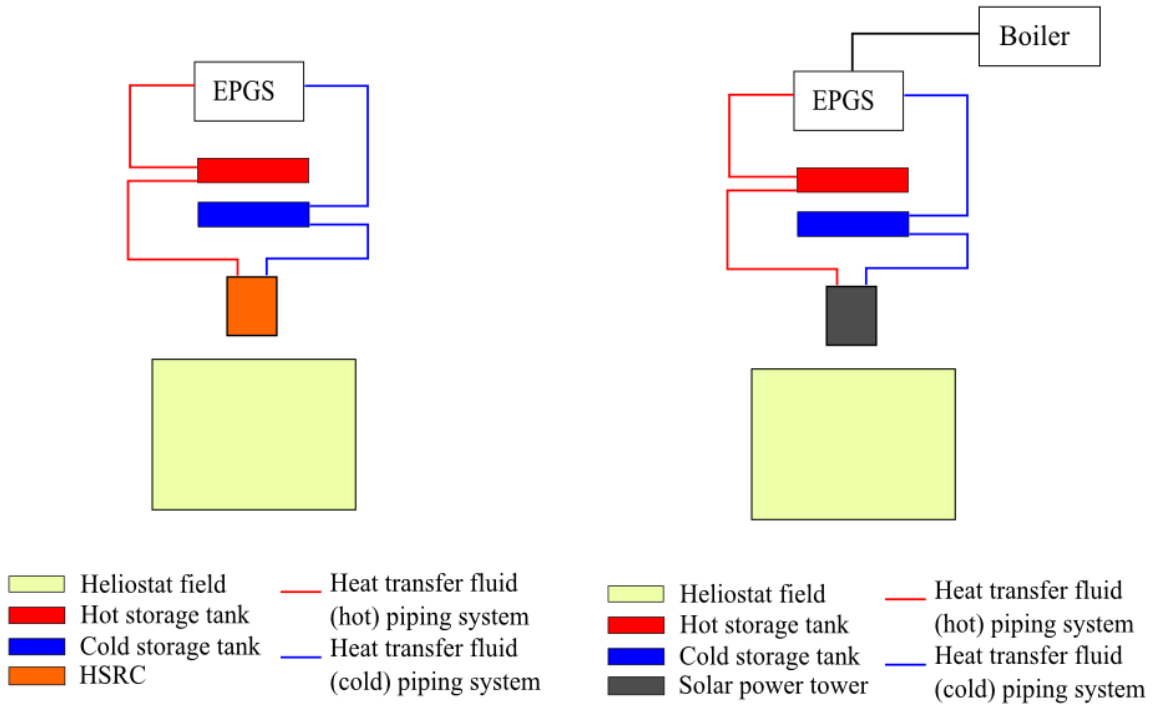

(a)

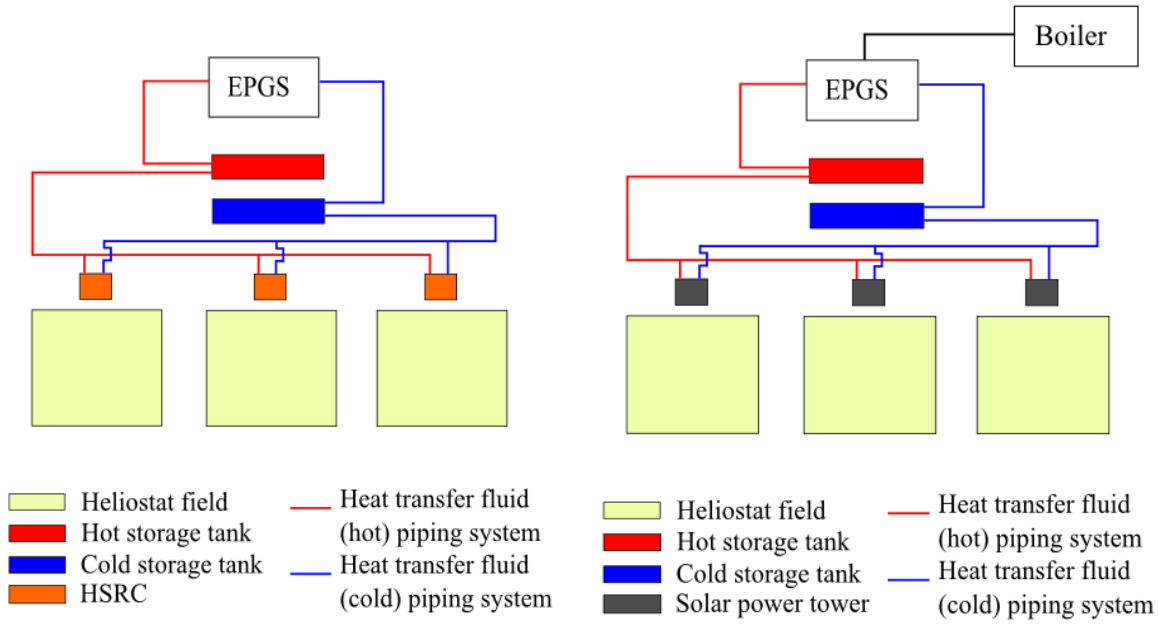
EPGS
Heliostat field
Hot storage tank
Cold storage tank
HSRC
Heat transfer fluid
(hot) piping system
Heat transfer fluid
(cold) piping system
Boiler
EPGS
Heliostat field
Hot storage tank
Cold storage tank
Solar power tower
Heat transfer fluid
(hot) piping system
Heat transfer fluid
(cold) piping system

(b)

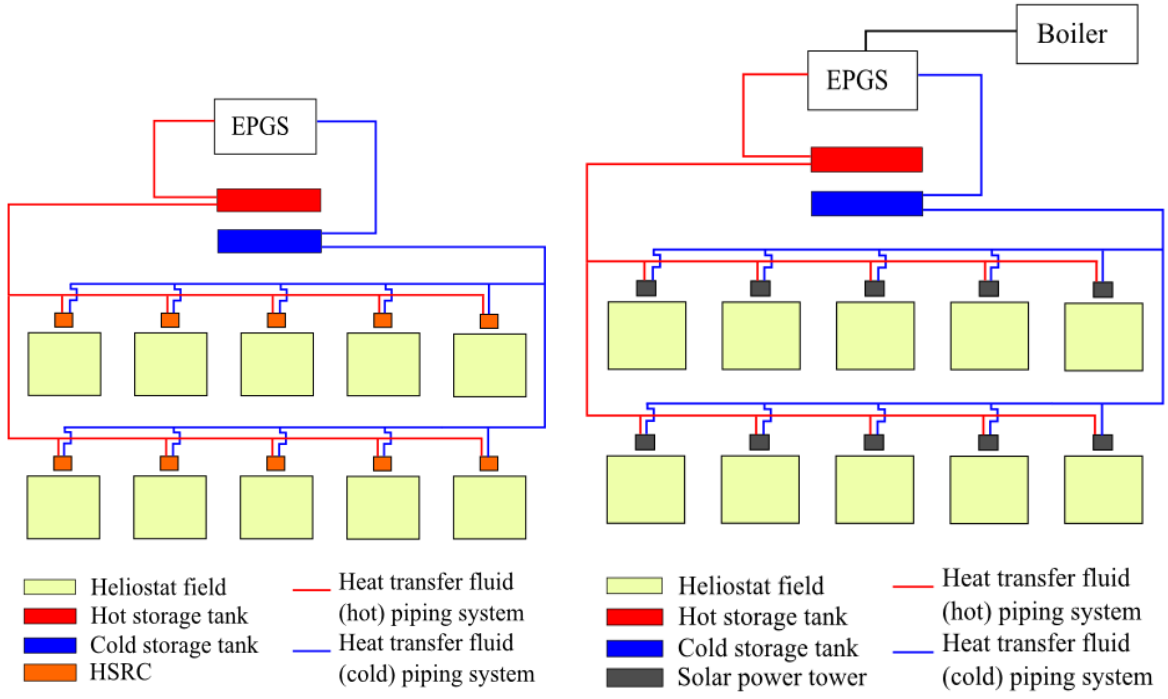
EPGS
Heliostat field
Hot storage tank
Cold storage tank
HSRC
Heat transfer fluid
(hot) piping system
Heat transfer fluid
(cold) piping system
Boiler
EPGS
Heliostat field
Hot storage tank
Cold storage tank
Solar power tower
Heat transfer fluid
(hot) piping system
Heat transfer fluid
(cold) piping system

(c)

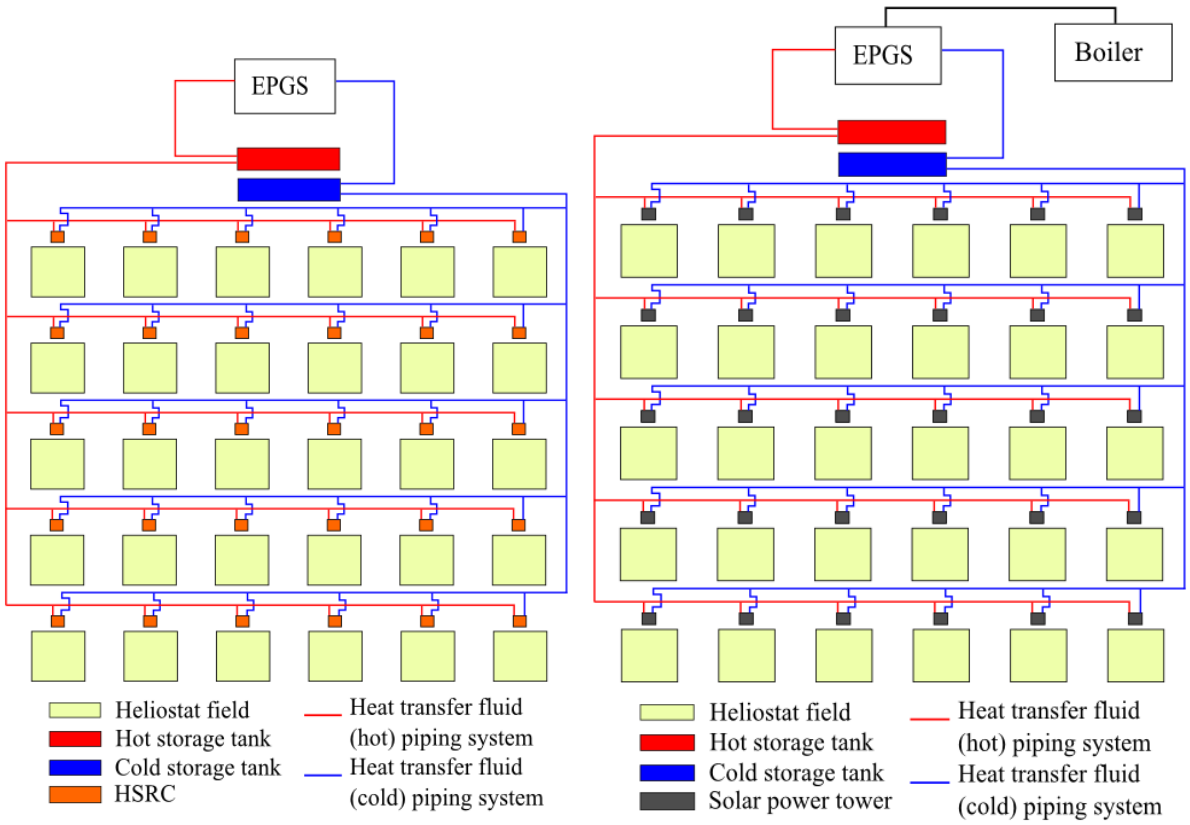

(d)

Fig.5. Plant layouts assumed for the HSRC system (left) and SGH system (right) for different module sizes of (a) 30MW$_{th}$, (b) 10MW$_{th}$, (c) 3MW$_{th}$ and (d) 1MW$_{th}$, with all systems producing a total thermal output of 30MW$_{th}$.

2.7 Electrical Trace Heating

The model assumes that electrical trace heating is used whenever the temperature of the HTF falls below a critical value for the receiver, piping system and the hot and cold storage tanks (refer to Fig. 5) to prevent the HTF from solidifying. Trace heating is used for both systems during periods when the plant is operated from stored thermal storage, while the SGH also requires additional trace heating at times when $\dot{Q}_{helio}$ is below its minimum threshold for which the gains exceed the losses [6]. We also report the primary energy associated with electrical

trace heating, assuming that the electricity is generated at an efficiency of 35% and that the power is purchased from the electrical grid [2].

To calculate the electrical trace heating of the pipes, the following equation was used (for molten salt as the HTF):

$$\dot{Q}_{trace} = \frac{1}{0.35} \times n_{mod} \times 1.1 \times (((\dot{Q}_{trace,per\ pipe,low} \times (n_{pipe} \times l_{pipe,salt,rec})) + \dot{Q}_{trace,per\ pipe,high} \times ((l_{pipe,base\ to\ tank} \times 2) + (h_{tower} \times 2))) \quad (1)$$

Here, the values of $\dot{Q}_{trace,per\ pipe,low}$ and $\dot{Q}_{trace,per\ pipe,high}$ are the average power required per meter of piping obtained from Rodriquez-Garcia et al. [23]. An additional 10% was also added to the overall power to account for the need to heat the storage tanks and other miscellaneous components [6].

The length of pipes from the base of the towers to the EPGS, $l_{pipe,base\ to\ tank}$, was taken to be the average value of those reported for operating power plant layouts, assuming a constant optical efficiency for each of the heliostat fields, while the diameter of the pipes were assumed to range from 0.05m to 0.254m for each scale [24-26]. The average value in length considered the vertical distance of the furthest receiver to the tower for plant sizes of $1MW_e$ and $10MW_e$ which are equal to approximately $3.3MW_{th}$ and $33.3MW_{th}$ respectively. This distance was then extrapolated to estimate the distances for other scales. The estimated total length of piping carrying the HTF from the base of each tower to the hot and cold storage tanks are presented in Table 3.

Table 3. The estimated total length of piping carrying the heat transfer fluid (HTF) from the base of each tower to the hot and cold storage tanks for different scales.

Receiver Scale (MW_{th})	Estimated total piping length from base of tower(s) to tanks (m)
30	200
10	2100
3	7000
1	12000

Table 4 presents the height of the solar power towers, h_{tower}, for different module sizes. The values of h_{tower} were obtained from literature for scales of $3MW_{th}$, $30MW_{th}$ and $100MW_{th}$, while the height for the other scales were predicted following a logarithmic equation of the three known tower heights, while also assuming a constant optical efficiency for each of the heliostat fields:

$$h_{tower} = 47.91 \times \dot{Q}_{rec}^{\ 0.1948} \quad (2)$$

Table 4. Heights of solar power towers for different scales both obtained from literature and predicted based on a logarithmic equation.

Receiver Scale (MW_{th})	Height(m)	Reference
100	120	[6]
30	90	[27]
10	78	-
3	60	[28]
1	40	-

2.8 Levelized Cost of Electricity

The equation from International Energy Agency (IEA) was used to calculate the Levelized Cost of Electricity (LCOE) as follows [29]:

$$LCOE_{overall} = \frac{\sum_t((Invest_t + O\&M_t + Fuel_t + Carbon_t + Decom_t) * (1+r)^{-t}}{\sum_t (Elec_t * (1+r)^{-t})} \quad (3)$$

where *t* represents the year, $Invest_t$ is the cost of investment in year *t*, $O\&M_t$ is the operations and maintenance costs for year *t*, $Fuel_t$ is the fuel costs for year *t*, $Carbon_t$ is the total cost of

carbon emissions (e.g. from a carbon tax) for year *t*, $Decom_t$ is the decommissioning cost of the power plant for year *t*, *r* in the term $(1+r)^{-t}$ is the discount factor for year *t*, and $Elec_t$ is the amount of electricity produced in year *t*. The life of the plant was assumed to be 30 years, while the present comparison conservatively ignores the costs of carbon emissions [11]. Decommissioning effects are also ignored following previous work by Lim et al [6] while the cost estimates were previously adjusted to account for inflation using the Chemical Engineering Plant Cost Index [5]. The discount factor is assumed to be equivalent to the assumed internal rate of return of 10% over the project life for most of the calculations done.

Table 5 presents the values and correlations used in the cost estimations for the different module sizes of the HSRC and SGH. Because the cost of the HSRC is not yet known (being pre-commercial), a factor, f_{HSRC}, was introduced as a multiplier of the cost of a solar-only cavity receiver when estimating the capital cost of the HSRC. This factor was varied between 1.5 and 2.5 times that of a solar-only cavity receiver, with most of the calculations assuming f_{HSRC}=2. This is because it is expected that the HSRC will cost more than a solar-only cavity receiver because of the addition of boiler components such as heat exchangers. Previous analysis has estimated that the addition of these components can double the weight of a solar-only cavity receiver (to achieve the same thermal efficiency to that of its counterpart), so that this can be taken as a first-order estimator for cost. However, the previous analysis did not account for the use of heat exchanger enhancement methods such as fins and dimples which may reduce its overall weight and cost. On the other hand, additional capital cost may be inquired by the HSRC due to the need to install piping for its fuel supply line which was estimated to be 1.5 times the overall cost of piping for the SGH. This also results in a slight increase in parasitic losses required to pump the fuel to the HSRC by around 1-2%. Additionally, to account for the type of material used to manufacture each modular component, in particular the heliostats, tower, and both the solar-only cavity receivers and HSRC we

introduced a correction factor, f_{mod}, which accounts for cheaper, more readily available parts/materials for the components in the smaller modules with a cost reduction of up to 40% [30]. Following this, the value of f_{mod} was varied between 0.2 and 1 with a value of 0.6 as the reference case. This value is also used to set targets for the cost reduction by mass production and technological advancements. Finally, it is also worth noting that the increased cost of sodium relative to molten salt included the additional costs of addressing the safety issues associated with sodium.

Table 5. Values and correlations used in the Levelized Cost of Electricity, LCOE, calculations (US dollars).

Component cost	**Correlation/value**	**Unit**	**Reference**
Heliostats	$f_{mod} \times 120$	\$/m^2	[31]
Solar-only cavity receiver	$n_{mod} \times f_{mod} \times 3.52\dot{Q}_{rec,max}^{0.44}$	\$M	[5]
HSRC	$n_{mod} \times f_{mod} \times f_{HSRC} \times 3.52\dot{Q}_{rec,max}^{0.44}$	\$M	[5]
Tower	$n_{mod} \times f_{mod} \times 0.0305\dot{Q}_{rec,max} + 0.961$	\$M	[5]
Piping	9	\$/m^2	[2]
Thermal storage (molten salt)	$0.0153\dot{Q}_{sto} + 0.502$	\$M	[5]
Thermal storage (sodium)	$3.2 \times (0.0153\dot{Q}_{sto} + 0.502)$	\$M	[18]
Steam generator	$0.212\dot{Q}_{SG,out,max}^{0.7}$	\$M	[5]
EPGS	$1.84\dot{Q}_{SG,out,max}^{0.7}$	\$M	[5]
Gas-fired boiler	$1.69\dot{Q}_{boil,max}^{0.7}$	\$M	[5]
Operation & Maintenance			
Solar field	$1.88A_{helio} + 0.189$	\$M/yr	[5]
Plant	$0.0151\dot{W}_{elec,net} + 2.92$	\$M/yr	[5]
Fuel cost (Natural gas)	$3\ to\ 15$	\$/GJ	[32]
Levelized cost calculation parameters			
Internal rate of return	$5\%\ to\ 20\%$		
Plant life	$30\ years$		

Most of the calculations assumed the cost of fuel to be $3USD/GJ to allow a direct comparison with the earlier assessment of Nathan et al. and Lim et al. [5, 6]. This price is within the range of which the current price of natural gas fluctuates [32]. Because the cost of fuel is a significant factor in determining the LCOE of electricity generating technologies [29] and also varies worldwide, [32] a sensitivity analysis to the cost of natural gas ranging from $3USD/GJ to $15USD/GJ was also performed.

2.9 Learning Rates

The assessment employed the approach to learning rates proposed by the IEA to analyse the cost and benefits of emerging clean energy technologies, which includes solar thermal systems [33]. These rates are used to estimate the relative cost reduction of a component for each of its doubling in cumulative production accounting for all aspects of the component including manufacturing, capital costs and O&M costs [34-36]. The equations used to estimate the cost of a component based on learning rates after a fixed cumulative installed capacity are [37]:

$$Cost_{cap_{cum}} = Cost_{initial} \times Cap_{cum}{}^{\varepsilon} \quad (4)$$

$$Learning\ rate = 1 - 2^{-\varepsilon} \quad (5)$$

Here, Cap_{cum} represents the cumulative production capacity while the learning rate is a function of ε, which represents the experience parameter that characterises its inclination. Jamasb and Kohler proposed the general "rule of thumb" learning rate for electricity generation technologies to be 20% [38]. They also predicted a learning rate of 22.5% for CSP technologies [38]. Hinkley et al calculated a learning rate of 15% while Neij et. al assumed a learning rate of 10±5% for the same technology respectively [34, 39]. Following this, a sensitivity study for learning rates in the range of 0% to 25% was performed with most of the calculations assuming a learning rate of 20%. In addition, all calculations were performed within the range of 30MW_{th} to 3,000MW_{th} of cumulative installed capacity with the reference case being 300MW_{th}.

3.0 Results and Discussion

Fig. 6 presents the distribution of power inputs and losses calculated to be necessary to achieve 30MW of continuous thermal output for the HSRC and SGH systems with module sizes and thermal storage capacities of 1, 5 and 10 hours using molten salt as the HTF and storage medium. The figure shows that trace heating losses increase with decreasing receiver size to be dominant for the smallest two module sizes of $3MW_{th}$ and $1MW_{th}$. Losses are also greater for the SGH than the HSRC for all storage capacities assessed. For the case of 1 hour of thermal storage capacity the power required for trace heating with 30 units of $1MW_{th}$ receivers ($HSRC_{Qrec1,Qsto1,salt}$), is greater than that for a single $30MW_{th}$ receiver ($HSRC\ 30_{Qrec30,Qsto1,salt}$) by a factor of ~10, while the equivalent factor for the SGH is ~8. This factor is ~8 for both the HSRC and SGH systems for the cases of 5 and 10 hours of thermal storage capacity. Also, the power required for trace heating for the $SGH_{Qrec1,Qsto1,salt}$ system is greater than that for the $HSRC_{Qrec1,Qsto1,salt}$ system by ~450. This factor decreases with each module size but the trend remains the same. In addition, the power needed for combustion is higher for all cases of the SGH systems than the HSRC systems by a factor of ~1.2 to ~1.5, predominantly due to start-up and shut-down losses, consistent with the previous assessment of Lim et al. [6].

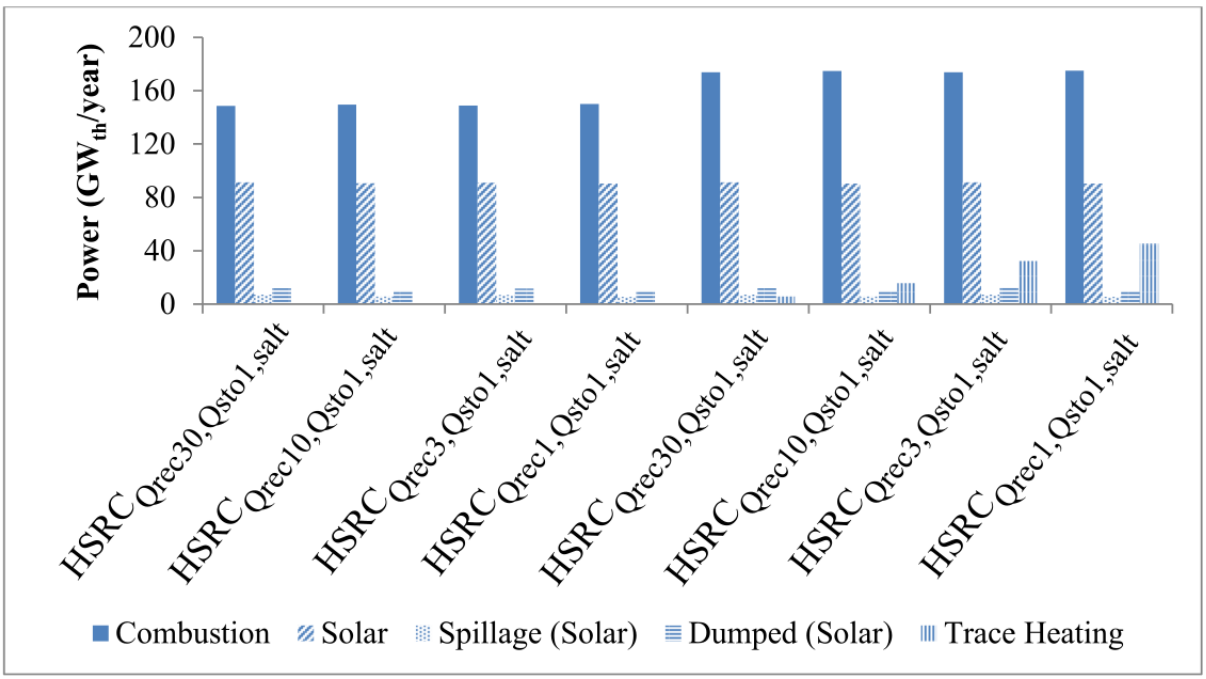
Power (GWth/year)
200
160
120
80
40
0
HSRC Qrec30,Qsto1,salt
HSRC Qrec10,Qsto1,salt
HSRC Qrec3,Qsto1,salt
HSRC Qrec1,Qsto1,salt
HSRC Qrec30,Qsto1,salt
HSRC Qrec10,Qsto1,salt
HSRC Qrec3,Qsto1,salt
HSRC Qrec1,Qsto1,salt
Combustion
Solar
Spillage (Solar)
Dumped (Solar)
Trace Heating

(a)

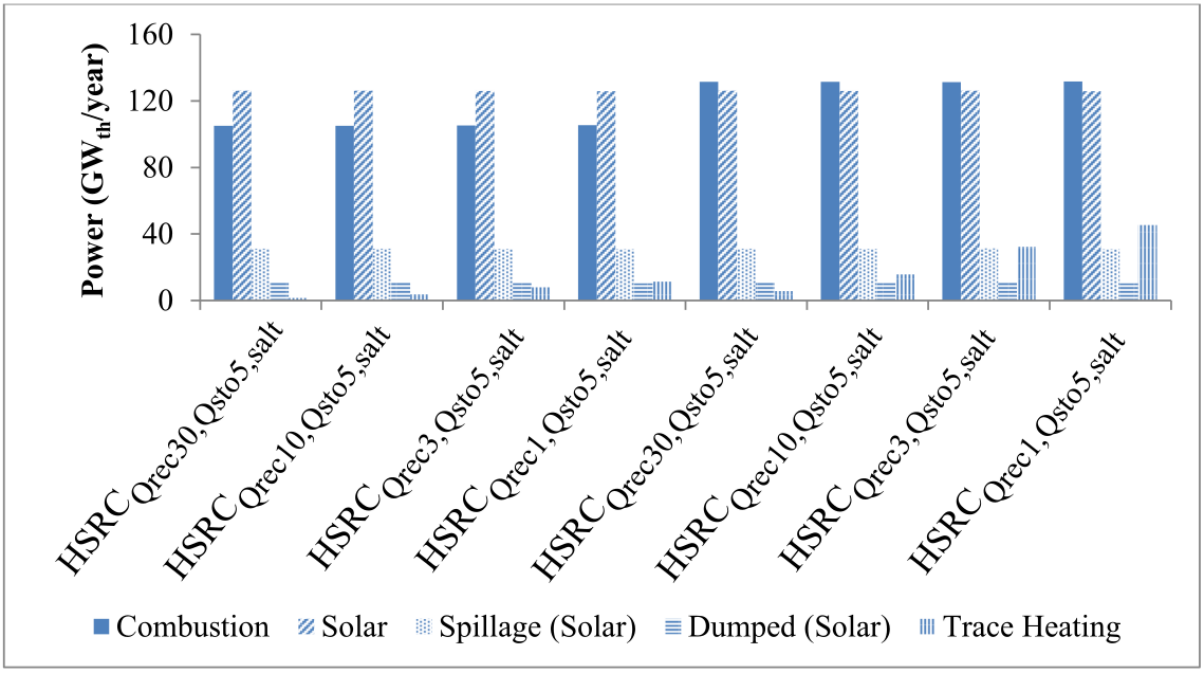
Power (GWth/year)
160
120
80
40
0
HSRC Qrec30,Qsto5,salt
HSRC Qrec10,Qsto5,salt
HSRC Qrec3,Qsto5,salt
HSRC Qrec1,Qsto5,salt
HSRC Qrec30,Qsto5,salt
HSRC Qrec10,Qsto5,salt
HSRC Qrec3,Qsto5,salt
HSRC Qrec1,Qsto5,salt
Combustion
Solar
Spillage (Solar)
Dumped (Solar)
Trace Heating

(b)

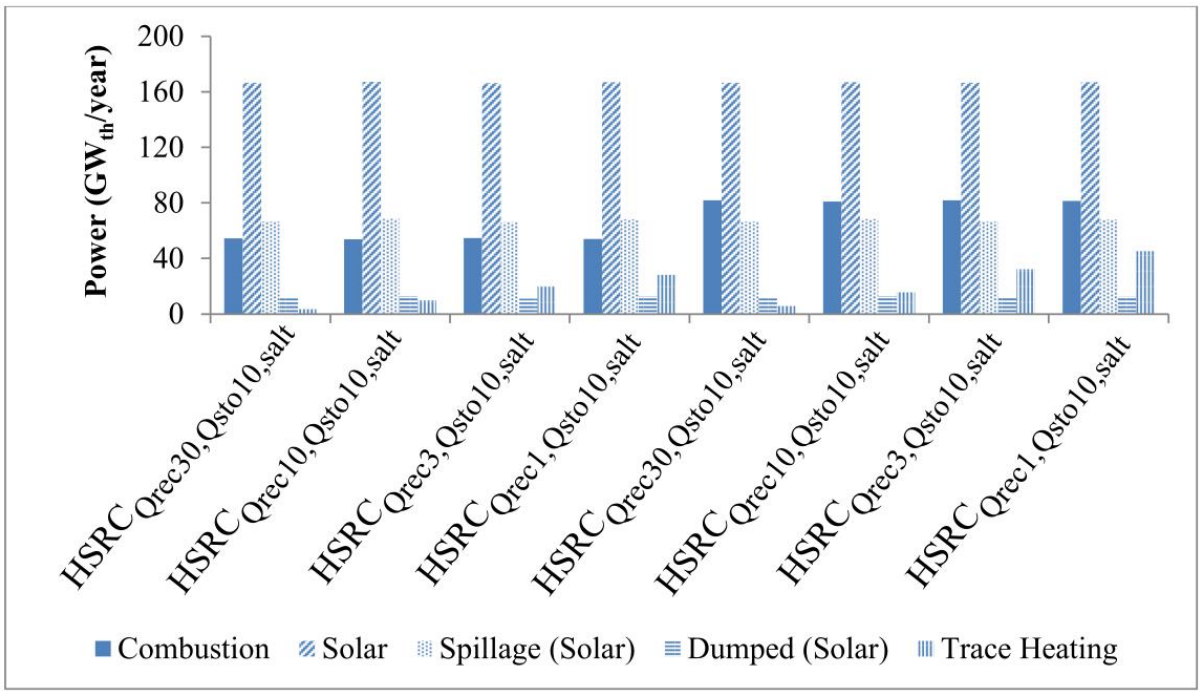

(c)

Fig.6. Annually averaged distribution of power inputs and losses calculated to achieve 30MW_{th} continuous output for both the Hybrid Solar Receiver Combustor (HSRC) and Solar Gas Hybrid (SGH) for modular sizes of 1MW_{th}, 3$MW_{th,}$ 10MW_{th} and 30MW_{th} using molten salt as the heat transfer fluid with a thermal storage capacity of (a) 1 hour, (b) 5 hours and (c) 10 hours. Note that all data are reported as gross thermal power to and from the Electrical Power Generating System (EPGS).

Fig. 7 presents the power required for trace heating for the case of the HSRC and SGH systems with 5 hours of thermal storage capacity using molten salt and sodium as the HTF and with the learning rate fixed at 20%, f_{mod}=0.6 and f_{HSRC}=2, calculated after 300MW_{th} of cumulative installations. It can be seen that the trace heating losses decrease with an increase in module size for all the cases of the SGH and HSRC systems. It was also found that the power required for trace heating decreases by a factor of ~2.7 when sodium is used as the HTF and storage

medium. For SGH systems with a thermal storage capacity of 5 hours, the power required for trace heating decreases from ~45.3GW_{th}/year to ~5.7GW_{th}/year and ~16.8GW_{th}/year to ~2.1GW_{th}/year with an increase in module size from 1MW_{th} to 30MW_{th} for the case of molten salt and sodium as the HTF, respectively. This is equivalent to ~2.7% to ~21.4% of the total LCOE for each system for the case of molten salt as the HTF and ~1% to ~7.9% for the case of sodium as the HTF. The trend is similar for the case of the HSRC, albeit with a decrease in trace heating losses relative to the SGH, with the losses contributing to less than 5.5% and 2% of the total LCOE for all cases of receiver size for molten salt and sodium as the HTF, respectively. That is, the use of sodium as a HTF decreases both the trace heating losses and the LCOE significantly relative to molten salt.

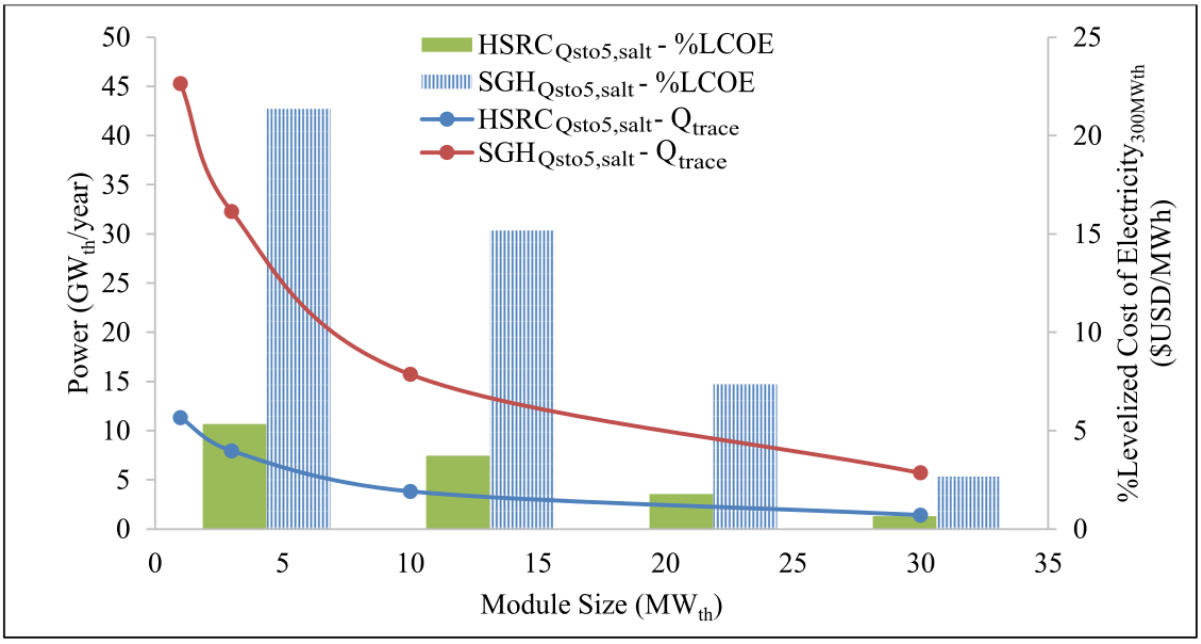

(a)

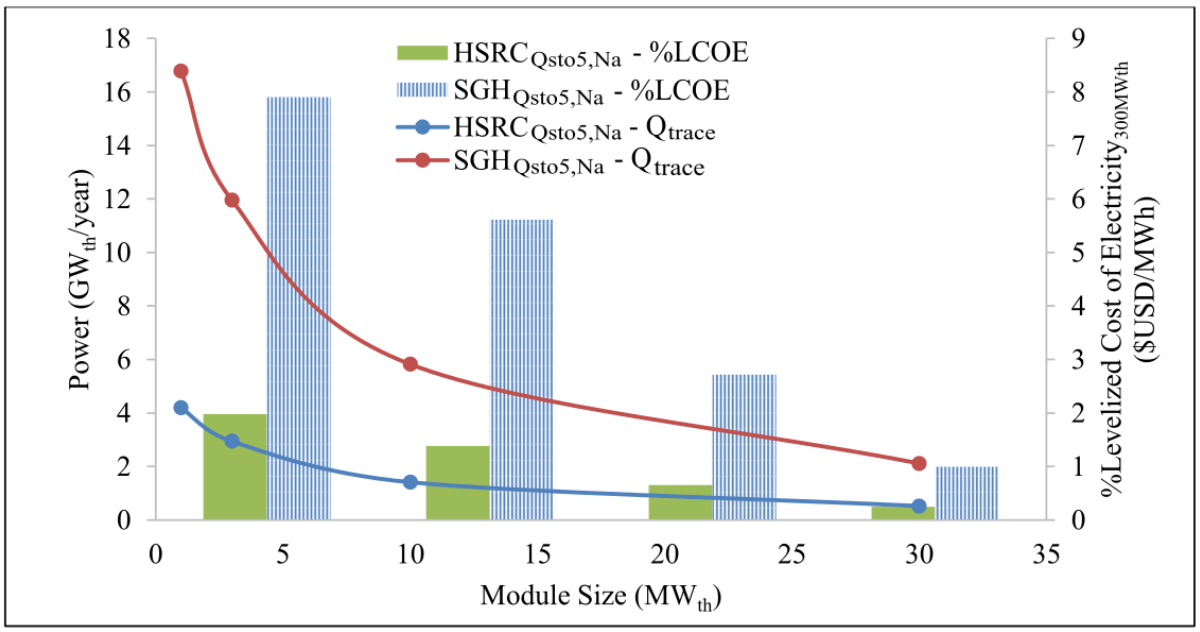

(b)

Fig.7. Annually averaged power required for trace heating and its corresponding equivalent Levelized Cost of Electricity for both the Hybrid Solar Receiver Combustor (HSRC) and Solar Gas Hybrid (SGH) for modular sizes of $1MW_{th}$, $3MW_{th}$, $10MW_{th}$ and $30MW_{th}$ for a thermal storage capacity of 5 hours after a cumulative installed capacity of $300MW_{th}$ with (a) molten salt and (b) sodium, as the heat transfer fluid with the learning rate is fixed at 20%, f_{mod}=0.6 and f_{HSRC}=2. Note that all data are reported as gross thermal power to and from the Electrical Power Generating System (EPGS).

Fig. 8 presents the LCOE calculated for the different module sizes for the reference case of 5 hours of thermal storage capacity for both molten salt and sodium as the HTF, for the case with the learning rate fixed at 20%, f_{mod}=0.6 and f_{HSRC}=2 as a function of cumulative installed capacity. As is implicit for a learning-curve, the LCOE for all modular systems decreases with an increase in cumulative installed capacity. However, the rate of learning is much steeper for the HSRC than for the SGH. In addition, the LCOE decreases as the module size increases in

all cases, i.e. modularisation increases the LCOE for the case of fixed values of f_{mod}. For example, for the case of molten salt as the HTF, the LCOE of the $1MW_{th}$ system is higher than that of $30MW_{th}$ by a factor of ~2.0 and ~1.8 for the HSRC and SGH systems respectively after a cumulative installed capacity of $30MW_{th}$, although this factor decreases to ~1.2 for both systems after a cumulative installed capacity of $30{,}000MW_{th}$. Additionally, for the case of $1MW_{th}$ module size, the LCOE for the HSRC system is slightly higher than the SGH system after cumulative installed capacities of only ~$80MW_{th}$, because the initial capital cost of each HSRC unit is higher than that of a solar-only cavity receiver. However, for greater installed capacities, the LCOE of the HSRC becomes lower than the SGH systems. A similar trend was obtained for the case of sodium as HTF, although the LCOE of the SGH is lower than the HSRC for the case of module sizes of $3MW_{th}$ and $1MW_{th}$ before a cumulative installed capacity of ~$200MW_{th}$ and ~$800MW_{th}$, respectively. This shows that the use of sodium benefits the SGH system more than the HSRC system due to higher trace heating losses from the former. Nevertheless, a reduction in the values of f_{mod} and f_{HSRC} and/or an increase in learning rates will decrease the LCOE of modularised systems further.

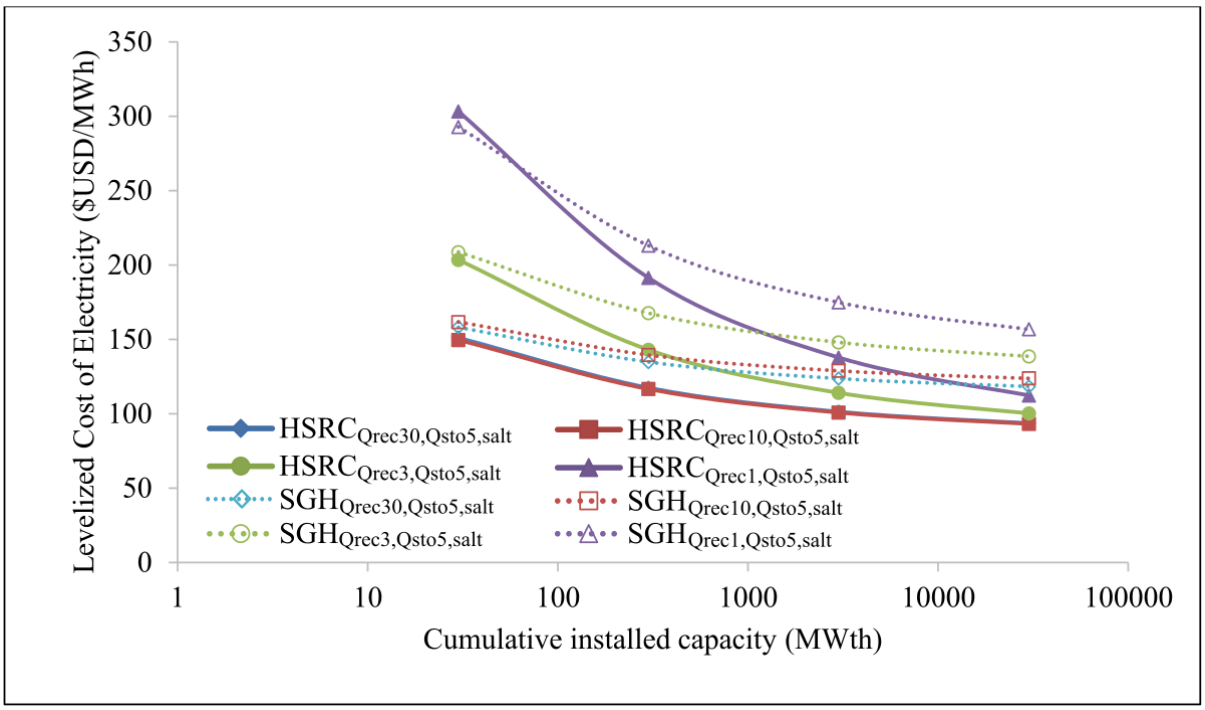

(a)

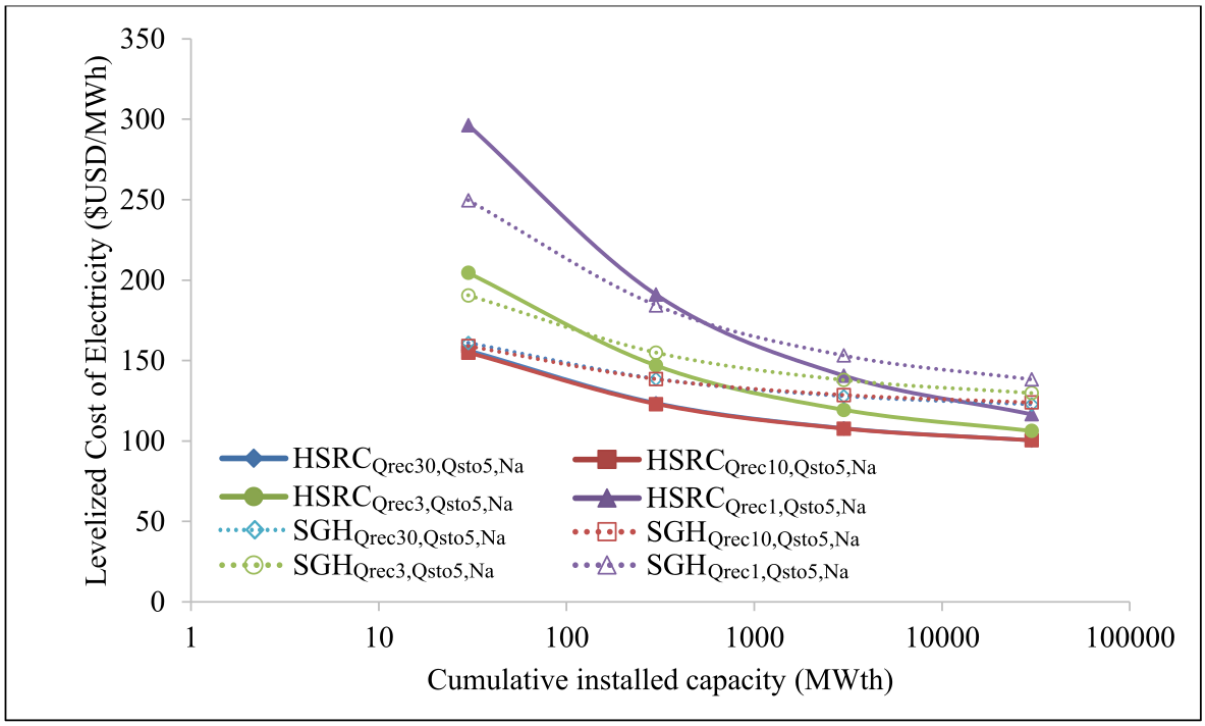

(b)

Fig.8. The dependence of the Levelized Cost of Electricity (LCOE) on different module sizes for the Hybrid Solar Receiver Combustor (HSRC) and the Solar Gas Hybrid (SGH) for the case of 5 hours of thermal storage capacity where f_{mod}=0.6 and f_{HSRC}=2, as a function of its cumulative installed capacity using (a) molten salt and (b) sodium as the heat transfer fluid.

Fig. 9 presents the sensitivity of the LCOE to the value of f_{mod} for the case of 5 hours of thermal storage capacity, a learning rate of 20%, and f_{HSRC}=2, calculated after 300MW_{th} of cumulative installations in which the systems employ either molten salt or sodium as the HTF. For the molten salt systems, it can be observed that the LCOE for the module size of 1MW_{th} for the HSRC system is higher than its 30MW_{th} counterpart for all cases of f_{mod}, while for the module size of 10MW_{th} and 3MW_{th}, the equivalent LCOE is lower than its 30MW_{th} counterpart

when f_{mod} < 0.6 and f_{mod} < 0.3, respectively. For all the module sizes of the SGH system, the LCOE is higher than that of its 30MW$_{th}$ counterpart, except for the case of a module size of 10MW$_{th}$ and f_{mod} < 0.4. There is also a steeper gradient for all the cases of modularised HSRC system because the capital cost of the HSRC has a greater influence than a solar-only cavity receiver for the SGH system. For the systems that employ sodium as the HTF, the trends are similar for all cases of module sizes for the HSRC. However, for the SGH systems, the LCOE for the module size of 10MW$_{th}$ is lower than its 30MW$_{th}$ counterpart for all values of f_{mod} while for the module sizes of 3MW$_{th}$ and 1MW$_{th}$, the LCOE is lower than its 30MW$_{th}$ counterpart for values of f_{mod} < 0.75 and f_{mod} < 0.38, respectively.

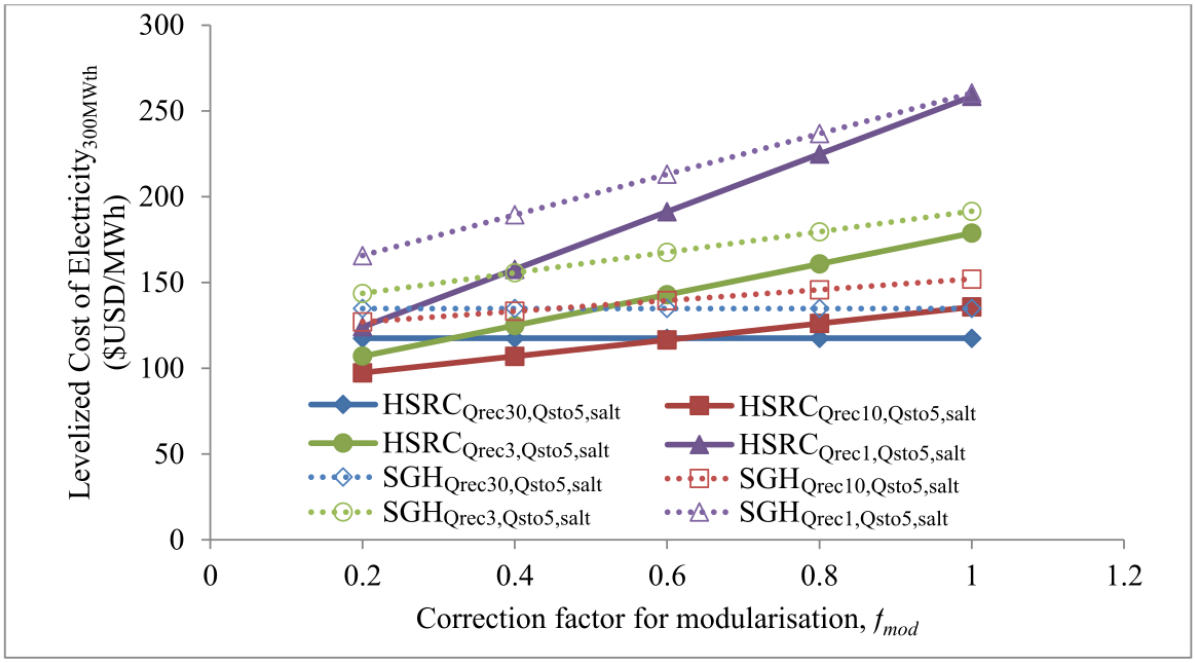

(a)

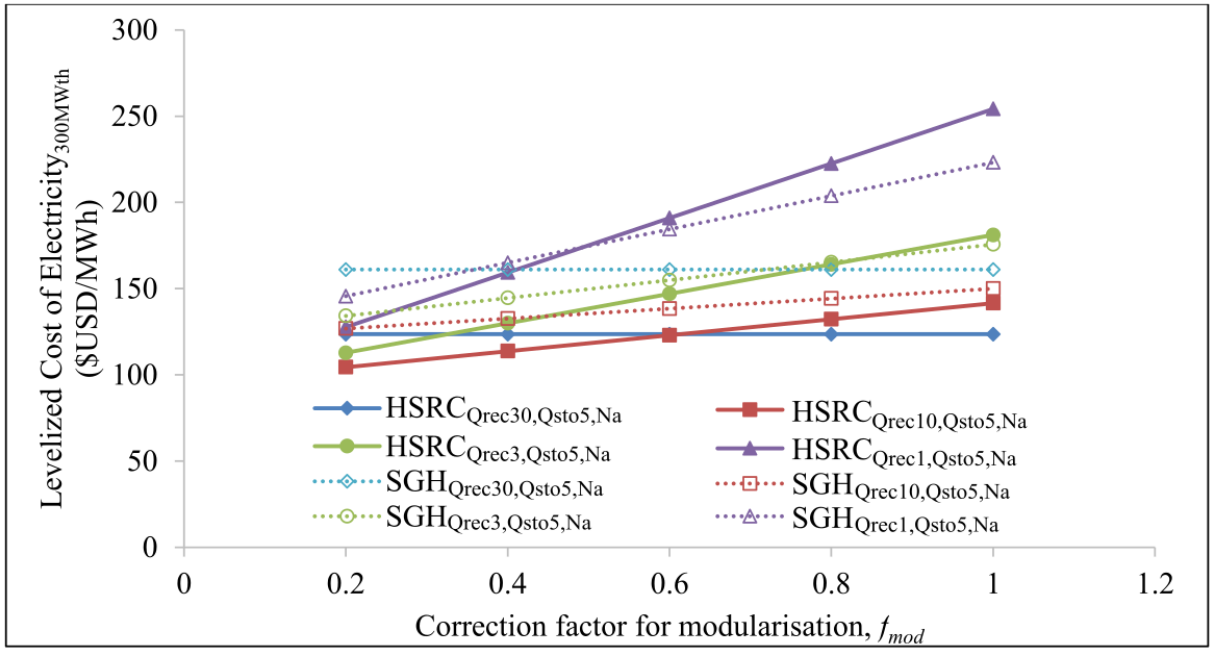

(b)

Fig. 9. The dependence of the Levelized Cost of Electricity (LCOE) on the modularisation correction factor, f_{mod}, for the Hybrid Solar Receiver Combustor (HSRC) and Solar Gas Hybrid (SGH) for the case of 5 hours of thermal storage with a learning rate of 20% and f_{HSRC}=2 after 300MW$_{th}$ of cumulative installations using (a) molten salt and (b) sodium as the heat transfer fluid.

Fig. 10 presents the sensitivity of the LCOE to the value of the learning rate, for the case of 5 hours of thermal storage capacity, f_{mod}=0.6 and f_{HSRC}=2 after 300MW$_{th}$ of cumulative installations. It can be seen that the percentage reduction in LCOE is greater because the learning rates increase for all cases of the HSRC (up to 43%) compared with the SGH (up to 32%). This is due to the higher initial capital cost of a HSRC compared with a solar-only cavity receiver.

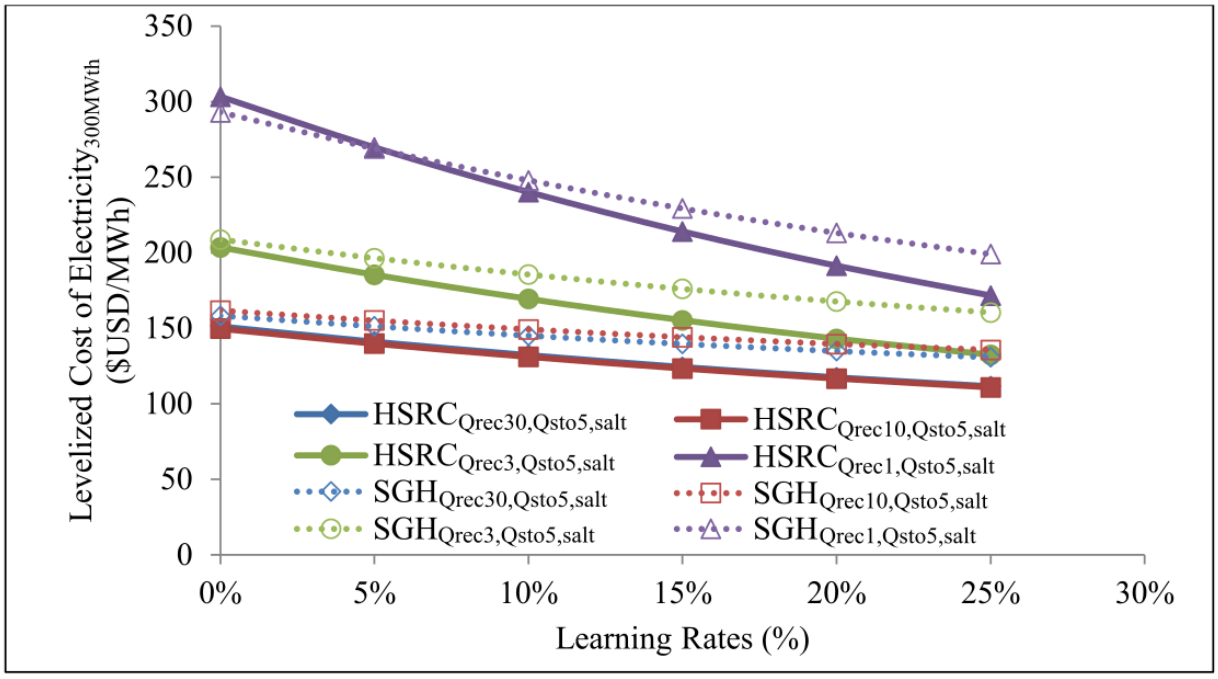

Fig.10. The dependence of the Levelized Cost of Electricity (LCOE) on different module sizes for the Hybrid Solar Receiver Combustor (HSRC) and the Solar Gas Hybrid (SGH) for the cases of 5 hours of thermal storage where f_{mod}=0.6, f_{HSRC}=2 and molten salt as the heat transfer fluid, as a function of its learning rate.

Fig. 11 compares the relative sensitivity of the LCOE to changes to each parameter (i.e. the "tornado chart") for systems employing molten salt as the HTF. Data are presented for cumulative installed capacities ranging from 30MW_{th} to 3,000MW_{th} for both the cases of $HSRC_{Qrec3,Qsto1}$ and $HSRC_{Qrec3,Qsto10}$. It is evident that the fuel cost has the greatest influence on the LCOE for the $HSRC_{Qrec3,Qsto1}$ system and that this influence increases with cumulative installed capacity. However, for $HSRC_{Qrec3,Qsto10}$, the discount factor has the greatest influence on LCOE for cumulative installed capacities of 30MW_{th} and 300MW_{th}. This is because the amount of fuel required for these systems is lower due to higher solar fractions resulting from an increase in thermal storage capacity. For cumulative installations of 300MW_{th} and above,

the fuel cost has the greatest influence on LCOE. This implies that the selection of fuel is a significant factor when designing a hybrid solar thermal power plant, especially for systems with relatively small thermal storage capacities.

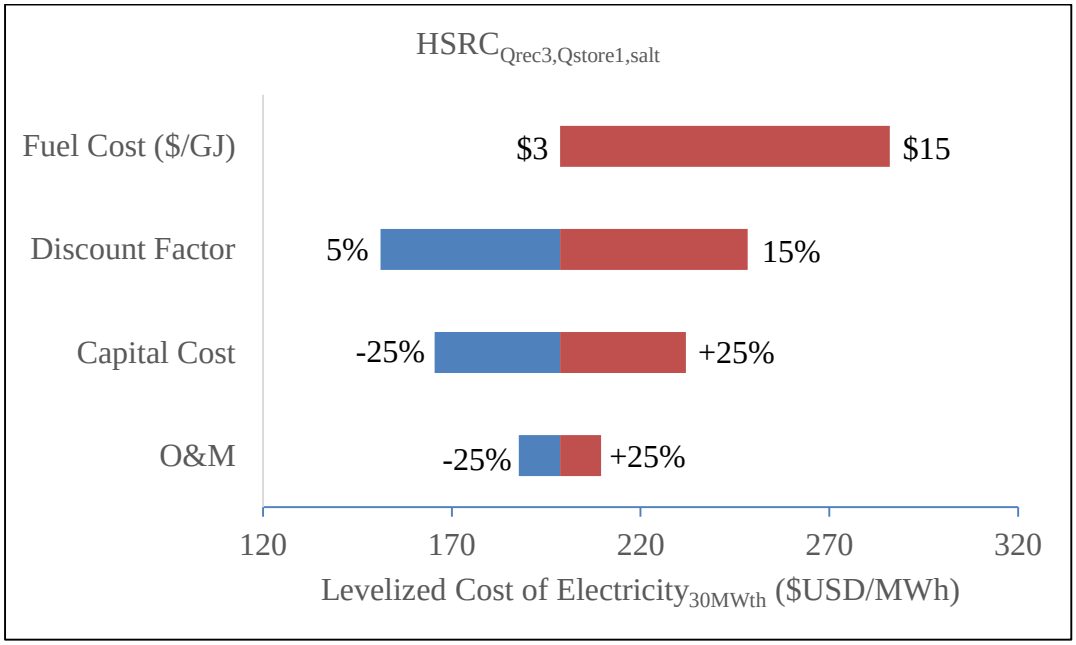

(a)

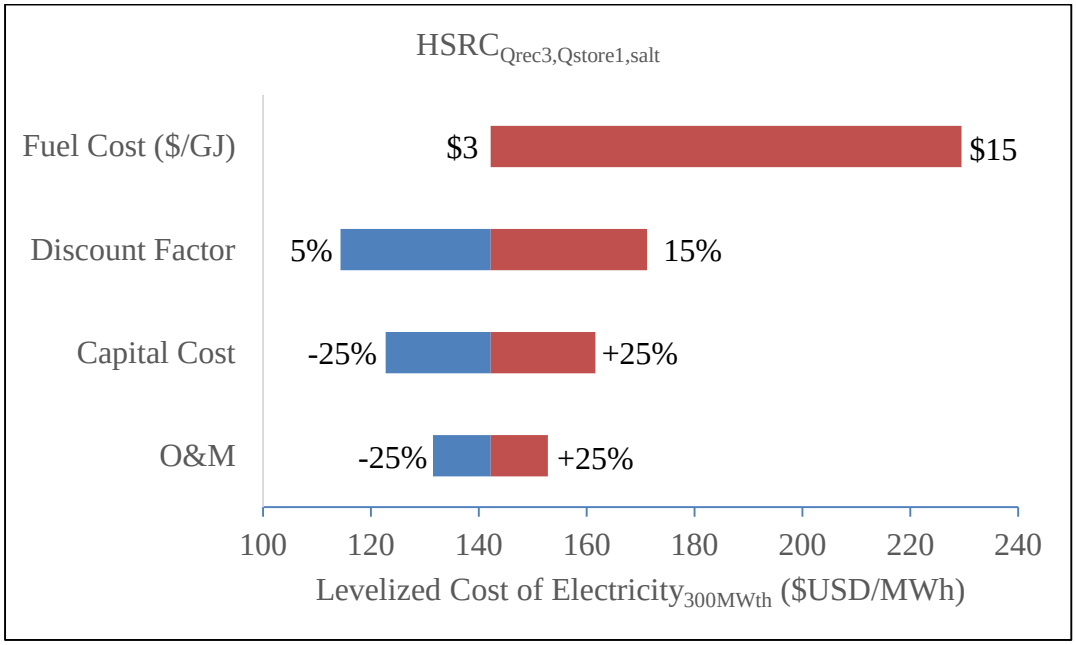

(b)

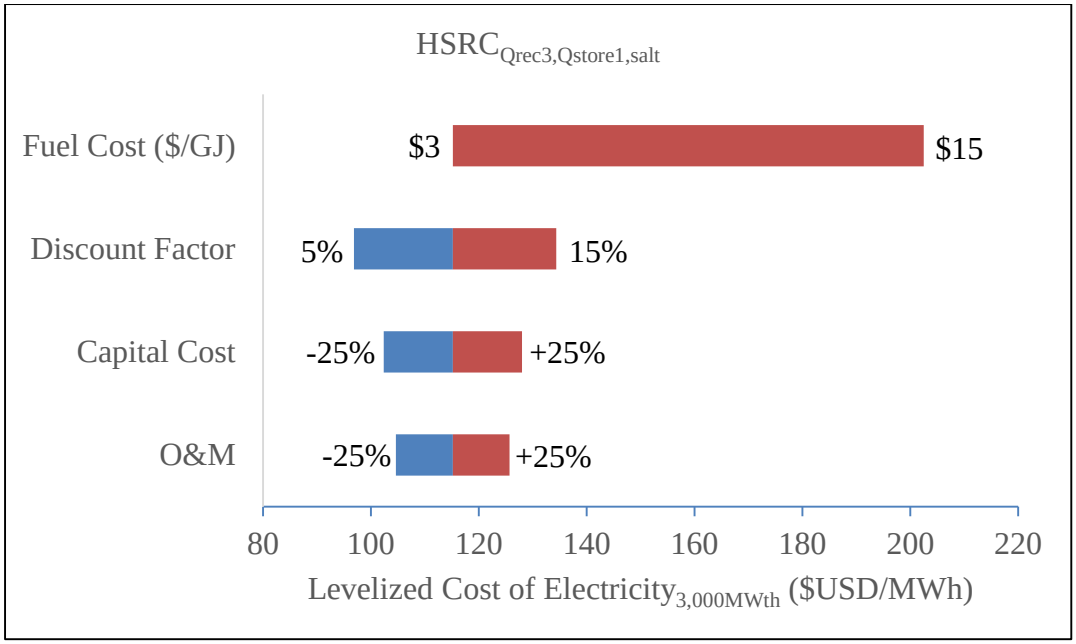
HSRC Qrec3,Qstore1,salt
Fuel Cost ($/GJ)
$3
$15
Discount Factor
5%
15%
Capital Cost
-25%
+25%
O&M
-25%
+25%
80
100
120
140
160
180
200
220
Levelized Cost of Electricity 3,000MWth ($USD/MWh)

(c)

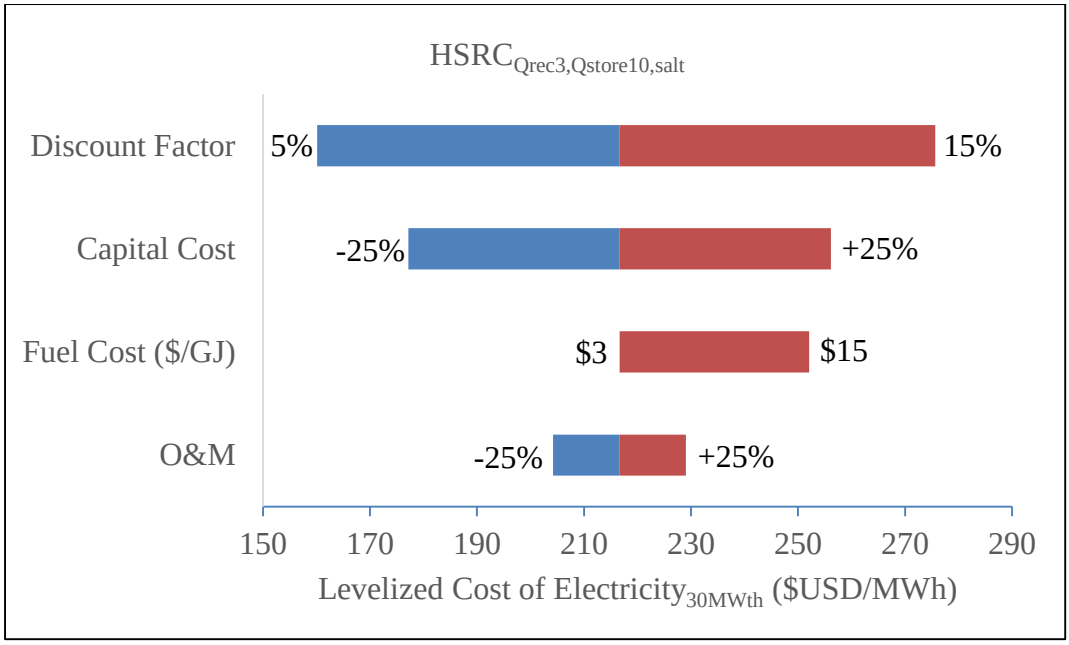
HSRC Qrec3,Qstore10,salt
Discount Factor
5%
15%
Capital Cost
-25%
+25%
Fuel Cost ($/GJ)
$3
$15
O&M
-25%
+25%
150
170
190
210
230
250
270
290
Levelized Cost of Electricity 30MWth ($USD/MWh)

(d)

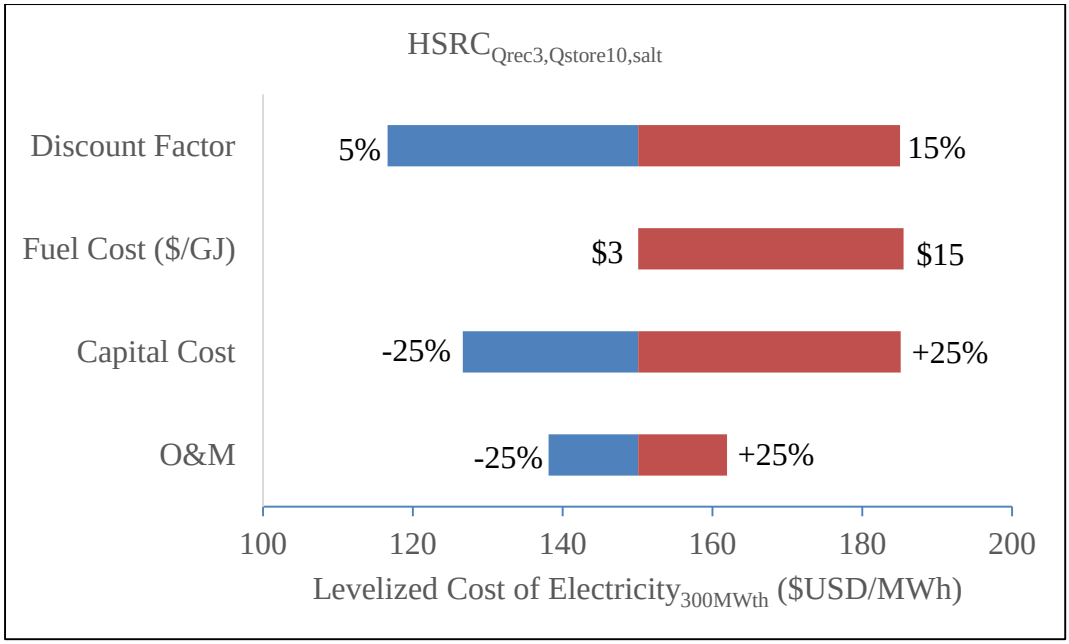

(e)

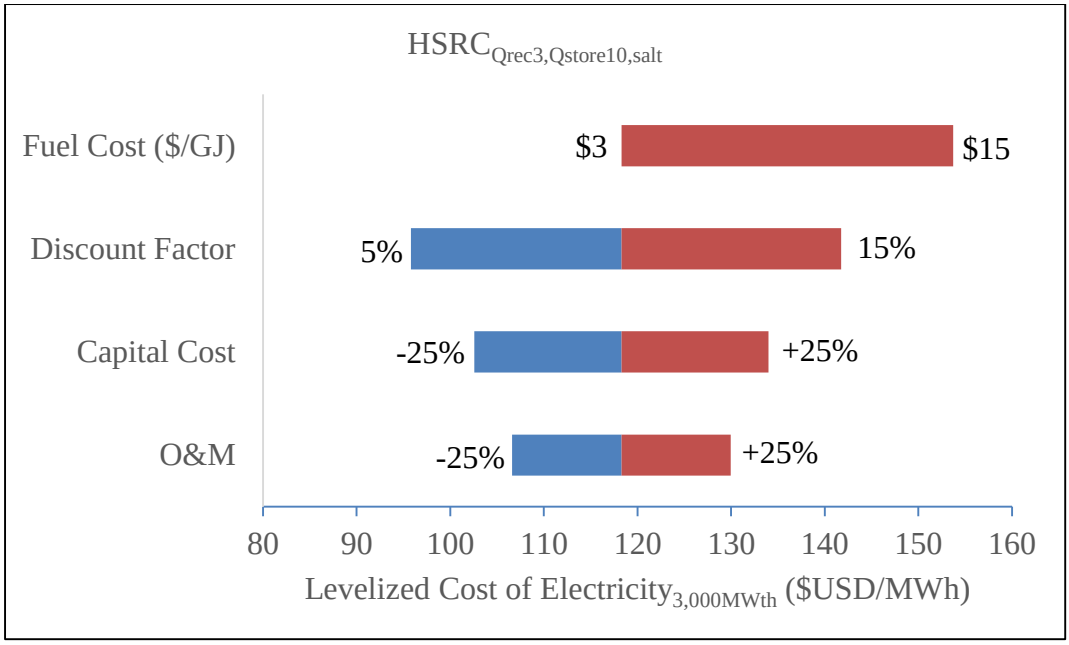

(f)

Fig.11. The influence of each parameter of the Levelized Cost of Electricity (LCOE) for module size of 3MW_{th} for the Hybrid Solar Receiver Combustor (HSRC) for the case of (a) to (c) 1 hour and (d) to (f) 10 hours of thermal storage capacity where the learning rate is fixed at 20%, f_{mod}=0.6, f_{HSRC}=2 and molten salt as the heat transfer fluid.

Fig. 12 presents the sensitivity of the LCOE to the value of the cost multiplier for the HSRC, f_{HSRC}, for the case of 5 hours of thermal storage, a learning rate of 20%, and f_{mod}=0.6 and for 300MW$_{th}$ of cumulative installations. It can be seen that the LCOE for all module sizes of the HSRC system is dependent on the cost multiplier. The LCOE of the HSRC is lower than the SGH for f_{HSRC} < 2.5 with all module sizes. This approach can be used to set a target for the cost reduction required from mass production and/or from advancements in the design of the HSRC.

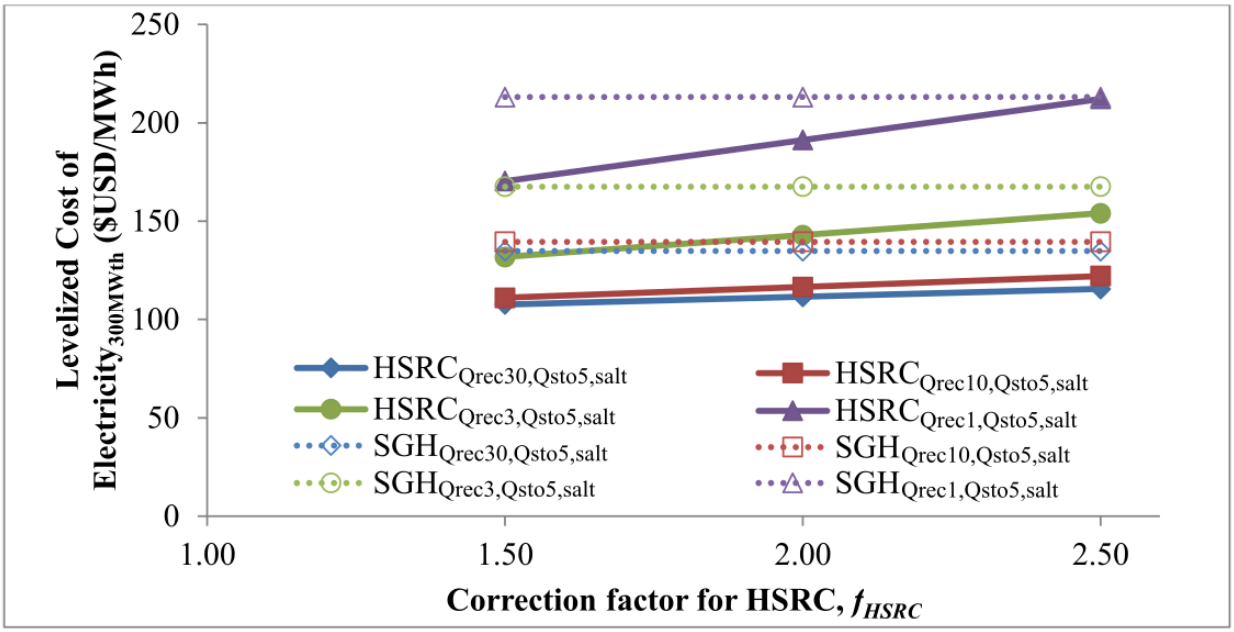

Fig. 12. The dependence of the Levelized Cost of Electricity (LCOE) on the HSRC cost multiplier, f_{HSRC}, for the Hybrid Solar Receiver Combustor (HSRC) and Solar Gas Hybrid (SGH) for the case of 5 hours of thermal storage with a learning rate of 20%, f_{mod} = 0.6 and molten salt as the heat transfer fluid.

4.0 Conclusions

The techno-economic implications of modularisation of hybrid solar thermal systems have been presented, derived from calculations with a pseudo-dynamic model. This shows that:

- The benefits of the learning curve of CSP technologies alone is not sufficient to yield a benefit from modularisation of hybrid CSP systems. To lower the LCOE also requires that modularisation allows the technology to utilise (or adapt) alternative components whose costs have already been lowered through mass production of other types of technology.
- The losses for smaller sized modules, namely $1MW_{th}$ and $3MW_{th}$, using molten salt as its HTF, are dominated by trace heating owing to the increased piping over their larger receiver counterpart. These losses are significantly reduced if an alternative low melting temperature fluid (e.g. sodium) is used.
- The HSRC reduces trace heating (for a molten salt system) by a factor of ~450 for the case of 1 hour of thermal storage capacity for 30 units of $1MW_{th}$ power plant relative to the SGH. However, the initial investment (and resulting LCOE) required to construct the HSRC modules is greater than that for solar-only cavity receivers employed in the SGH system. For a total cumulative installed capacity of greater than ~$70MW_{th}$ the cost of the HSRC becomes lower than the SGH assuming a learning rate of 20%. With the use of an alternative HTF with lower melting temperature, the benefits of the HSRC compared with the SGH are less significant.
- The LCOE for both the HSRC and SGH systems decreases significantly with an increase in total installed capacity. The LCOE of smaller modules becomes competitive with a single larger module after the total installed capacity reaches ~$300MW_{th}$ (i.e. after 10 plants are installed), if the cost of the modularised components can be decreased by >80% and >40% for systems that employ molten salt and sodium as its HTF,

respectively. Nevertheless, the actual value depends on other factors such as learning rates and the reduced cost of modularised components.

- Learning rates greatly influence the LCOE of emerging power technologies, and are more significant for the case of the HSRC than the SGH due to the higher capital cost of the HSRC relative to a solar-only cavity receiver. The learning rates influence the LCOE of the HSRC and SGH systems by up to 43% and 32%, respectively.
- The cost of fuel is a major factor when calculating the LCOE, especially for the case of systems with a small thermal storage capacity, such as 1 hour. The selection of fuel in hybrid solar thermal systems has a large influence on its overall LCOE.

Acknowledgements

The authors would like to acknowledge the support of the Australian Research Council and of FCT Combustion Pty. Ltd. and Vast Solar Pty. Ltd. through the ARC Linkage Grant LP110200060.

References

1. Romero, M., et al., *Distributed power from solar tower systems: a MIUS approach.* Solar Energy, 1999. **67**(4): p. 249-264.
2. Sargent & Lundy LLC Consulting Group, *Assessment of Parabolic Trough and Power Tower Solar Technology Cost and Performance Forecasts*. 2003, NREL: Chicago, Illinois.
3. Kueh, K.C., G.J. Nathan, and W.L. Saw, *Storage capacities required for a solar thermal plant to avoid unscheduled reductions in output.* Solar Energy, 2015. **118**: p. 209-221.
4. Zhang, H.L., et al., *Concentrated solar power plants: Review and design methodology.* Renewable and Sustainable Energy Reviews, 2013. **22**: p. 466-481.
5. Nathan, G.J., D.L. Battye, and P.J. Ashman, *Economic evaluation of a novel fuel-saver hybrid combining a solar receiver with a combustor for a solar power tower.* Applied Energy, 2014. **113**: p. 1235-1243.
6. Lim, J.H., E. Hu, and G.J. Nathan, *Impact of start-up and shut-down losses on the economic benefit of an integrated hybrid solar cavity receiver and combustor.* Applied Energy, 2016. **164**: p. 10-20.
7. Lim, J.H., et al., *Analytical assessment of a novel hybrid solar tubular receiver and combustor.* Applied Energy, 2016. **162**: p. 298-307.
8. Lim, J.H., et al., *Techno-economic assessment of a hybrid solar receiver and combustor.* AIP Conference Proceedings, 2016. **1734**(1): p. 070020.
9. Nathan, G.J., et al., *A Hybrid Receiver-Combustor*, A.R.I.P. Ltd, Editor. 2013.
10. Neber, M. and H. Lee, *Design of a high temperature cavity receiver for residential scale concentrated solar power.* Energy, 2012. **47**(1): p. 481-487.
11. Cooper, M., *Small modular reactors and the future of nuclear power in the United States.* Energy Research & Social Science, 2014. **3**: p. 161-177.
12. Locatelli, G., C. Bingham, and M. Mancini, *Small modular reactors: A comprehensive overview of their economics and strategic aspects.* Progress in Nuclear Energy, 2014. **73**: p. 75-85.
13. Vast Solar, *Dissemination Report: Heliostat Field and High Temperature Receiver Development*. 2014.
14. Want, A. *Commercially Sustainable CSP Scalable, High Efficiency, Low Cost*. in *ASTRI Symposium*. 2015.
15. Johansson, T.B., *Renewable energy: sources for fuels and electricity*. 1993: Island press.
16. Sohal, M.S., et al., *Engineering Database of Liquid Salt Thermophysical and Thermochemical Properties*. 2010, Idaho National Laboratory. p. 2.
17. Behar, O., A. Khellaf, and K. Mohammedi, *A review of studies on central receiver solar thermal power plants.* Renewable and Sustainable Energy Reviews, 2013. **23**: p. 12-39.
18. Boerema, N., et al., *Liquid sodium versus Hitec as a heat transfer fluid in solar thermal central receiver systems.* Solar Energy, 2012. **86**(9): p. 2293-2305.
19. Hsieh, T.-C.A., W.J. Dahm, and J.F. Driscoll, *Scaling laws for NO x emission performance of burners and furnaces from 30 kW to 12 MW.* Combustion and Flame, 1998. **114**(1): p. 54-80.
20. Weber, R. and F. Breussin, *Scaling properties of swirling pulverized coal flames: From 180 kW to 50 MW thermal input.* Symposium (International) on Combustion, 1998. **27**(2): p. 2957-2964.

21. CIBO, *Boilers*, in *Energy Efficiency Handbook*, R.A. Zeitz, Editor. 1997, Council of Industrial Boiler Owners: Burke, Virginia. p. 20.
22. Fisher, J., *Low cost, high efficiency, dispatchable concentrated solar thermal power (CSP)*. 2015, Vast Solar.
23. Rodriguez-Garcia, M.-M., M. Herrador-Moreno, and E. Zarza Moya, *Lessons learnt during the design, construction and start-up phase of a molten salt testing facility.* Applied Thermal Engineering, 2014. **62**(2): p. 520-528.
24. Yao, Y., Y. Hu, and S. Gao, *Heliostat field layout methodology in central receiver systems based on efficiency-related distribution.* Solar Energy, 2015. **117**: p. 114-124.
25. Yu, Q., et al., *Modeling and simulation of 1 MWe solar tower plant's solar flux distribution on the central cavity receiver.* Simulation Modelling Practice and Theory, 2012. **29**: p. 123-136.
26. Wei, X., et al. *Optimization procedure for design of heliostat field layout of a 1MWe solar tower thermal power plant*. in *Solid State Lighting and Solar Energy Technologies, November 12, 2007 - November 14, 2007*. 2008. Beijing, China: SPIE.
27. Romero, M., R. Buck, and J.E. Pacheco, *An Update on Solar Central Receiver Systems, Projects, and Technologies.* Journal of Solar Energy Engineering, 2002. **124**(2): p. 98-108.
28. Siala, F.M.F. and M.E. Elayeb, *Mathematical formulation of a graphical method for a no-blocking heliostat field layout.* Renewable Energy, 2001. **23**(1): p. 77-92.
29. International Energy Agency and OECD Nuclear Energy Agency, *Projected Costs of Generating Electricity*. 2010.
30. Kahlbetzer, J., *Delivering on the promise of low-cost dispatchable concentrating solar thermal power*. 2015.
31. DOE, U., *Sunshot vision study.* US DOE, Washington, DC, 2012.
32. NAB Group Economics, *Natural Gas Market Update – August 2014*, N.A.B. Limited, Editor. 2014.
33. Wene, C.-O., *Experience curves for energy technology policy*. 2000: OECD.
34. Neij, L., *Use of experience curves to analyse the prospects for diffusion and adoption of renewable energy technology.* Energy Policy, 1997. **25**(13): p. 1099-1107.
35. McDonald, A. and L. Schrattenholzer, *Learning rates for energy technologies.* Energy policy, 2001. **29**(4): p. 255-261.
36. Arreola-Risa, A. and B. Keys, *Designing Supply Chains for New Product Development*, ed. B.E. Press. 2013.
37. Jamasb, T., *Technical change theory and learning curves: patterns of progress in electricity generation technologies.* The Energy Journal, 2007: p. 51-71.
38. Jamasb, T. and J. Kohler, *Learning curves for energy technology: a critical assessment.* 2007.
39. Hinkley, J., et al., *Concentrating solar power–drivers and opportunities for cost-competitive electricity.* Clayton South: CSIRO, 2011.

CHAPTER 7

CONCLUSIONS

Chapter 7 - Conclusions

The present thesis provides new understanding about the potential economic benefits of directly integrating a solar cavity receiver with a natural gas combustor, termed the Hybrid Solar Receiver Combustor (HSRC), to provide firm supply of electricity with low emissions. The performance of the HSRC was evaluated using analytical models that calculate heat transfer, mass flow rates and energy balance in the device and pseudo-dynamic models that evaluated the device's performance over periods of up to five years. The study identified research targets into which parameters (e.g. length of cavity to diameter of cavity ratio, heat exchanger length etc.) are important in terms of influencing the HSRC's performance. The benefits of the HSRC which include a reduction in start-up and shut down losses and parasitic losses, relative to its equivalent hybrid (termed the Solar Gas Hybrid (SGH)) were also estimated. In addition, the study considered operation of the HSRC with both conventional combustion and Moderate or Intense Low-oxygen Dilution (MILD) combustion, and contrasted the results under different operating conditions. Finally, the study considered the concept of modularisation of selected components, in particular, the heliostat, tower, and receiver, for both HSRC and SGH systems by comparing their Levelized Cost of Electricity (LCOE).

The following are the main conclusions from the research project:

- The size and the weight of the HSRC is typically controlled by the heat transfer requirements of the combustor, rather than the solar receiver, because additional length (and hence, weight) is required for the heat exchanger component to recover the heat from the combustion products. In addition, the heat flux that can potentially be achieved by a solar concentrator is greater than that from combustion.

- For the HSRC to achieve a similar efficiency to a conventional boiler requires it to be integrated with a sufficiently effective heat exchanger. It was estimated that this will double the cost of the device relative to a solar-only cavity receiver, although it is possible to integrate more efficient (lighter and cheaper) heat exchanger components such as fins and dimples. Nevertheless, the total cost of the device was estimated to still be lower than that of two separate devices, i.e. a gas boiler and a solar cavity receiver.
- When implemented in a typical power plant, the HSRC was estimated to reduce the net fuel consumption by up to 31%, and LCOE by up to 17%, relative to an equivalent hybrid CSP system that employs a standalone solar-only cavity receiver and backup boiler, called the Solar Gas Hybrid (SGH), for a reference receiver capacity of $100MW_{th}$. This is because the HSRC reduces start-up and shut-down losses of a conventional boiler and reduces parasitic losses due to electrical trace heating. These results are most sensitive to the thermal storage capacity and cost of fuel (natural gas).
- Further improvements can potentially be made to the HSRC by configuring it to operate in the conditions required for Moderate or Intense Low-oxygen Dilution (MILD) combustion. By doing this, there is also potential to reduce the LCOE relative to the HSRC operating with conventional combustion by up to 4% for a reference receiver capacity of $30MW_{th}$.
- Modularisation of selected components in a hybrid CSP plant (i.e. heliostats, towers, solar receivers) has the potential to be economically beneficial relative to a single large scale power generation system through the use of alternative, low-cost manufacturing methods. In particular, for a plant of 30 units of $1MW_{th}$ modules, the LCOE was estimated to be competitive, compared with a single unit of $30MW_{th}$, after ~10 plants

are installed if the cost of the components can be decreased by >80% for systems that employ molten salt as its Heat Transfer Fluid (HTF).

- The use of a low melting point HTF, e.g. sodium, in a modular hybrid CSP plant was estimated to significantly increase the benefits of modularisation, relative to a modular system that employs molten salt as its HTF, predominantly by decreasing the amount of parasitic losses. Specifically, the LCOE for a plant of 30 units of $1MW_{th}$ modules was estimated to be competitive, relative to a single unit of $30MW_{th}$, after ~10 plants are installed if the cost of the modular components can be decreased by >40%.
- For a modular system, the HSRC technology was estimated to reduce the amount of electrical trace heating losses of an SGH system by a factor of up to ~450 if both systems employ the use of molten salt as the HTF, although the initial investment required to construct the HSRC modules is greater. The LCOE of the HSRC was estimated to be lower than the SGH after a total cumulative installed capacity of $>70MW_{th}$ if both systems employ the use of molten salt, assuming a learning rate of 20%. This is because the learning rate influences the LCOE of the HSRC more significantly than the SGH. However, the benefits of the HSRC compared with the SGH are less significant when an alternative HTF with a lower melting point, e.g. sodium, is used.

In light of this, the results obtained have further advanced the fundamental understanding of the HSRC and better identified the conditions where the HSRC technology would offer economic benefits relative to equivalent hybrid CSP systems, thus justifying its on-going development.

CHAPTER 8

RECOMMENDATIONS FOR FUTURE WORK

Chapter 8 – Recommendations for future work

It is recommended that more advanced modelling techniques are to be used to reduce the uncertainties and assumptions of the analytical model (refer to Chapter 3). More complex modelling tools such as Computational Fluid Dynamics (CFD) studies of the device could be used to improve the predictions of the performance of the Hybrid Solar Receiver Combustor (HSRC). The outcomes of these studies should provide the knowledge required to construct a prototype of the HSRC for experimental research. In particular, important aspects that may potentially influence the performance of the HSRC, such as the effects of coking and condensation, could be analysed. Experimental studies that can demonstrate this concept and provide further verification of this technology would accelerate its development towards potential commercialization.

Additionally, combining the HSRC technology with other hybrid CSP-combustion systems, such as feedwater heating, has not yet been considered. This combination will no doubt increase the solar share of the electrical power system. However, the overall capital cost of the system will be increased. Hence, this trade-off needs to be assessed, and it could ultimately increase the benefits of adopting the HSRC technology in an electrical power system.

The final recommendation for future work is to study the performance of the HSRC using different Heat Transfer Fluids (HTFs). Thus far, assessments have only been done assuming molten salt as the HTF. The use of other types of HTFs have yet to be explored. In particular, air, which has been shown to be able to operate at higher temperatures of approximately 900°C. Such high temperatures are well suited for cavity receivers. Air is also relatively cheap compared with molten salt, although a lot more volume is required due to its lower specific heat capacity. Another potential advantage of using air relative to molten salt is the ease of pumping it up a tower, which may result in lower parasitic losses.